Characterization of Anti-Ricin Monoclonal Antibodies and the Construction of a Chimeric Murine-Human IgG2/K Anti-Ricin Monoclonal Antibody

by

Robert Matthew Vendramelli

A thesis submitted to the Faculty of Graduate Studies of

The University of Manitoba

In partail fulfilment of the requirements of the degree of

MASTER OF SCIENCE

Department of Medical Microbiology

University of Manitoba

Winnipeg, Manitoba, Canada

Abstract:

Ricin toxin is a very deadly plant protein that is synthesized by the plant *Ricinus communis*. The toxin has been used in covert assassinations, and holds concern for public safety due to its wide availability, ease of purification, and potential use in a bioterrorism event. As such, ricin toxin has been classified as a Category B agent by the Centers for Disease Control and Prevention (CDC) and as a Schedule 1 agent under the Chemical Weapons Convention. The molecular structure of ricin toxin places it in a group of similar proteins called ribosome inactivating proteins (RIP). More specifically, ricin toxin is classified as a Type II RIP because of its heterodimeric construction; it is composed of a toxic A-chain possessing enzymatic action, and a receptor binding B-chain. For this study, monoclonal antibodies (mAbs) were obtained with binding activities against either the A-chain or B-chain, and a surrogate non-toxic ricin analogue, TST10114, was determined to be suitable for characterization of the anti-ricin monoclonal antibodies. The immunoglobulin variable region genes encoding for the binding domains of the mAbs were sequenced via reverse transcriptase polymerase chain reaction from hybridoma cell RNA. One potent anti-ricin A-chain neutralizing monoclonal antibody was chosen for chimerization, RAC18, which exhibited strong binding affinity and neutralizing properties. The constant regions of a human immunoglobulin G2 (IgG2) were used as the backbone for the recombinant chimeric antibody. The resulting chimeric RAC18-huG2 was transiently expressed in human-derived HEK 293F cells, purified, and assessed for binding characteristics and functional attributes.

Acknowledgements:

First, I would like to thank Dr. Jody Berry for providing me the opportunity to work in his laboratory, and providing me with the resources that allowed me to dedicate my time to this thesis. The insights and encouragement you provided were indispensable and greatly appreciated during my time in the mAb lab, as well as the fact that I was able to work in a field that did – and still does - greatly interest me. I was also guided through my research by the comments provided to me by my advisory committee members: Dr. Xiaojian Yao, Dr. Abdel Soussi-Gounni, and especially to Dr. Cindi Corbett whose help in organization and tone of the writing was greatly appreciated – seriously! I'm also very thankful to have had the input of hybridomas, information and resources from Dr. Seth Pincus in New Orleans, LA, and the help provided by his generous lab staff and students. A big "thanks" to all the staff and students that I worked with in the mAb lab, Xin and Amrit provided me with great training in new techniques, as well as fellow Master's students Kevin Hay, Darren Boese and Ryan Gaudet.

I would also like to thank the Department of Medical Microbiology at the University of Manitoba for helping me gain the tools necessary to succeed in my thesis – not only through the education, seminars and symposia, but also the geniality offered by all members of the department, student and staff alike – I know I have finished with many new friends.

Finally, a big acknowledgement and thanks to my friends and family! To my parents, Loris and Donna for giving me an affordable home during the beginning of this endeavor (i.e. free!), as well as your encouragements and guidance not only in these past few years, but ever since I can remember. To Liz, who has put up with me being mostly broke, and paying most of the rent for the last year (or more) – thanks for being so understanding and always putting a smile on my face!

Table of Contents:

Abstract: II
Acknowledgements: III
Table of Contents: IV
List of Figures: VII
List of Tables: VIII
1.0 Introduction 1
1.1 History of Biowarfare 1
1.2 Treaties and Conventions 3
1.3 Agents of bioterrorism 4
1.4 Ricin as a biothreat weapon 5
1.5 Methods of dispersion 6
1.6 Detection 9
1.7 Source 11
1.8 A scientific history of ricin 12
1.9 Ricin biosynthesis 13
1.10 Toxic action of Ribosome-Inactivating Proteins 13
1.11 Entry into mammalian cells 15
1.12 Mechanisms of toxic action 16
1.13 Immunoglobulin G 17
1.14 Monoclonal antibodies and hybridomas 18
1.15 Therapeutic application 19
1.16 Decreasing mAb immunogenicity 20
1.17 Summary 21
1.18 Project Introduction 22
1.19 Hypothesis 24
2 Materials and Methods 25
2.1 Hybridoma cell lines 25
2.2 Growth and maintenance of hybridoma cell lines 25
2.2.1 Maintenance 25
2.2.2 Collection and storage of hybridoma supernatant 26

2.3 Isolation of mAb V-region coding sequence 26
2.3.1 Isolation of total hybridoma RNA and production of cDNA 26
2.3.2 PCR amplification of IgG variable regions 27
2.3.3 Cloning into pCR2.1 (TOPO vector) 29
2.3.4 IMGT/V-quest search and V-region comparison 30
2.4 Cloning into mammalian expression vector 30
2.4.1 Expression vectors utilized 30
2.4.2 Insertion of RE sites into the variable regions 34
2.4.3 Cloning new V-regions into pCR2.1 36
2.4.4 Ligation of anti-ricin mAb V-regions into vectors 37
2.4.5 Analyzing vectors and Sequencing (PCR primer design) 38
2.5 Expression of recombinant mAb in HEK 293F cells 39
2.5.1 Growth and maintenance of HEK 293F cells 39
2.5.2 Small-scale screening transfection 40
2.5.3 ELISA screening for rAb production 41
2.5.4 Large-scale transfection 42
2.6 Antibody Purification 43
2.6.1 Concentration of supernatant 43
2.6.2 Protein G purification of murine mAb 43
2.6.3 Purification of chimeric mAb 43
2.6.4 Buffer exchange 45
2.6.5 Protein determination by bicinchoninic acid assay 45
2.7 Antibody characterization 46
2.7.1 Denaturing protein gel (SDS-PAGE) 46
2.7.2 Western Immunoblot 47
2.7.3 ELISA of purified Abs 48
2.7.4 mAb affinity determination (BIAcore) 48
2.7.5 Determination of epitope specificity inferred via cELISA 50
3 Results 51
3.1 Isolation of mAb variable regions 51
3.2 Chimeric Ab development 53

3.2.1 Insertion of restriction enzyme sites..... 53
3.2.2 Ligation into vectors..... 55
3.3 Expression of rAb in HEK 293F cells..... 57
3.3.1 ELISA screening of transfection supernatant..... 57
3.3.2 Large scale transfection for chimeric Ab expression..... 60
3.4 Antibody purification..... 61
3.4.1 Chimeric antibody purification..... 61
3.5 Antibody characterization..... 62
3.5.1 Denaturing protein gel (SDS-PAGE)..... 62
3.5.2 Western Immunoblot..... 63
3.5.3 ELISA..... 65
3.5.4 Affinity determination (BIAcore)..... 70
3.5.5 Determination of epitope specificity inferred via cELISA..... 73
4.0 Discussion..... 76
4.1 Selection of RAC18 anti-ricin mAb for IgG2 chimerization..... 76
4.2 Construction of expression system for chRAC18-huG2..... 79
4.3 Optimization of expression system and purification..... 82
4.4 Characterization of chRAC18-huG2..... 82
4.5 Summary and future directions..... 84
Appendix A: Expression system coding sequences:..... 88
Appendix B: Variable region Sequences of the 6 mAbs provided in this thesis:..... 92
Appendix C: IMGT/V-Quest search of the RAC18 variable regions:References:..... 94
References:..... 102

List of Figures:

Figure 1.1: Schematic representation of TST10114, a non-toxic ricin analogue 23
Figure 2.1: The two vectors used for recombinant expression of the variable light chain of RAC18 mAb in HEK 293F cells..... 32
Figure 2.2: The two heavy chain vectors that were used for recombinant expression of the variable heavy region of the RAC18 mAb in HEK 293F cells. 33
Figure 3.1: Attempted PCR amplification variable heavy and variable light regions. 52
Figure 3.2: Amino acid sequence comparison of the VL regions and VH regions of two anti-ricin B-chain mAbs isolated from murine cDNA..... 53
Figure 3.3: PCR insertion of restriction enzyme sites flanking variable regions 54
Figure 3.4: Restriction enzyme digestion, ligation and screening of insertion of variable regions into expression vectors 57
Figure 3.5: ELISA screening of transfection supernatants 59-60
Figure 3.6: SDS-PAGE analysis of purified murine anti-ricin mAbs..... 62
Figure 3.7: Denaturing SDS-PAGE of the chimeric mAb purified by different methods 63
Figure 3.8: Testing the murine mAbs for binding by Western Blot. 64
Figure 3.9: Testing the chimeric recombinant chRAC18-huG2 for binding by Western Blot. 65
Figure 3.10: ELISA analysis of the murine mAbs..... 66
Figure 3.11: Comparison of binding between TST10114 and RAC by the anti-ricin A-chain mAbs 67-68
Figure 3.12: ELISA analysis of the transfection supernatant to determine expression of recombinant antibodies..... 69
Figure 3.13: Coating a flow cell of a CM5 chip in preparation of BIACore affinity analysis..... 70
Figure 3.14: Sensorgram data obtained from the BIACore analysis 72
Figure 3.15: ELISA demonstrating the competition for the binding site by the recombinant chRAC18-huG2 with the murine RAC18..... 75
Figure 4.1: Comparison of the sequences of 11 different A-chains from various ribosome inactivating proteins demonstrating conserved residues..... 86

List of Tables:

Table 1.1: Methods currently in use for the detection of ricin toxin..... 10

Table 2.1: Combinations of Light and Heavy chain vectors transfected into HEK 293F cells to express the full length chimeric anti-ricin A-chain mAb.....41

Table 2.2: Chimeric mAb purification methods..... 44

Table 3.1: Primer combinations successful in amplifying the variable regions from the cDNA of the six hybridoma lines. 51

Table 3.2: Concentration of purified antibody achieved through five different purification trials..... 61

Table 3.3: Brief summary of the activities and affinities of murine mAbs to their respective targets. 73

1 Introduction

1.1 History of Biowarfare

The use of biological agents for terrorist purposes seems to have gained much focus throughout the 20th century, although these agents have been documented in wartimes for millennia. A 2,000-year trend was initiated by Greeks that included contaminating potable water sources of enemies with animal corpses (Poupard and Miller 1992). This was first documented in 300 BC, and has been repeated throughout the years, including during the US Civil War in 1863. Even before the determination of bacterial etiologies, infectious agents were used. For example, in the Middle Ages, catapults were used to spread deadly infections by hurling plague victims, or excrement over walls (Khardori 2006). During the North American French and Indian wars (1754-1767), indigenous Native Americans were offered blankets that were laden with smallpox (Khardori 2006, Hilleman 2002). Pungi sticks (sharpened or pointed sticks stuck in the ground) were contaminated with fecal matter to promote infections when they pierced skin, and various native groups in Central and South America have used toxin-poisoned arrows in hunting (Hilleman 2002).

The scientific research efforts of Robert Koch and Louis Pasteur led to the discovery of the infectious agents behind many diseases, and this ushered in the modern era related to the development of biological weapons (Khardori 2006, Hilleman 2002). After the germ theory of disease, specific organisms were exploited as potential weapons (Hassani *et al.* 2004). During World War I, Germany was accused of many plots revolving around biowarfare (Hilleman 2002, Blancou and Pearson 2003), however, chemical warfare supplanted the role of biological agents (Khardori 2006). Japan used bioweaponry in China extensively before and during World War II,

from 1932-1945. During this time up to 260,000 people were killed by releasing laboratory bred plague infected fleas, and contaminating food and water with *Bacillus anthracis*, *Vibrio cholerae*, *Yersinia pestis*, *Shigella sp*., and *Salmonella sp*. (Khardori 2006). In addition, an estimated 5,000 – 10,000 prisoners died during WWII from experimental work with the above bacterial agents, as well as *Neisseria meningitidis* (Khardori 2006, Hilleman 2002). In 1942, inadequate training of the Japanese troops resulted in an outbreak of cholera, responsible for 1,700 deaths and 10,000 cases (Khardori 2006).

After WWII, the USSR developed an extensive bioweapons division which was operational up to, and possibly after 1993 (Hilleman 2002). The research included different bacterial and viral agents, as well as viral hemorrhagic fevers. An accidental anthrax release in 1979 killed many civilians and animals downwind of a weapons site in Sverdlovsk. The former Soviet government vehemently denied the presence of military biological research in the area (Binder *et al.* 2003), and it took in excess of 10 years of investigations to convince the scientific community that it was an accidental release of anthrax. Iraq began its bioweapons research and development around 1975, and has functionally weaponized bacteria (*B. anthracis* and *Clostridium perfringens*), anti-plant agents and toxins (including ricin and botulinus) (Hilleman 2002). Iraq confirmed that it has deployed weapons containing anthrax and botulinum toxin (Khardori 2006). Another recent attack of note was in 1995 when a Japanese group, Aum Shinrikyo, released the nerve gas sarin in a crowded Tokyo subway (Hamburg 2002). This group had also previously experimented with both anthrax and botulism, and had even sent an expedition to Zaire, with the hope of acquiring Ebola for production as a bioweapon.

Following the anthrax attacks in the US in September 2001, Binder *et al*. note that the overall aim of bioterrorist attacks is not necessarily mortality and lethality, but focuses more on

the societal disorganization and psychological effects of the population (fear, disorganization and panic) (Binder *et al.* 2003).

1.2 Treaties/Conventions

Worldwide, many institutes have compiled lists of agents of concern, and in North America, the Centers for Disease Control and Prevention (CDC) list of bioterrorism agents contains approximately 40 agents (http://www.bt.cdc.gov), and subdivides them into 3 categories. Category A agents are considered high priority, and would cause the most harm while being easy to disseminate. Category B is comprised of slightly less toxic substances that would not cause the same level of morbidity and mortality as Category A. Ricin toxin currently is classified as a Category B agent. Category C includes biological agents that are emerging pathogens that may be weaponized in the future. See also Table 1.1 below for a more complete description and list of the agents included in the categories.

The Geneva Protocol for the Prohibition of the use in war of asphyxiation, poisons, or other gases and the biologic methods of warfare (Hassani *et al.* 2004, Khardori 2006) was drafted after WWI by the League of Nations in 1925, and its function was to ban the use of chemical and biological weapons during war. However, it had a major weakness in that it did not ban the research and development or stockpiling of these weapons, which many signing countries, including Canada, took advantage of (Hilleman 2002).

The Biological and Toxin Weapons Convention (BWC) is a treaty that was developed in 1972 (Hamburg 2002), entered into force in 1975 (Hilleman 2002), and includes 171 signatories as of June 2005 (www.opbw.org). The main stipulations of the BWC are to prohibit the development, possession, stockpiling and use of biological weapons (Hamburg 2002, Hilleman

2002); however, it also suffered weaknesses. In regards to enforcement, Hilleman describes the BWC as "toothless" (Hilleman 2002), as it also fails to define a number of terms, and enforce or even monitor compliance. Different countries that signed responded in different ways: the US destroyed all bioweapon stockpiles under President Nixon, but continued biodefense research, while both the USSR and Iraq began huge offensive research campaigns, as did South Africa (to a much lesser extent) (Hilleman 2002).

The Chemical Weapons Convention (CWC) was signed in 1993, and lists highly toxic chemicals that could be used as weapons. Included in the list, are biological toxins, (including ricin and abrin) as well as various bacterial toxins (botulinum, *C. perfringens* toxin, *Staphylococcus aureus* toxin, shigatoxin, and tetanus toxin to name a few). Under the CWC, ricin is the only protein that is listed as a schedule 1 chemical (Ler *et al.* 2006).

1.3 Agents of bioterrorism

As previously mentioned, agents involved in a bioterrorism attack would be of a biological nature themselves (bacteria or viruses) or a biological product (toxin). Although the list of human and animal bacterial and viral pathogens is extensive, there is only a handful that could be of the greatest harm to public health in an attack (Kortepeter and Parker 1999). Agents that may be destined for use in bioterrorism exhibit a number of properties, which may include, but are not limited to: high lethality; ease of production in large scales; capability of aerosolization and dispersion; and/or communicability and lack of vaccine/treatment (Kortepeter and Parker 1999).

When compared with conventional weapons that may be used in a terrorist attack, bioweapons have many advantages. They are relatively inexpensive and can be produced and

transported fairly easily while still causing considerable damage (Hamburg 2002). One of the major advantages to an organization lacking funds (like a small organization or developing country) is that bioweapons can be very cheap, while still being effective. Considering an attack on a civilian population, and using estimated costs, a conventional weapon might cost $2,000 US per km^2, while bioweapons could be as low as $1 US per km^2 (Huxsoll *et al.* 1987). For this reason, they have been called a poor man's atomic bomb (Livingston and Douglas 1984).

1.4 Ricin as a biothreat weapon

Ricin is a proteinaceous toxin, and can lead to death very quickly, whereas some bacterial or viral agents may be contagious. Considering plant toxins, ricin is one of the most lethal (Ler *et al.* 2006). When inhaled or injected, the human lethal dose is estimated around 1-5 μg/kg (Marsden *et al.* 2005), while intoxication through food or water is higher, around 5-10 mg/kg (Pappas *et al.* 2006).

Ricin has bioweapon appeal because it ranks as "one of the most toxic and easily obtainable plant toxins" (Ler *et al.* 2006). Recent reports indicate that approximately 1 million tons of castor beans are processed each year (Garland and Bailey 2006, Patocka and Streda 2006, He *et al.* 2007). With ricin accounting for up to 5% of the weight of the bean, this means anywhere from 10,000 tons to 50,000 tons of ricin is produced as a byproduct every year. Ricin can either be cheaply extracted from the castor oil waste mash, or cheaply purified from whole beans (Mantis *et al.* 2006, Marsden *et al.* 2005). This makes ricin a good candidate for a 'poor man's atomic bomb,' since weaponizing ricin can be much cheaper and easier (in terms of production and concealment) than, for example, nuclear weapons (Patocka and Streda 2006).

1.5 Methods of dispersion

Depending on the target, the dispersal technique would be different. In the case of a single person being intoxicated, the best known lethal case was that of Georgi Markov, who was surreptitiously 'shot' with a ricin bullet in 1978 (Olsnes 2004). Other methods documented up to the year 2000 are covered extensively in a publication by W. Seth Carus (He *et al.* 2007), and include accounts of attempted murder through food poisoning; the attempted assassination of Nobel prize winning author Alexander Solzhenitsyn; murder of unwanted children in Malawi through feeding; attempted assassination of Internal Revenue Services agents; and many other attempted uses of ricin. Between 2003 and 2004, ricin appeared in various locations in the US, including a mail room in South Carolina, mail addressed to a US senator and mail addressed to the White House (Audi *et al.* 2005).

Injection

The most notorious incident involving ricin delivered by parenteral administration is the case of 49-year old Georgi Markov, who died 3 days post intoxication. Other cases involving injection are mostly seen in suicidal cases (Schep *et al.* 2009). Incidents involving individuals from 20- to 61-years old have been documented, with death occurring as soon as 33 hours post injection, and survival in other cases. Castor bean extracts in these cases ranged from masticated beans being injected subcutaneously (Targosz and Winnik 2002), to acetone extracts injected intravenously or subcutaneously (Coopman *et al.* 2009, Watson *et al.* 2004). Mice injected with radioactively labelled ricin only retained 11% radioactivity 24 hours post injection (with most of the radioactivity being excreted in the urine), indicating that the toxin does not stay within the biological system for an extended period of time (Ramsden *et al.* 1989). However, within that time, the toxin is able to disseminate rapidly to major organs such as the liver (accumulating

46% radioactivity 30min post injection), spleen, as well as muscle. A suspected leading cause of death is attributed to necrosis of cardiac tissue leading to heart block (Crompton and Gall 1980), while other cases report massive multiorgan failure (Targosz and Winnik 2002, Coopman *et al.* 2009).

Lethal doses (LD_{50}) of parenterally administered ricin toxin in mice are as low as 2.8µg/kg (Olsnes and Pihl 1973), and human lethal doses are estimated between 1-10µg/kg (Garland and Bailey 2006).

It seems unlikely that a large scale terrorist attack would involve the parenteral administration of ricin toxin, simply due to the difficulty and the necessity of close one-on-one contact with the intended target.

Dermal Absorption

In the mid 1990's, a group called the "Minnesota Patriots Council" was unsuccessful in executing a plot to smear doorknobs with a ricin extract that had been mixed with dimethylsulfoxide (DMSO) (Schep *et al.* 2009). Although an attempt of this nature would most likely create panic, there is little evidence that ricin can be absorbed through intact skin. Allergic reactions have been documented however (Thorpe *et al.* 1988).

Ingestion

The lethal doses of ricin via the oral route are much higher than other methods of intoxication. In mice the reported dose to achieve LD50 is 20mg/kg (Schep *et al.* 2009), while in humans it may be slightly lower, between 5-10mg/kg (Pappas *et al.* 2006). It has been speculated that as low as 1mg/kg is enough to cause mortality in humans, which corresponds to approximately eight beans (Audi *et al.* 2005, Balint 1974). This figure does not factor in the actual amount of ricin per bean which can vary, and mortality has been reported following the

ingestion of two beans (Challoner and McCarron 1990). Toxicity by ingestion is several orders of magnitude higher than other routes of administration, which may be due to different factors. While many proteins are susceptible to the proteolytic enzymes and acidic environment of the gastrointestinal tract, it seems that in vitro ricin is fairly resistant to degradation by these processes (Olsnes *et al.* 1975). However, ricin toxin is not well absorbed across the intestine resulting in little organ damage (Patocka and Streda 2006, Cook *et al.* 2006, Schep *et al.* 2009). There can be damage to the intestinal mucosa along with apoptotic cell death leading to substantial fluid loss. Hepatic damage has been reported as well but deaths appear to be rare (Doan 2004).

Schep *et al.* (2009) evaluate a possible scenario if ricin were to be used in a bioterrorist attack by contaminating a municipal water supply, and concludes that the logistics would make such an attack unfeasible. Assuming that a 0.2mg/kg dose would be enough to potentially cause human death (1/100th of a mouse LD_{50}), and that an average person drinks 2L of water a day, close to 7500kg of pure ricin would be needed for a population of around 60,000 (calculations made for residents weighing 60kg). Water treatment processes, such as chlorination, have shown to be effective at abrogating ricin toxicity (Mackinnon and Alderton 2000), lessening the possibility of a successful plot to intoxicate a metropolitan community via water. In this event, the mortality would be low, with the majority of exposed individuals making a full recovery, but the strain on the public health system could be taxing.

Inhalation

Some sources indicate that the most likely route of administration by an attack would be as an aerosol in a toxic cloud (Pappas *et al.* 2006, Patocka and Streda 2006). Death after inhalation could be observed between 36-48 hours post exposure. Others have stated that a ricin

attack would be unlikely to be spread as an aerosol, because it is would require vast quantities to be effective from a lethality standpoint (Garland and Bailey 2006). In order to cover a $100km^2$ area with 50% lethality, it would require somewhere in the order of 8 tons of ricin, compared with a few kilograms of anthrax (Kortepeter and Parker 1999). Not considering lethality, hospitals would still be overrun with patients, as well as the spread of fear and panic among the population.

Although the accounts of human exposure are limited, a low exposure dose may lead to allergic symptoms (Bradberry and Dickers 2003), as reported by workers exposed to ricin dust. A study involving rhesus monkey exposed to aerosolized lethal doses of ricin lead to death within 48 hours (Wilhelmsen and Pitt 1996). Death was attributed to asphyxiation of the monkeys following massive alveolar flooding, however, necrosis and inflammation was also observed along the entire airway.

While the LD_{50} of inhaled ricin shows the lowest LD_{50} in animals (1-5μg/kg), the observed mortality is dependant on the size of the particles aerosolized - also called the aerodynamic equivalent diameter (AED) (Roy *et al.* 2003). Larger AEDs (10μm or larger) result in ricin particles depositing higher in the airway, where they may be expelled by various biological mechanisms (such as being swept away by the mucociliary system (Audi *et al.* 1005)). Smaller sized particles (smaller than 3-5μm) would cause the most damage because they can actually be breathed all the way into the bronchioles and alveoli (Schep *et al.* 2009).

1.6 Detection

Environmental detection of ricin contamination via immunoassay has been the most used method, since diagnosis of exposed individuals is extremely difficult and there are very few

clinical symptoms (Pappas *et al.* 2006, Marsden *et al.* 2005). When radiolabeled ricin was injected into rats, it was taken up into organs within 30 minutes, and at 24 hours only 11% remained. A 2006 compilation of detection methods is presented in Table 1.1, however, the authors still make mention of the need for a sensitive and rapid method of detection and quantitation (Ler *et al.* 2006).

Table 1.1: Methods currently in use for the detection of ricin toxin. (Adapted from Ler *et al.* 2006)

	Ricin methodologies	Lowest level of detection (LOD)
1	Radioimmunoassay	100 pg for ricin
2	Enzyme-linked immunosorbent assay (ELISA)	(a) 100 pg/ml (Enhanced colorimetric) (b) 100 pg/ml (Gold particles with silver enhancement)
3	Fluorescence based fiber optic immunoassay	(a) 100 pg/ml in buffer solution (b) 1 ng/ml in river water
4	Fluorescence based immunoassay using quantum dots	30 ng/ml
5	Planar array immunosensor with charge-coupled device	25 ng/ml
6	Aptamer microarray	320 ng/ml
7	GSLs with QCM	5 μg/ml
8	Protein gel based microchip immunoassay	0.7 ng/ml
9	Magnetic microsphere with (a) ECL or (b) FCL	(a) 0.5 pg/ml (b) 1000 pg/ml
10	Gold-coated magnetoelastic sensor	5 ng/ml
11	Fourier transform near-infrared reflectance spectromerty	1.5 mg/500mg wheat flour
12	Capillary electrophoresis with UV	10 mg/ml

1.7 Source

Ricin toxin is produced by the plant *Ricinus communis* which is commonly called the ricin plant, castor bean plant or wonder tree. While all parts of the plant are considered poisonous, ricin toxin itself is primarily stored in the endosperm cells of the maturing beans (Hartley and Lord, 2004, Coopman *et al.* 2009). Castor bean oil is commercially extracted and used in various industries, including as a lubricant of mechanical parts (Olsnes 2004). By products of oil production contain toxic ricin and regulations are in place to monitor disposal of the crude toxic byproduct. The molecular weight of ricin toxin is approximately 63 kDa (Coopman *et al.* 2009), and it represents up to 5% of the bean by weight. When purified, it is a water soluble, white powder that is stable over a wide pH range, but may be inactivated by heat (Audi *et al.* 2005). Ricin is considered to be one of the most toxic proteins in the natural world, with lethal doses approaching 1.0 μg/kg (Coopman *et al.* 2009, Schep *et al.* 2009).

Ricin is associated with a large groups of heterodimeric toxins that contain two moieties – one for binding cells, and another for exerting action intracellularly (Sandvig 2002). Fitting in with this description, ricin can be classified as a type II ribosome inactivating protein (RIP), and by definition, is composed of a binding B-chain, and an enzymatically active A-chain. Ricin also belongs to the A-B family of toxic proteins (Olsnes 2004).

Like many other toxic plants, the plants that synthesize RIPs have been used in folk medicine for thousands of years. It is known that ancient Greeks and Egyptians used the beans from *Ricinus communis* - methods are described in medicinal Sanskrit works called the Susruta Ayurveda, a text from the sixth century BC (Park *et al.* 2004). The seeds from *Abrus precatorius* have been used in ancient Asian medicine, as well as a basis for weighing gold and jewels in south East Asia (Olsnes and Pihl 1976).

1.8 A scientific history of ricin

The name ricin was proposed by Hermann Stillmark in 1888, who extracted the toxin to a semi pure form (Stillmark, 1888). The initial mechanism of toxic action was incorrectly attributed to agglutination of red blood cells, and it was later discovered that Stillmark's preparations were a mixture of the ricin toxin, and a second, less toxic protein called ricin agglutinin (Olsnes 2004, Barbieri *et al.* 2004). In the 1890s, Paul Ehrlich made advances in immunological sciences through his use of ricin and abrin (Ehrlich 1891a and Ehrlich 1891b). Ehrlich was able to show that immunization with ricin produced protection from subsequent ricin exposure in animals, and that it was very specific to the immunizing molecule (antigen). He also observed that host proteins (antibodies) in the animal's sera acted specifically against the toxin they had been immunized with.

From a pure science perspective, ricin and abrin were relatively ignored until it was shown in 1968 that ricin down-regulated amino acid incorporation in rats (Dirheimer *et al.* 1968). Kinetic data obtained over the next decade demonstrated that a single type II RIP A-chain molecule can inactivate thousands of ribosomes per minute. For example, one ricin A-chain molecule can inactivate 2000 ribosomes per minute, which is faster than the cell can synthesize new ones. In this manner, a single ricin A-chain molecule can effectively kill a cell (Olsnes 2004). The elucidation of the exact ribosomal residue that ricin acts on, and the enzymatic method was reported in two papers from 1987. Endo and colleagues demonstrated that ricin cleaves a very specific adenine residue (A4324) in 28S rat rRNA via N-glycosidase activity (Endo *et al.* 1987, Endo and Tsurugi 1987)

Structural information can be important for understanding the functions of mAbs. The crystal structure of ricin B-chain was solved in 1991 to 2.5 Å, (Rutenber and Robertus 1991) and ricin A-chain in 1994 to 1.9 Å (Weston *et al.* 1994). Sequence comparisons of many different RIPs show many similarities, especially in the active site (Olsnes and Kozlov 2001).

1.9 Ricin biosynthesis

In the castor beans, ricin is initially synthesized as a single precursor protein, and is directed through the endoplasmic reticulum (ER) and Golgi apparatus into the vacuole (Hartley and Lord, 2004). Once inside the vacuole ricin is present in its intact A-B heterodimeric form. Ricin is not specific in the ribosomes it acts on, and this method of biosynthesis provides at least two mechanisms that protect the ribosomes of *Ricinus communis* from toxin inactivation. First, the toxin never encounters the substrate while inside the host cell by, sequestering it into specific organelles (Hartley and Lord, 2004). Second, in order for ricin A-chain to be fully active, it needs to be cleaved from the B-chain while in the final heterodimeric form, which normally happens in the ER of the intoxicated cell, not in the cytosol.

1.10 Toxic action of Ribosome-Inactivating Proteins

Ribosome-inactivating proteins (RIPs) are enzymatically active proteins that target cell substrates, and their main function is to catalytically inactivate ribosomes (Girbes *et al.* 2004). RIPs have been divided into three classes, or types, based on their protein structure and intra-molecular interactions (Girbes *et al.* 2004). Type I RIPs are composed of one polypeptide chain (approximately 30 kDa), they are the most common, and are relatively non-toxic to intact cells, however in cell-free system, they inhibit protein synthesis. Type II RIPs are heterodimers

composed of a binding B-chain, and an enzymatically active A-chain (which exerts similar effects as type I RIPs). These proteins are larger, approximately 65 kDa. Type III RIPs are less well defined, and there is much controversy in the literature as to the exact classification of these proteins (Girbes *et al.* 2004, Park *et al.* 2004, Barbie *et al.* 2004). RIPs can be found in a number of living organisms, including fungi, bacteria, and plants. Most RIPs have been identified as plant products, and although their exact biological role in the host cells is not well understood, they are most likely involved in plant defense (Olsnes 2004, Hartley and Lord, 2004). It is postulated that type II RIPs may provide defense against plant eating organisms, while type I RIPs would be more likely to defend against viruses and perhaps microorganisms (Peumans *et al.* 2001).

Ricin acts upon host ribosomes to shut down protein biosynthesis at a cellular level. The ribosome is an intracellular heterodimeric ribonucleoprotein that is composed of a large and small subunit, and is involved in the synthesis of proteins (Spirin 2002). When DNA is initially transcribed, it forms a messenger RNA (mRNA) that is then translated by the ribosome into a protein (Matsuura and Yomo 2006). Ribosomal RNA (rRNA) is single stranded, which allows it to fold into extensive tertiary structures with specific surface patterns, such as looped domains, many of which contain invariant residues (Spirin 2004, Robertus and Monzingo 2004). In the 28S rRNA of the large ribosomal subunit, one of these universally conserved domains is a stem-loop structure that plays a large role in binding elongation factors, and it is here that RIPs exert their toxic effect (Hartley and Lord, 2004). Through their active A-chain, RIPs depurinate a specific adenine at residue 4324 (A_{4324}) in the 28S rRNA (He *et al.* 2007). This greatly interferes in protein biosynthesis, and causes cell death (Ho *et al.* 2009).

Although ribosomes are the primary target of RIPs, there have been other enzymatic activities discovered over the past decade, including nuclease (DNase and RNase), superoxide dismutase and phospholipase activities (Park *et al.* 2004). As a group, RIPs are better understood and studied as N-glycosidases, and this is their defining characteristic.

1.11 Entry into mammalian cells

Before ricin can exert any of its intracellular toxic effects, it needs to be internalized into the cell. Similar to other type II RIPs, this is accomplished by the B-chain lectin. Ricin B-chain binds to cell surface glycoproteins and glycolipids that contain a terminal saccharide, and it is subsequently endocytosed by different mechanisms (Sandvig *et al.* 2002). Once internalized in an early endosome, ricin is transported through the Golgi apparatus in a retrograde fashion to the ER (Hartley and Lord, 2004, Sandvig *et al.* 2002). A recent study indicates that prevention of the transport from the early endosome to the trans-Golgi network can abrogate lethality in mice (Stechmann *et al.* 2010). Host cell machinery in the ER reduce the disulfide bond that tethers the ricin A-chain to the ricin B-chain, releasing the A-chain into the cytosol, where it can exert its toxic effects. (Audi *et al.* 2005). Only a small amount of ricin A-chain actually makes it into the cytosol as some is recycled to the cell surface or degraded in lysosomes (Olsnes 2004). It has been reported that as little as 5% of the ricin that is endocytosed actually makes it into the ER. This may be dependent on the cellular receptor that is initially bound by the ricin B-chain, and recent data is increasingly in favor of this hypothesis (Spooner 2006). It has also been noted that the galactose-binding ability of ricin B-chain is necessary for the successful release of the ricin A-chain into the cytosol. Youle *et al.* (1981) modified the ricin B-chain so that it would bind the

mannose-6-phosphate receptor, and they found that the modified ricin had lost most of its toxicity (Youle *et al.* 1981).

Ricin toxin is able to avoid proteasomal destruction through the use of a host cell machinery. Mammalian cell ER contains a protein complex called Sec61 - a quality control pathway which is responsible for removing any incorrectly folded proteins from the ER (Hartley and Lord, 2004). These misfolded proteins are ubiquinated and targeted for destruction by the proteasome (Olsnes 2004). It has been recognized that ricin A-chain interacts with the Sec61α protein, which might help it escape from the ER. Ricin A-chain contains minimal lysine residues, which are required for ubiquitination in the cytosol. By preventing polyubiquitin from attaching to the molecule, ricin A-chain can escape the proteasomal degradation pathway.

1.12 Mechanisms of toxic action

In 28S rRNA A_{4324} is near the middle of a G-A-G-A highly conserved RNA sequence called the sarcin/ricin domain. As a matter of fact, this domain has been described as "the most highly conserved sequence present in the large subunit of rRNA" (Hartley and Lord, 2004). Sarcin is another class of ribotoxin which is produced by the fungus *Aspergillus giganteus*. The sarcin/ricin domain is one of the most studied domains in ribosomes, simply because it is highly conserved is recognized by numerous toxins from different plants, bacteria and fungi. It has further been demonstrated that laboratory prepared smaller RNA stem-loops that retain the GAGA tetraloop sequence, and DNA stem-loops with the GAGA loop sequence are also substrates for ricin A-chain (Narayanan 2005).

The structure of the GAGA stem-loop structure is dependant on the surrounding nucleotide sequence, which forms the hairpin loop at the end of the stem allowing for the

presence of the correct bond acceptors and donors for the glycosidase reaction (Correll *et al.* 1998). It is in this hairpin loop that the specific GAGA sequence exists in an extremely conserved nature. The fact that ricin chooses A_{4324} from a possible 7000 nucleotides in the ribosome indicate that it is not strictly the nucleotide that is being recognized, nor is it the hairpin structure, since other such structures are left intact.

It has been shown that damage to the 28S rRNA by ricin leads to activation of kinases; including stress activated protein kinases (SAPK), also called cJun NH_2-terminal kinases (JNKs) (Kopferschmidt *et al.* 1983, Iordanov *et al.* 1997); and mitogen-activated protein kinases (MAPKs) through the p38 signaling cascade (Jetzt *et al.* 2009). These activation pathways are a result of ribotoxic stress, and leads to apoptosis of the cell. Previously, it has been hypothesized that cell death was through necrosis as a response to the arrest of protein synthesis.

1.13 Immunoglobulin G

The structure of immunoglobulin G (IgG) contains both the constant (C) and variable (V) domains of the antibody (Ab). The basic 'Y' shape of an Ab contains a mirror set of identical C- and V-domains, and may be divided into four total subunits – two light chains and two heavy chains. The heavy chain of IgG1 is comprised of three constant regions (CH1, CH2 and CH3), as well as a variable chain region (VH). The light chain is made up of a constant light region (CL), and a variable light region (VL), and is tethered to the heavy chain through disulfide bonds. The amino termini of one pair of VH and VL come together to form the antigen binding domain (Lipman 2005). There are three complementarity determining regions (CDRs) on each of the VH and VL chains, so each antigen binding domain is made up of a total of six CDRs. Mature, activated B cells secrete Abs that are all the same, that is, once out of the germinal

center in the lymph node, there is no more affinity maturation. Upon another infection, the memory B cells undergo clonal expansion – they replicate to large numbers, but each new cell is an exact clone of its initial cell.

Each invading pathogen presents numerous antigens (Ags) that may be recognized by numerous Abs. In this instance, when protecting the host against a pathogen, the adaptive immune system creates Abs that can bind to different regions on an antigen. These regions, also called epitopes, can either be a linear sequence of amino acids, or they can be a conformational epitope, based on the three dimensional structure of the Ag. In this manner, an antigen may contain different epitopes, and thus may elicit the production of Abs targeting these different epitopes. This is exactly what happens in a normal human response to a foreign Ag – many Abs are created that have different targets on the same Ag. This normal response is termed polyclonal (Lipman 2005), because there are many different clones of B cells, with different recognition capabilities. On the other hand, when a clonal population of B cells arises from one single progenitor B cell, they are by definition all producing the exact same Ab, and this is termed a monoclonal antibody (mAb).

1.14 Monoclonal antibodies and hybridomas

B cells are normal cells of the human body, and as such, they are subject to senescence, as well as other physiological properties that do not make them suitable for the continual expression of mAbs in a laboratory setting. In 1975, Nature published a paper by Georges Kohler and Cesar Milstein which described a new technology for the controlled production of mAbs involving hybridomas (Nissim and Chernajovsky 2008). In their Nobel Prize winning work, Kohler and Milstein fused immunized mice spleen cells with myeloma tumor cells,

creating immortalized cells that continuously produce mAbs (Laffly and Sodoyer 2008). It was now possible to immunize a mouse with a specific Ag, and select for the B cells secreting relevant antibodies, and produce hybridomas that will produce your specific antibody. These hybridomas are grown in cultures, and Kohler and Milstein mentioned in a rather humble statement that "such cultures could be valuable for medical and industrial use" (Kohler and Milstein 1975).

1.15 Therapeutic application

The ability to produce mAbs on a large scale meant that their "exquisite specificity" (Eccles 2001) could be harnessed for use in a therapeutic and/or diagnostic setting. Another attractive feature of Abs is their structural organization into different functional domains (Kim *et al.* 2005). Indeed, mAbs have proven extremely useful in diagnostics (Hwang and Foote 2005), where it is important to have the ability to recognize a single epitope in a mixture of antigen. However, there appeared to be some limited application for their future in therapeutics - they were shown as early as 1985 to induce natural human immunological responses against the mAbs themselves (Shawler *et al.* 1985), termed an anti-antibody response (AAR) (Hwang and Foote 2005). Around this time, the first therapeutic murine mAb was approved for use in kidney transplants, but its high levels of AAR lead to its failure as a sustainable treatment (Kim *et al.* 2005). This is not extremely surprising, considering the fact that the mAbs used in these early trials were of a murine (or mouse) origin, and even as a therapeutic, mAbs that are obtained from a murine model are foreign proteins inside a human host, and thus, elicit an immune response. In addition, murine mAbs had very short half lives inside humans, and they do not effectively

activate effector functions such as complement-dependent cytotoxicity (CDC) or antibody-dependent cell-mediated cytotoxicity (ADCC).

1.16 Decreasing mAb immunogenicity

The immune response generated by murine mAbs has been termed a human anti-mouse antibody (HAMA) response (Hwang and Foote 2005), and there has been much focus on reducing this type of response in humans. There are methods that try to keep the mouse V-domains, or the CDRs intact, while reducing the amount of mouse protein in the overall mAb.

One such method is by creating chimeric mAbs. Only the V-regions of the murine mAb are retained in chimeric mAbs – the constant regions are replaced with a human C-region scaffold (Laffly and Sodoyer 2005). This offers many advantages over murine mAbs: the specificity of the V-regions is left intact, so the high affinity for the Ag is retained, and they are viewed as less foreign by the host immune system. As mentioned, the Fc portions of mouse mAbs do not stimulate human effector functions very well, and the entire mAb has a much shorter serum half life. By incorporating the Fc portion from a human origin, longer half lives are observed, as well as increased effector function response. Overall, many of the problems associated with administering murine mAbs to humans can be overcome through chimerization, however, human anti-chimeric antibody responses (HACA) have also been noted, but to a much lesser extent than HAMA (Laffly and Sodoyer 2005, Hwang and Foote 2005). The second approved therapeutic Ab was ReoPro in 1994.

1.17 Summary

The number of deaths caused by bioterrorism may not be as high as other chronic health hazards (such as smoking), but they have garnered a lot of attention (Bomlitz and Brezis 2008). Although media coverage of these events may be a misrepresentation of the risk of these bioterrorist agents, these are still real risks that are present in the world today. As a point, bioterrorism killed less than 12 people in the US in 2003, and were the main subject of over 100,000 reports in the media, while smoking killed close to 500,000 people, with media reports less than 10,000 (Bomlitz and Brezis 2008). Regardless of these numbers, the protection of the public health from bioterrorist action is still a very active and valid research avenue. The use of bioweapons in future conflicts is a major threat, and the "proliferation of biological weapons is today a reality" (Binder *et al.* 2003). Although ricin may not be as toxic as other biothreat agents (anthrax or botulinum for example), it is still widely regarded as a serious threat to both humans and animals (Garland and Bailey 2006), and some have recommended that it be moved up to a Category A agent in the CDC list. The Geneva Protocol and the BWC attempted to rid the world of bioweapons unsuccessfully, and further measures are needed to end the development and application of bioweapons, including basic measures such as reducing hunger and poverty to discourage war (Hilleman 2002).

There is a ricin subunit vaccine – RiVax – currently in human phase I clinical trials (Neal *et al*. 2010) which has shown adequate protection in mice studies (Smallshaw *et al.* 2007, Marconescu *et al*. 2010). In a small trial involving 15 volunteers, the vaccine demonstrated the ability to illicit a dose-dependant response, however, the neutralizing ability of the antibodies varied greatly between some individuals (Vitetta *et al*. 2006). If a ricin vaccine is approved it is unlikely to be made available to the general population (rather being used for military exercises),

leaving the remainder of the population (non-vaccinated individuals) at risk in the event of a release of ricin. It is in this circumstance that an anti-ricin therapeutic would be most beneficial, and that is why the search for potential therapeutic candidates is important at this time.

Hybridoma technology for the production of mAbs has come a long way since Kohler and Milstein's 3 page Nature article (Kohler and Milstein 1975). The various setbacks experienced beginning with HAMA responses in the 1980s have been resolved enough to allow for US FDA therapeutic approval of at least 29 mAbs. With the widespread use of antibiotics in the 1940s, the use of polyclonal animal or human sera was largely abandoned (Xiao and Dimitrov 2007). However, with today's technologies, exploiting animal and human Ab reservoirs for new drugs has become a pharmaceutical reality.

1.18 Project Introduction

Ricin is a potent toxin that has increased in production over the past decades – both as a byproduct of industry and for potential uses in biowarfare and bioterrorism. There is currently no antidote to counteract or stop the toxic properties of the toxin, and it is thus desirable to engineer potential therapeutics. Murine hybridoma cell lines have been provided that produce potent neutralizing monoclonal antibodies against ricin toxin (a kind gift of Dr. S. Pincus). However, as mentioned previously murine mAbs are not desirable for therapeutic use. Therefore, the murine anti-ricin mAbs were chimerized for potential therapeutic use.

Although the hybridomas used in this thesis were producing mAbs with specificity against intact active ricin, a surrogate biotoxin was utilized for increased laboratory safety. This non-toxic ricin analogue TST10114 (Figure 1.1), was obtained from Twinstrand Therapeutics. TST10114 is constructed from ricin A-chain covalently linked to ricin B-chain. The composition

of the recombinant TST10114 abrogates any cellular toxicity, permitting its use in biosafety level 2 containment laboratories.

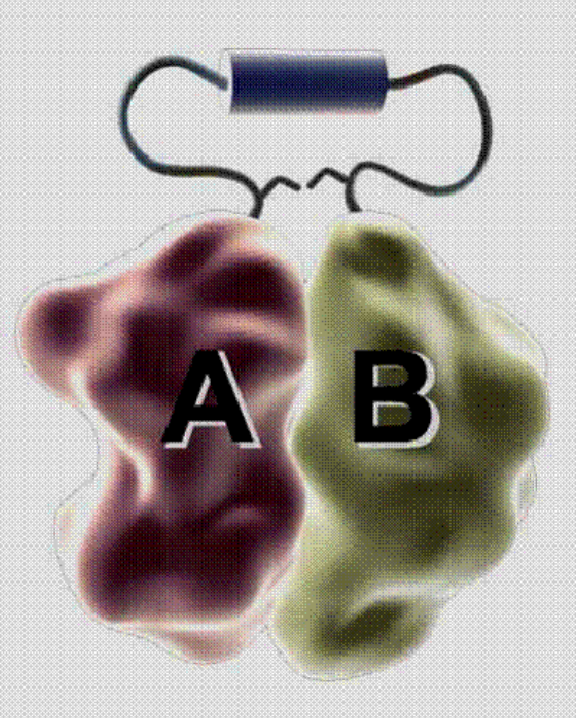

Figure 2.1: Schematic representation of TST10114, a non-toxic ricin analogue. Visible in the diagram is the toxic A-chain covalently linked to the binding B-chain. (Image provided by Dr. Jody Berry, Cangene Corporation)

Using reverse genetic techniques, the variable regions of the murine antibodies were isolated and sequenced, and purified anti-ricin mAbs were characterized. Primers for PCR were designed to amplify the DNA of the variable regions, and also to insert restriction enzyme sites. The variable regions were ligated into antibody expression vectors containing a backbone of the constant regions from a human IgG molecule.

One of the murine mAbs, RAC18 was chosen as the most suitable candidate for chimerization and expression due to its target, binding affinity, neutralizing ability and potential for cross reactivity with related toxins. Some of these characteristics have been studied and reported (Maddaloni *et al*. 2007), allowing for a natural chimerization starting point of this

project. For the expression of the chimeric RAC18, an IgG2 isotype was selected, and two heavy chain expression vectors were obtained. Once the expression vectors were constructed, the efficiency of recombinant antibody expression was assessed via immunoassay. Human embryonic kidney (HEK) 293 Free Style cells were chosen as the cells to transiently express the recombinant mAb, using a serum free growth media. Analyzing the supernatants of the four transfections allowed for the selection of an expression system that would yield the largest quantity of mAb by volume. The purification of the chRAC18-huG2 chimeric mAb out of the supernatant was another step for optimization, as many buffers and columns exist for the purification of antibodies. Once the final chRAC18-huG2 had been purified, it was characterized in a similar manner to the parental murine mAb in order to test the hypothesis that the binding characteristics of the parental mAb were retained throughout the chimerization process.

1.19 Hypothesis

A chimeric murine-human anti ricin A-chain IgG2 monoclonal antibody will be produced from a parental murine IgG1 monoclonal antibody via recombinant technology. Expression and characterization of the chimeric monoclonal anti-ricin antibody will demonstrate that the binding characteristics of the parental antibody have been conserved through the chimerization process.

2 Materials and Methods

2.1 Hybridoma cell lines

Hybridoma cell lines producing anti-ricin monoclonal antibodies were obtained from two different sources. The two cell lines TFTA1 (anti-ricin A-chain) and TFTB1 (anti-ricin B-chain) were purchased from the American Type Culture Collection (ATCC), submitted by R. Jerrold Fulton (Fulton 1986). The four remaining cell lines were obtained as a kind gift from Dr. Seth Pincus (Louisiana State University Health Sciences Center, New Orleans), and included two anti-ricin A-chain hybridomas (RAC14 and RAC18), and two anti-ricin B-chain hybridomas (RBC7 and RBC11) (Maddaloni 2004). Hybridoma lines RAC14 and RAC18 were created by immunizing BALB/c mice with purified ricin A-chain, while RBC7 and RBC11 were created by immunizing BALB/c mice with purified ricin B-chain as per Maddaloni *et al.*, 2004 (Maddaloni 2004).

2.2 Growth and maintenance of hybridoma cell lines

2.2.1 Maintenance

Hybridoma growth media was composed of (by volume) 85% BD Cell MAb Quantum Yield (BD), 10% fetal bovine serum (non-irradiated; heat inactivated) (Hy-Clone), 1% L-glutamine (Gibco), 1% antibiotic-antimycotic (Multicell), 1%HT Hybri-Max (Sigma) and 2% Hybridoma Cloning Factor (BioVeris). This growth media was stored at 4°C for up to 21 days, and warmed in a water bath to 37°C prior to use. For purification of monoclonal antibody from the supernatant, cells were weaned off fetal bovine serum by passaging into differing ratios of Hybridoma growth media and Hybridoma serum-free media. Hybridoma serum-free media was

composed of 96% HyQ CCM1 (Thermo Scientific), 1% L-glutamine (Gibco), 1% antibiotic-antimycotic (Multicell), 1% HT Hybri-Max (Sigma) and 2% Hybridoma Cloning Factor (BioVeris). Cells were grown in a 1:1 mixture, followed by a 4:1 mixture of hybridoma serum-free media:hybridoma growth media for 2-3 days each then passaged into hybridoma serum-free media.

Hybridoma cell lines were stored at a concentration of 1.0×10^7 cells/mL at -150°C in freezing media, which was composed of 80% fetal bovine serum (non-irradiated; heat inactivated) (Hy-Clone), 10% BD Cell MAb Quantum Yield (BD), and 10% dimethyl sulphoxide hybri-max (Sigma-Aldritch). Cells were counted using a hemacytometer every 2 or 3 days, and were passaged when a concentration of $5.0 \times 10^4 – 5.0 \times 10^5$ cells/mL was reached. Cells were diluted 1:10 in fresh pre-warmed media to increase viability, or 1:5 to increase total number of cells.

2.2.2 Collection and storage of hybridoma supernatant

Hybridoma cells were grown in 1 litre when the purification of monoclonal was desired. Supernatant was centrifuged in conical centrifuge tubes (Corning Incorporated) at 3000xg for 30 minutes in the Beckman Coulter Allegra X-12R, and collected in storage bottles (Nalgene). Supernatant was stored at 4°C for short term or -20°C for long term storage.

2.3 Isolation of mAb V-region coding sequence

2.3.1 Isolation of total hybridoma RNA and production of cDNA

Total RNA was isolated from 1.0×10^7 cells using the RNeasy Mini Kit (QIAGEN), following the manufacturer's protocol. RNA was eluted in 40µL DNase/RNase free water. RNA

concentrations were determined spectrophotometrically using the ND-1000 Spectrophotometer (NanoDrop), and samples were either used immediately or frozen at -80°C for a short period of time.

The total RNA isolated from the hybridoma cells was used to make complementary DNA (cDNA) by combining 1µL oligo$(dT)_{20}$ primer, 2µL of the eluted RNA, 2µL 10mM dNTP Mix, and 6µL DEPC treated water, and following the instructions provided with the ThermoScript™ RT-PCR kit (Invitrogen). In order to minimize the possibility of creating any aberrant Kappa cDNA, a 3-prime biotin blocked primer (AbVk: 5′-TAATGTGCTGACAGTAATAGGT-3′-Biotin) was added to the initial reaction mix (Yuan 2004). Amplified aberrant variable regions were identifiable as 100-150 base pair fragments visualized by ethidium bromide following electrophoresis on an agarose gel. When the aberrant cDNA could not be avoided, a protocol involving rapid amplification of cDNA ends (RACE) was used. In this case, total cDNA was created from total RNA using the GeneRacer™ kit (Invitrogen). Sequencing was accomplished using known internal primer pairs (T7, M13R) which aligned to regions directly prior to and directly after the inserted variable region in the pCR2.1 vector.

2.3.2 PCR amplification of IgG variable regions

Polymerase chain reaction (PCR) was set up to retrieve the variable region DNA from the cDNA. A panel of PCR primers that are complementary to conserved regions flanking the murine Ab V-region specific were chosen, and included:

V_H 5':

UmIgVH	TGAGGTGCAGCTGGAGGAGTC
MHcL-1	ATGGACTT(GCT)G(GAT)A(CT)TGAGCT

MHcL-2	ATGGAATGGA(GC)CTGG(GA)TCTTTCTCT
MHcL-3	ATGAAAGTGTTGAGTCTGTTGTACCTG
MHcL-4	ATG(GA)A(GC)TT(GC)(TG)GG(TC)T(AC)A(AG)CT(TG)G(GA)TT
MHC1	AGGTCCAGCTGCTCGAGTCTGG
Sheriff IgG	GCCGGTACCCAGCTCCAGCTTCAGGAGTC

V_H 3':

MG1-3Seq	AGATGGGGGTGTCGTTTTGGC
Sheriff IgG	GCGTCGACCAGGGGCCAGTGGATAGAC
MG2a/b-3Seq	GAC(TC)GATGGGG(CG)TGTTGTTTTGGC
MH125	GGATACAGTTGGTGCAGC

V_L 5':

MVL	GTGCCAGATGTGAGCTCGTGATGACCCAGTCTCCA
Sheriff Kappa	GCCGAATTCGACATTGTGCTGACCCAATCTCCAGCTTC
MKcL-1	ATGAAGTTGCCTGTTAGGCTGT
MKcL-2	ATGGACTTTCAGGTGCAGATCT
MKcL-3	TTGCTGTTCTGGGTATCTGGTA
MKcL-4	ATGGAGACAGACACACTCCTGCTAT
UmIgVK	GACATTCTGATGACCCAGTCT

V_L 3':

MK-3Seq	TACAGTTGGTGCAGCATCAGC
IgKappa	GCGCCGTCTAGAATTAACACTCATTCCTGTTGAA
MKC1	GGATACAGTTGGTGCAGC
Sheriff Kappa	GCGAATGCGGATGTTAACTGCTCACTGGATGGTGGG

Primer sequences from Dr. Jody Berry, PhD thesis (1999), University of Manitoba.

A total volume of 50μL was set up per reaction with 46μL of Platinum® Blue PCR SuperMix (Invitrogen), 2μL of a 1/10 dilution of the purified cDNA, and 1μL each of the 5' and 3' primers at a concentration of 20μM each. Reactions were cycled in the Techne Touchgene Gradient Thermal Cycler (Techne) with the following conditions: 94°C for 2 minutes; 30 cycles of 94°C for 1min, 62°C for 1min, and 72°C for 1min 30s; the final extension was 10 minutes at 72°C.

The reactions were then analyzed in a 1% agarose gel with ethidium bromide (Invitrogen). The bands were visualized using UV light and viewed on the GelDoc XR (BioRad) and relevant bands in the 350-500 base pair range were purified using the QIAquick Gel Extraction Kit (Qiagen). During the final step, DNA was eluted from the QIAquick column using 30uL of autoclaved Milli-Q water. DNA concentration was determined using the ND-1000 Spectrophotometer (NanoDrop®). Purified DNA samples were either cloned into pCR2.1 vector immediately, or frozen at -20°C

2.3.3 Cloning into pCR2.1 (TOPO vector)

Relevant PCR products or gel purified PCR products were cloned into the vector pCR2.1 using the TOPO TA Cloning® Kit (Invitrogen). *Escherichia coli* cells were transformed (either by chemical transformation and electroporation) with 2μL of the PCR product following the manufacturer's protocol, and were allowed to recover for 1 hour in SOC media (Invitrogen). Transformed *E. coli* cells were plated onto Luria Bertani with ampicillin agar plates (LB-Amp, 100μg ampicillin/mL) that had also been coated with 40μL of 100mg/mL 5-bromo-4-chloro-3-indoyl-β-D-galactoside (X-gal), and were incubated at 37°C over night. The following day, white colonies were identified and single colonies were sub cultured into 3-5 mL of LB-Amp

broth. Broth cultures were grown in a shaking incubator at 250RPM at 37°C over night. The following day, glycerol stocks were made of the cultures and stored at -80°C. To isolate plasmid DNA, the bacterial cultures were pelleted, and plasmids were purified using the QIAprep® Miniprep Kit (QIAGEN) according to the manufacturer's protocol, and eluted with 35µL sterile water. DNA concentrations were determined using the ND-1000 Spectrophotometer (NanoDrop®). Purified plasmids were diluted to 150ng/µL in 10µL total volume, and sent to the Genomics Core Facility at the National Microbiology Laboratory to be pyrosequenced on the Applied Biosystems 3730-XL. Primers for sequencing were the M13Reverse (5′-CAGGAAACAGCTATGAC-3′) and T7 (5′-TAATACGACTCACTATAGGG-3′). Sequences were analyzed and aligned using Lasergene suite software (DNAstar).

2.3.4 IMGT/V-quest search and V-region comparison

The consensus variable region sequences were analyzed using the International Immunogenetics Information System® V-Quest (http://www.imgt.org/IMGT_vquest/share/textes/) to ensure that functional variable regions had been cloned. The sequences were then aligned using the MacVector program to identify any similarities.

2.4 Cloning into mammalian expression vector

2.4.1 Expression vectors utilized

A total of four vectors were used for mammalian expression of recombinant IgG2 antibody (rAb). The two heavy chain vectors were pFUSE-CHIg-hG2 (Invivogen) and pINFUSE-hIgG2-Fc2 (Invivogen), each used for expression of human IgG2 heavy chain

fragment. The two light chain vectors used were pcDNA3.1 (Invitrogen) and p-dbKappa (modified from a commercial vector, see D. Boese, M.Sc thesis, 2009, University of Manitoba). All vectors carried the zeocin resistance gene. For ease of manipulation of the variable heavy regions into the various vectors, they were first ligated into the p-dbIgG1 vector (created in house, see D. Boese, M.Sc thesis, 2009, University of Manitoba). The pFUSE-CHIg-hG2 vector lacked the interleukin-2 secretion signal (IL2ss), which was inserted from p-dbIgG1, while the pINFUSE-hIgG2-Fc2 vector lacked the huCH1 sequence, which was also inserted from the p-dbIgG1 vector, to form a secretable heavy chain and a full length heavy chain respectively. While only the RAC18 mAb was chosen for expression as a chimerized IgG2, all other variable light and variable heavy regions were ligated into the p-dbKappa and p-dbIgG1 vectors respectively for long term storage, or future use. The pcDNA3.1 vector was supplied by the lab of Dr. Seth Pincus, with the variable light RAC18 sequence already ligated into it.

Both the kappa chain and heavy chain p-db vectors were constructed with the restriction enzyme site EcoRV (5'-GATATC-3') 5' of the variable region and NcoI (5'-CCATGG-3') 3' of the variable region. These two restriction enzyme sites are not in frame, which had to be taken into consideration during PCR primer design to insert the sites flanking the variable regions. Briefly, forward primers were constructed with six irrelevant base pairs followed by the EcoRV site, a guanine base pair (to ensure the variable region is in frame), and the first 23-27 base pairs of the respective variable region (see also Appendix A for RE placement). Reverse primers were constructed with 4-6 irrelevant base pairs followed by the NcoI site, a cytosine, and the reverse complement of the final 20-32 base pairs of the variable region. PCR primers are listed below, and cycling parameters are outlined in section 2.3.2.

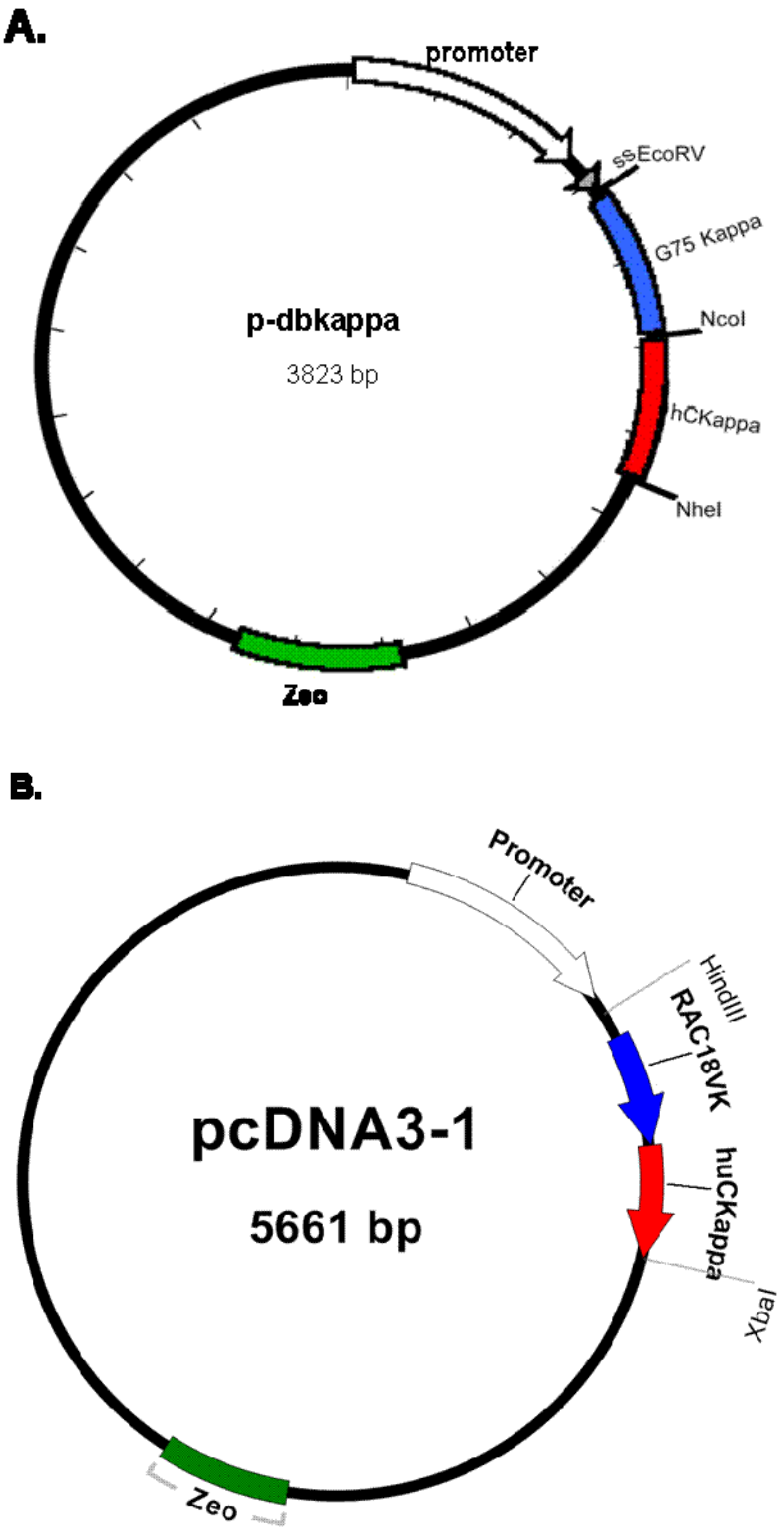

Figure 2.1: Light chain vectors used for recombinant mAb expression in HEK 293F cells. (**A.**) p-dbKappa showing an anti-anthrax G75 variable region that was removed for the insertion of the RAC18VK sequence. (**B.**) pcDNA3.1 as received from Dr. Seth Pincus, containing the RAC18VK sequence. RE sites used for ligations are included.

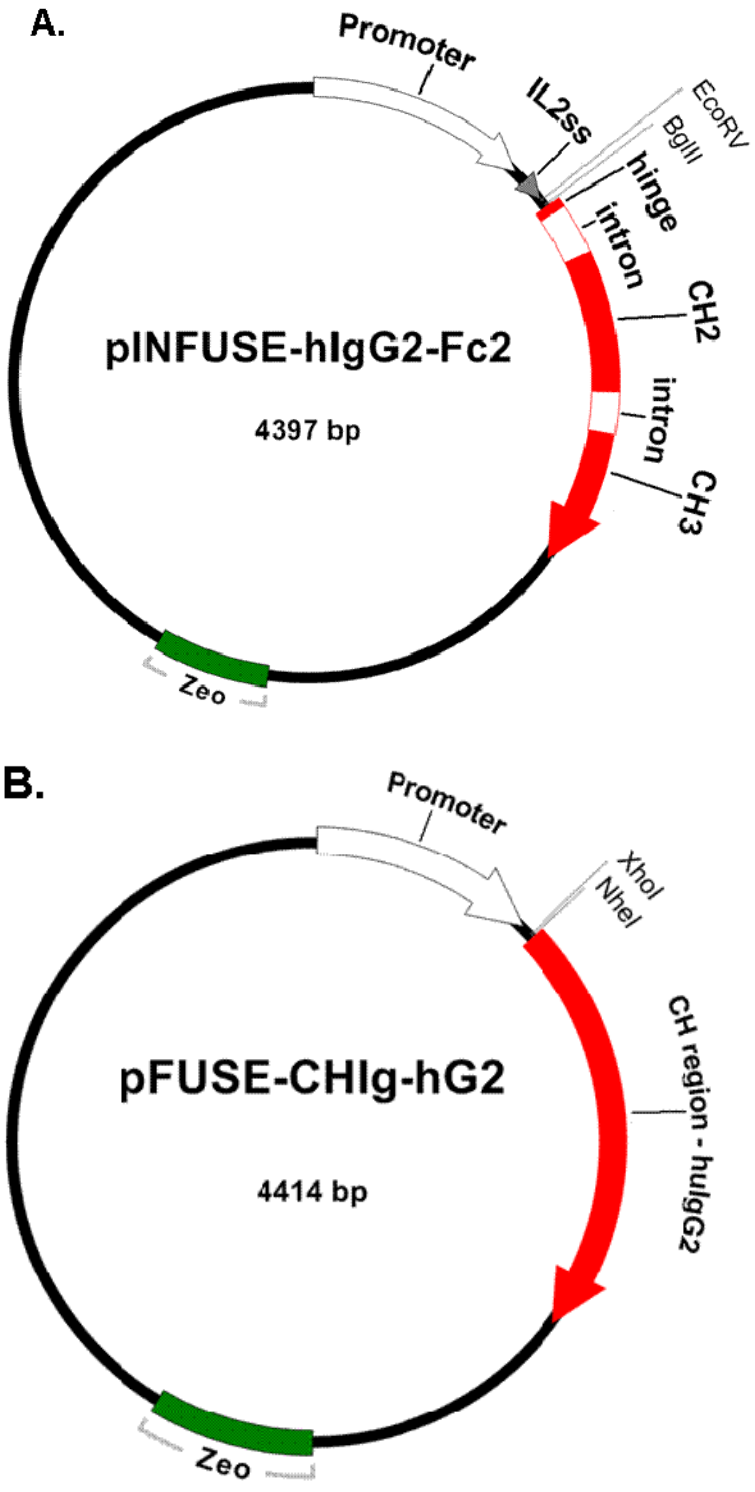

Figure 2.2: Heavy chain vectors for recombinant mAb expression in HEK 293F cells. (**A**.) pINFUSE-hIgG2-Fc2 required the insertion of the RAC18VH and CH1 sequences. (**B.**) pFUSE-CHIg-hG2 required the insertion of the Il2ss and RAC18VH. RE sites used for ligations are included.

2.4.2 Insertion of RE sites into the variable regions

The RAC18VH was subcloned into the human IgG2 vector by PCR amplification with built in flanking RE sites. Once the RAC18 variable heavy region was inserted into p-dbIgG1, it was necessary to subclone it into the huIgG2 expression vectors pFUSE-CHIg-hG2 and pINFUSE-hIgG2-Fc2. For insertion into pFUSE-CHIg-hG2, primers were designed to insert the XhoI (5'-CTCGAG-3') before the IL2ss, and NheI (5'-GCTAGC-3') at the end of the RAC18VH sequence. The forward primer was designed with 6 irrelevant base pairs followed by the XhoI sequence and the initiation codon of the IL2ss. The reverse primer was designed to insert the NheI sequence directly after the variable heavy sequence, in frame. Preparing the RAC18CH-CH1 sequence for insertion into pINFUSE was achieved using the EcoRV RE site (present before the RAC18VH sequence) and BglII RE site (present and after the CH1 sequence).

5' Primer to insert XhoI before IL2ss
IL2XhoF GAATTC*CTCGAG*ATGTACAGGATGCAACTCCTG

5' Primers to insert EcoRV before VK
TFTA1:
A1KEcoRVFdbK GAATTC*GATATC*GGATGTTGTGATGACCCAGACTCCACTC

RAC18:
A18KEcoRVFdb GAATTC*GATATC*GGACATCCAGATGACACAGTCTCCATCC

TFTB1:
B1KEcoRVFdbK GAATTC*GATATC*GAAGCTCGTGATGACCCAGTCTCCATCT

RBC7:
B7KEcoRVFdbK GAATTC*GATATC*GGAGCTTGTGATGACCCAGTCTCCAGCT

RBC11:
B11EcoRVFdbK GAATTC*GATATC*GGAGCTCGTGATGACCCAGTCTCCATCC

3' Primers to insert NcoI after VK
TFTA1:

A1KBdbKNco1 AGTAC*CCATGG*CTTTTATTTCCAGCTTGGTCCCCCCTCCGAACG

RAC18, TFTB1:
B1A18KBdbNco AGTAC*CCATGG*CTTTGATTTCCAGCTTGGTGCCTCCACCGAACG

RBC7:
B7KBdbKNco1 AGTAC*CCATGG*CTTTTATTTCCAATTTTGTCCCCGTGCCGAACG

RBC11:
B11KBdbKNco1 AGTAC*CCATGG*CTTTGATTTCCAGCTTGGTGCCTCCACCGAACG

5' Primers to insert EcoRV before VH
TFTA1:
A1HEcoRVF GAATTC*GATATC*GCAGCTCCAGCTTCAGGAGTCAGG

RAC18, TFTB1, RBC7:
A18B7B1HEcRF GAATTC*GATATC*GGAGGTGCAGCTGGAGGAGTCTGG

RBC11:
B11HEcoVFdbG GAATTC*GATATC*GGAGGTGCAGCTGGAGGAGTCTGG

3' Primers to insert NcoI after VH
TFTA1:
A1HNcoIBdbG TGGAGG*CCATGG*CTGAGGAGACTGTGAGAGTGGTGCCTG

RAC18:
A18SP18HNcoB TGGAGG*CCATGG*CTGCAGAGACAGTGACCAGAG

TFTB1
B1HNcoIBdbG TGGAGG*CCATGG*CTGAGGAGACGGTGACTGAGGTTCCTTG

RBC11:
B11HNcoIFdbG TGGAGG*CCATGG*CTGAGGAGACTGTGAGAGTGGTG

3' Primer to insert NheI after RAC18 VH
A18VHBhG2Nhe GAATTC*GCTAGC*TGCAGAGACAGTGACCAGAGTCCCTTG

PCR cycling parameters are outlined in section 2.3.2

During design of the primers, the initiation codon in the recipient vectors had to be identified, as to ensure the variable regions were translated in the correct frame. It was determined that base pairs of the EcoRV RE site were not present in frame in the vector (3' of the variable region), and as a result, the primers designed required an extra guanine residue

inserted directly after the EcoRV site, and immediately before the first base of the variable region. The choice of guanine as the base pair was made so that the pre-existing serine animo acid was not altered before the start of the variable region. Similarly, in the construction of the reverse primers (5'), the 6 base pairs composing the NcoI site were identified as not being in frame with the end of the variable regions. In order to keep the constant regions in frame (for both the constant Kappa region and the constant heavy region), an extra cysteine was added directly after the NcoI site, and immediately prior to the reverse complement of the last base pairs of the variable region. This ensured that when the variable region was amplified, the end of the variable region would contain an extra guanine residue at the 5' end of the sequence. The cysteine was chosen in the reverse complement to ensure that when the construct was translated, it would retain the alanine amino acid in the sequence (see also Appendix A).

After the amplification PCR was completed, the products were run on a 1% agarose gel and gel purified (see Figure 3.3 and section 2.3.2). The concentration of the purified PCR product was determined spectrophotometrically (ND-1000 Spectrophotometer), and if the DNA concentrations were below 100ng/μL, the purified product was cloned into pCR2.1 as per section 2.3.3.

2.4.3 Cloning new V-regions into pCR2.1

The PCR reactions completed in section 2.4.2 was run on a 1% agarose gel as outlined in section 2.3.2. Upon visualization with ethidium bromide (EtBr), relevant bands were identified in the 350-400 base pair range, and were excised and purified as per section 2.3.2 followed by cloning into TA vector as per section 2.3.3. Sequencing was carried out as described, using the M13R and T7 primers.

2.4.4 Ligation of anti-ricin mAb V-regions into vectors

Restriction enzyme digestions were accomplished using enzymes and buffers from either New England Biolabs or Fermentas Life Sciences, following the manufacturers' provided protocols. A double enzyme digestion was used to cleave both ends of the insertion sequence, as well as the recipient vector, allowing for ligation of the insertion sequence in the proper orientation. The initial digestion of the variable regions for insertion into p-db vectors was accomplished using EcoRV and NcoI restriction enzymes. Both the TA vector containing the RAC18 variable sequence, as well as the recipient p-db vector were digested along side each other. Cleavage out from the vector (as opposed to a PCR product) ensured that all purified cDNA had both ends cut. One microlitre of calf intestinal alkaline phosphatase (CIAP) was added to the digestion reactions of the recipient vectors, and the vial was incubated at 50°C for 20 minutes to reduce religation of the vector ends. Digestions were analyzed by running reactions on a 1% agarose gel via electrophoresis, and visualized by staining with EtBr and exposure to UV light. The correct sized bands were excised and purified using the QIAquick Gel Extraction Kit as described in 2.3.2. DNA concentrations were determined using the ND-1000 Spectrophotometer. Following the ligation of the RAC18VH into p-dbIgG1 (see section 2.4.4), the p-dbIgG1-RAC18VH vector was used as a PCR template to insert the XhoI site before the IL2ss, and the NheI site after the variable heavy region by PCR primer templated change. The PCR product was gel purified and cloned into TA vector which acted as a shuttle vector. This allowed for the digestion of the TA-cloned IL2ss-RAC18 variable heavy sequence with the XhoI and NheI restriction enzymes in preparation for insertion into pFUSE-CHIg-hG2. Again, this digestion was carried out alongside the recipient vector, pFUSE-CHIg-hG2, then analyzed

and purified as described above. In the final digestion, the p-dbIgG1-RAC18VH and the pINFUSE-hIgG2-Fc2 vectors were double digested with EcoRV and BglII, then analyzed and purified as described above.

Ligation reactions were set up in a total of 20µL. This consisted of 4µL T4 ligation buffer (Invitrogen), 1µL T4 DNA ligase (Invitrogen) and a 3:1 molar ratio of insert to vector. Autoclaved Milli-Q water was used to reach the final 20µL if necessary. Reactions were incubated at 14°C overnight. The following morning, the ligation was precipitated by adding 2µL Mussel glycogen (Invitrogen), 2µL of 3M sodium acetate (Ambion), 44µL of 95% ethanol, and incubated at -80°C for two hours. The reaction was then spun down at full speed in a bench-top centrifuge for 20 minutes at 4°C. Supernatant was carefully discarded, and the pellet was washed two times with 100µL of 70% ethanol, spinning for 5 minutes at 4°C each time. The pellet was then left to dry for one hour in a biosafety cabinet, and resuspended with 8µL autoclaved Milli-Q water. The precipitated vector was then used to transform electro-competent Top10 *E. coli* cells similar to the described method in section 2.3.3, however, in this case, the precipitated vector replaced the PCR product, and the TOPO vector was left out. Following the one hour recovery time, aliquots were dispensed onto LB agar plates containing 25µg/mL Zeocin, and the plates were incubated at 37°C over night. The next day six to ten colonies were picked and subcultured in 3-5mL LB broth with 25µg/mL Zeocin, which were again incubated at 37°C over night. Plasmid DNA was isolated from these cultures and purified as described in section 2.3.3

2.4.5 Analyzing vectors and Sequencing (PCR primer design)

Once purified mammalian expression vectors were obtained, they were screened for variable region inserts by double RE digestions using the respective enzymes that were used in the ligation reactions. For example, screening of the p-db vectors was accomplished by digesting with the EcoRV and NcoI RE.

Furthermore, sequencing primers were designed that flanked the variable regions or would bind to areas in the constant regions. The returned sequencing data ensured that the variable regions had been inserted in the correct orientation, in frame, and without mutations. Primer sequences and descriptions are included as follows:

IgG1CHR	AGATCATGAGGGTGTCCTTG
IgG2CHR	GACTGAAGGTCCTGCCACAG
pFUSER	CACTGCATTCTAGTTGTGG
pFUSEF	CAGATCCAAGCTGTGACCG
phG2CH1R	AACTGTCTTGTCCACCTTGG
phG2CH2R	GGAGATGGTTTTCTCGATGG

2.5 Expression of recombinant mAb in HEK 293F cells

2.5.1 Growth and maintenance of HEK 293F cells

Suspension human embryonic kidney (HEK) FreeStyleTM 293F cells were grown in serum-free FreeStyleTM 293 Expression Media (GIBCO). Cells were grown in Erlenmeyer Polycarbonate Sterile Flasks (VWR) in a shaking incubator at 37°C supplemented with 8% CO2, and shaking at 125 RPM. Cells were monitored and counted using a hemacytometer every 2-3 days, and when a density of 1.5-2.5 x 10^6 cells/mL was reached, cells were passaged into fresh media to a final concentration of 2-3 x 10^5 cells/mL.

2.5.2 Small-scale screening transfection

Transfection of HEK 293F cells was achieved using the 293fectin™ reagent (Invitrogen) following the manufacturer's protocol. Small scale screening transfections were carried out in 6-well cell culture plate in triplicate for each combination of heavy- and light-chain vectors. There were a total of two Kappa chain vectors and two heavy chain vectors, leading to four total combinations as outlined in Table 2.1 (below). Each 6mL transfection required $6.0x10^6$ cells ($1.0x10^6$ cells/mL) to be transfected with 6µg of heavy chain plasmid, and 12µg of light chain plasmid. Plasmids were diluted into a total of 200µL Opti-MEM media (Gibco), while 12µL 293fectin™ was also diluted to 200µL in Opti-MEM media and allowed to incubate at room temperature for 5 minutes. The diluted plasmid DNA preparation was added to the diluted 293fectin™ and incubated for 30 minutes at room temperature. Following this incubation, the 400µL DNA-293fectin™ complexes were added to the fresh suspension of $1.0x10^6$ 293F cells/mL in the 6-well plate. Plates were incubated in a shaking incubator at 37°C supplemented with 8% CO2, and shaking at 125 RPM for 5 days.

Supernatant was harvested by aspirating the contents of each well into a separate 15-mL Falcon tube, followed by a rinse of the well with 3mL phosphate buffered saline (PBS) which was added to the respective tubes. The tubes were then spun in a centrifuge at 3500 RPM for 15 minutes, and the supernatant was decanted into new tubes. Supernatant was stored at 4°C for short term or -20°C for long term storage. This particular procedure was recognized as sub-optimal, but was adequate for the needs of this project.

Table 2.1: Transfection combinations. Combinations of Light and Heavy chain vectors were dual-transfected into HEK 293F cells to express the full length chimeric anti-ricin A-chain mAb.

Transfection	Heavy chain vector	Kappa chain vector
1.1	pFUSE-CHIg-hG2-RAC18VH	pcDNA3.1-RAC18VK
1.2	pFUSE-CHIg-hG2-RAC18VH	p-dbKappa-RAC18VK
2.1	pINFUSE-hIgG2-Fc2-RAC18VH	pcDNA3.1-RAC18VK
2.2	pINFUSE-hIgG2-Fc2-RAC18VH	p-dbKappa-RAC18VK

2.5.3 ELISA screening for rAb production

Transfection supernatant was screened for recombinant antibody (rAb) production via enzyme-linked immunosorbent assay (ELISA). A MaxiSorp 96 well plate (NUNC^{TM}) was coated with 100ng per well of each of the following target antigens: TST10114 (a ricin analogue used to determine functionality of the rAb); goat anti-human Kappa (CK) (Gαhu IgK-CK) specific polyclonal antibody (Southern Biotech) and goat anti-human F(Ab)'2 (Gαhu IgG-F(Ab)'2) specific polyclonal antibody (Jackson ImmunoResearch) were used to confirm expression. Control wells were coated with PBS and 0.4% w/v bovine serum albumin (BSA) (Sigma) in PBS pH7.2. The plate was incubated overnight at 4°C, and then blocked with 0.4% BSA for 2 hours at 37°C. The plate was washed twice with Milli-Q(R) water using the Power Washer 384 (TECAN) automated plate washer. A 2-fold dilution was set up in a round bottom 96 well dilution plate as follows: first 70µL PBS was added to rows B-H, then 70µL of the neat supernatant was added to both rows A and B of the ELISA plate; row B was mixed by pipetting up and down, and 70µL was then transferred down the column, mixing each step. A total of 60µL/well was transferred from the dilution plate to the precoated, blocked ELISA plate. The plate was incubated with Ab for 2 hours at 37°C, followed by washing 8 times with Milli-Q®

water. A 1:2000 dilution of goat anti-human immunoglobulin G heavy chain Fc specific polyclonal antibody conjugated to horseradish peroxidase (Gαhu IgG-γ-HRP) (Jackson ImmunoResearch) was prepared, and 60µL was added to each well, followed by a 1 hour incubation at 37°C. The ELISA plate was then washed another 8 times with Milli-Q® water, and 60µL of 2,2'-azino-bis(3-ethylbenzthiazoline-6-sulphonic acid) (ABTS) substrate (Roche) was added to each well. The plate was incubated at room temperature and color development was monitored by reading the plate at 30 minutes and 60 minutes using the SpectroMax250 Spectrometer (Molecular Devices) set to 405nm. The absorbance readings were recorded with SoftMax Pro 4.6 Software (Molecular Devices), and graphed using GraphPad software.

2.5.4 Large-scale transfection

A large scale transfection of 293 Free Style cells was carried out in a total media volume of 600mL. This required 600µg of heavy chain plasmid and 1200µg of light chain plasmid each to be diluted to 20mL in Opti-MEM media. The heavy chain plasmid dilution was mixed with 1200µL 293fectin™ diluted to 20mL and incubated for 5 minutes at room temperature, while the light chain plasmid dilution was mixed with 3000µL 293fectin™, also diluted to 20mL and incubated for 5 minutes at room temperature. The complexes were allowed to incubate for 30 minutes at room temperature before adding them to $6.0x10^8$ cells. The transiently transfected cells were incubated at 37°C supplemented with 8% CO_2 and were grown to log phase. Cells were then centrifuged at 2095 x g for 15 minutes in the Beckman Coulter Allegra X-12R, and the supernatant was collected. The cells were resuspended in 500mL of fresh FreeStyle™ 293 Expression Media, and incubated a second time with another supernatant harvest.

2.6 Antibody Purification

2.6.1 Concentration of supernatant

The spent supernatant from transfected cells (transfection supernatant) was filter sterilized under negative pressure through a Millipore Stericup with a 0.45µm HV Durapore Membrane, followed by filtration through a Nalgene Surfactant-Free Cellulose Acetate (SFCA) Filter Unit with a 0.2µm filter (Nalgene Corporation). Both hybridoma supernatant (section 2.2.2) and transfection supernatant was concentrated tenfold under positive pressure of N_2 using an Amicon 8000 stirred cell (Millipore) with a 30kDa cut off membrane.

2.6.2 Protein G purification of murine mAb

A 1mL HiTrap Protein G column (GE HealthCare) was equilibrated with 10 column volumes of room temperature Pierce Binding Buffer (pH8.0) (Thermo Scientific). Concentrated hybridoma supernatant was mixed 1:1 v/v with Pierce Binding Buffer and 10-20mL was applied to the column. The flow through was collected and reapplied to the column two more times, followed by a wash of 10 column volumes of Pierce Binding Buffer. Antibody was eluted with 5 column volumes of Pierce Elution Buffer (pH2.8) (Thermo Scientific), and collected in 1mL aliquots in Eppendorff tubes containing 100µL of Pierce Binding Buffer to neutralize the pH. The fractions were analyzed spectrophotometrically at 280nm using the BioRad SmartSpec™ Plus, and all fractions with readings above 0.5 absorbance units were pooled and diluted 1:5 v/v in PBS.

2.6.3 Purification of chimeric mAb

A total of five different trials were conducted to purify the chimeric recombinant antibody from an initial volume of either 6mL or 8mL of tenfold concentrated supernatant. Purification was achieved by using either a 1mL HiTrap Protein A column (GE HealthCare) or a 1mL HiTrap Protein G column. A list of the buffers and columns used is presented in Table 3**.**

Table 2.2: Chimeric mAb purification methods. Five methods were attempted to determine the ideal way to purify chRAC18-huG2.

Trial	Column	Binding Buffer	Elution Buffer	Neutralization Buffer
1	Protein A	PBS pH7.2	0.5M Acetic Acid pH3.0	1.0M Tris-HCl pH8.0
2	Protein A	Pierce Binding Buffer	Pierce Elution Buffer	PBS pH7.2
3	Protein A	PBS pH7.2	Pierce Elution Buffer	PBS pH7.2
4	Protein G	PBS pH7.2	0.01M glycine-HCl pH1.7	9:1 (PBS:Tris-HCl pH8.0)
5	Protein G	Pierce Binding Buffer	Pierce Elution Buffer	9:1 (PBS:Pierce Binding Buffer)

The same method from section 2.6.2 was used for purification except the final neutralization step after elution. In these trials, final eluate was collected in neutralization buffer equivalent to five times the volume of elution buffer. This ratio was determined by ascertaining the pH of the final solution when elution buffer was mixed with neutralization buffer. Samples were not assayed for absorbance, instead, samples immediately underwent buffer exchange as described in section 2.6.4.

2.6.4 Buffer exchange

In order to remove the elution buffer from the purified antibody samples, samples were dialyzed with PBS using Centriprep® Centrifugal Filter Units, Y-30 series (Millipore) which contain a 30kDa cut off membrane. Samples from the column purification were collected in the Centriprep reservoir, and immediately centrifuged for 30 minutes at 1500xg in the Beckman Coulter Allegra X-12R centrifuge. Upon completion of the spin, the sample flowthrough was collected, fresh PBS was added to the centriprep reservoir, and the spin was repeated. This method was repeated until a total of 4 spins was achieved. A final volume of 1-4mL was collected, and stored at -20°C.

2.6.5 Protein determination by bicinchoninic acid assay

Protein concentrations were determined using the bicinchoninic acid (BCA™) Protein Assay Kit (Pierce). A 96-well round bottom plate was used for dilutions of a BSA standard (in triplicate) and unknown samples (in duplicate). Aliquots of 25µL of PBS were added to each well on the plate, except row A which was used for undiluted samples. Column 1 was used as a blank, and no samples were added to that column. Columns 2-4 were used for the standard (2mg/mL) and the remaining columns were used for samples. A total of 50µL of standard and samples were added to their respective wells in row A, and 25µL was transferred to row B. Two-fold dilutions were repeated in this manner down the plate, discarding the final 25µL. The BCA working reagent was made by diluting the provided Reagent B into Reagent A in a 50:1 manner (400µL Reagent B into 20mL Reagent A for a 96-well plate), and 200µL of the working reagent was aliquoted into each well of the plate. The plate was placed on a shaker for one minute, and then incubated for one hour at 37°C. The plate was read at 562nm using the

SpectroMax250 Spectrometer, and absorbance readings were recorded using the SpectroMax Pro software. A standard curve was generated by the software which allowed for the protein concentration determination of the unknown samples. Samples with high protein concentrations were re-assayed in a diluted manner, while samples with low protein concentrations were re-assayed using either a diluted standard, or the microBCA Kit (Pierce).

2.7 Antibody characterization

2.7.1 Denaturing protein gel (SDS-PAGE)

Purified antibody was analyzed for purity using sodium dodecyl sulfate (SDS) polyacrylamide gel electrophoresis (SDS-PAGE). For purified murine mAbs, 5µg of antibody was mixed with denaturing sample buffer (consisting of Laemmli sample buffer with 0.05% B-mercaptoethanol (BME) (BioRad)) to a total volume of 20µL, and was denatured by boiling for 5 minutes at 95°C. Samples were cooled on ice for a further 5 minutes. The entire volume was loaded onto a Criterion 4-20% Tris-HCl gradient gel (BioRad), along with the Kaleidoscope Prestained Standard (BioRad) molecular weight marker. Running buffer was composed of 25mM Tris, 192mM Glycine and 0.1% w/v SDS buffer pH8.3 (BioRad), and the gel was electrophoresed for 55 minutes at 200V. The gel was then removed from the cassette, and excess gel was removed. The gel was stained with Bio-Safe™ Coomassie (BioRad) on a rocking platform for one hour. The gel was destained with Milli-Q water until most of the blue background on the gel was removed. The gel was then analyzed on the Odyssey Infrared Imager (Li-Cor) to acquire digital images.

Purified chimeric antibodies were run with 750ng per lane when analyzed by SDS-PAGE. The gel was processed as above, however the gel was stained with Pierce GelCode® Blue Stain Reagent, and destained with Milli-Q water.

2.7.2 Western Immunoblot

The initial steps of the western immunoblot are as described in section 2.7.1 involving running SDS-PAGE. When the gel cassette was opened, the gel was assembled into the transfer apparatus with an Immobilon-P Polyvinylidene Fluoride (PVDF) membrane (Millipore), and a buffer composed of 20% v/v methanol and 0.15M Tris/Glycine buffer pH8.8 (BioRad). The transfer was allowed to run at 120V for 60-90 minutes. Following transfer, the PVDF membrane was washed three times for five minutes each time, with Tris-buffered Saline (TBS) on a shaking platform. The membrane was blocked overnight at 4°C with 10% skim milk in TBS. The membrane was then washed three times in TBS with 0.05% Tween-20 (Sigma) (TBST) followed by a one hour incubation in a 1:2000 dilution of G α hu IgG-γ-HRP secondary antibody, placed on a shaker. The membrane was washed three more times in TBST, and submersed in Diaminobenzidene (DAB)/Metal substrate (Pierce) until bands developed.

In order to examine antibody-antigen interactions by Western immunoblot, 5µg of antigen was diluted into denaturing sample buffer, and boiled as described in section 2.7.1. Antigens used included TST10114, ricin toxin A-chain, 0.4% BSA and PBS. The antigens were run down the gel, transferred to Immobilon-P PVDF and blocked as described above. The membrane was then incubated in neat supernatant or 1:10 dilution of supernatant for two hours on a shaker. The incubation with secondary antibody and development steps were processed as described above.

Purified murine mAbs were diluted 1:1,000 from a 1mg/mL starting concentration into 10% skim milk. The PVDF membranes were incubated in 10mL of the diluted mAbs as the primary antibody, and the procedure was completed as described above.

2.7.3 ELISA of purified Abs

To compare the relative binding of the purified mAbs to TST10114, an ELISA was set up as described in section 2.5.3. The entire 96-well plate was coated with 100ng per well TST10114 and blocked. Purified anti-ricin mAbs were diluted down the columns in duplicate, starting at either 1mg/mL and diluting 1/2 down the plate, or starting at 10mg/mL and diluting 1/10 down the plate.

2.7.4 mAb affinity determination (BIAcore)

Antibody binding affinities were determined using the BIACore 2000 unit, with a CM5 (carboxymethyl cellulose) chip and HBS-P buffer (BIACore) for dilutions. The flow rate of buffers and samples was set to 5µL/minute.

First, a flow cell of the CM5 chip was coated with the antigen TST10114 in the following manner. A new CM5 chip was docked into the BIACore 2000. A 'prime' command was run twice to prime the tubing with room temperature HBS-P buffer. The actual coating consisted of four steps: activation; coating; blocking; and scrubbing. First, the parameters of the software were set to 25°C with a single detection mode, using flow cell 1 with a flow rate of 5µL/minute. The chip was activated with 20µL of a 1:1 mixture of EDC:NHS (BIACore) using the KINJECT command, with ExtraClean. Coating involved the command QUICKINJECT, with 35µL of a 1:5 dilution of 1mg/mL TST10114 in 10mM sodium acetate buffer (pH4.0) (BIACore). The

chip was blocked with a 35µL QUICKINJECT (ExtraClean) of 1.0M ethanolamine (BIACore). Finally, the chip was scrubbed with a 15µL QINJECT of 100mM hydrochloric acid.

Antibody samples were diluted into HBS-P buffer, and placed in 0.2mL BIACore tubes. A total of four to eight dilutions were prepared per sample. Tubes were placed in the BIACore rack, along with a tube of glycine-HCl (pH1.5) (BIACore) which was used to regenerate the chip after each sample analysis. The following program was written to analyze samples in an automated fashion:

```
DEFINE      LOOP  dilutions
        LPARAM      %volume             %position
        TIMES       1
                    15                  r1a1
                    13                  r1a2
                    10                  r1a3
                    8                   r1a4
                    5                   r1a5
END

DEFINE      APROG antiricin
        PARAM %volume %position
        KEYWORD  dilution %volume
        FLOW 5                                      !sets flow to 5ul/min
 1:00   KINJECT %position  40  1200                 !inject 40ul of sample
20:00   INJECT r1b1   35                            !injects 35ul glycine
END

MAIN                                                !run program using the
                                                     LOOP block
        FLOWCELL 2
        LOOP dilutions STEP
                APROG antiricin %volume %position
        ENDLOOP
        APPEND continue
END
```

2.7.5 Determination of epitope specificity inferred via cELISA

A 96-well plate was coated with 100ng TST10114 per well overnight at 4°C and blocked as described in section 2.5.3. To examine if the murine IgG1 RAC18 competed with the chimeric IgG2 RAC18, mixtures of the two antibodies were prepared by altering the amount of each antibody depending on the competing antibody. For the murine competition, 50ng of chimeric RAC18 was mixed with amounts of murine RAC18 varying from 10ng to 100ng. The chimeric competition used the opposite; 50ng of murine RAC18 was mixed with the same range of chimeric RAC18. Each mixture was brought up to a final volume of 60µL with 0.4% BSA, and aliquoted onto the plate, in duplicate for each mixture. The plate was incubated and washed as described above.

For the secondary antibody, each murine competition and chimeric competition were detected with G α mouseIgG-HRP and G α humanIgG-HRP respectively, using previously described dilutions of secondaries. The remainder of the test was completed as described in section 2.5.3.

3 Results

3.1 Isolation of mAb variable regions

Complementary DNA was successfully created from the isolated mRNA of the hybridomas. From this cDNA template, the variable region coding DNA was isolated using mouse specific primers. Primer combinations that amplified the variable regions are presented in Table 4 (see section 2.3.2 for primer sequences).

Table 3.1: Primer combinations that were successful in amplifying the variable regions from the cDNA of the six hybridoma lines.

mAb	Variable Heavy		Variable Light	
	5'	**3'**	**5'**	**3'**
TFTA1	UmIgVH; MHC1	MG1-3Seq; Sheriff IgG 3'	MVL; Sheriff Kappa 5'	MKC1; Sheriff Kappa 3'
RAC14	MHC1	MG1-3Seq	GeneRacer 5'	Sheriff Kappa 3'
RAC18	UmIgVH; MHC1	MG1-3Seq	GeneRacer 5'	Sheriff Kappa 3'
TFTB1	UmIgVH; Sheriff IgG 5'; MHcL-3; MHC1	MG1-3Seq; Sheriff IgG 3'	MVL; Sheriff Kappa 5'	MKC1; Sheriff Kappa 3'
RBC7	UmIgVH	MG1-3Seq; Sheriff IgG 3'	MVL	Sheriff Kappa 3'
RBC11	UmIgVH; MHC1	MG1-3Seq	MVL; Sheriff Kappa 5'	IgKappa; MKC1; Sheriff Kappa 3'

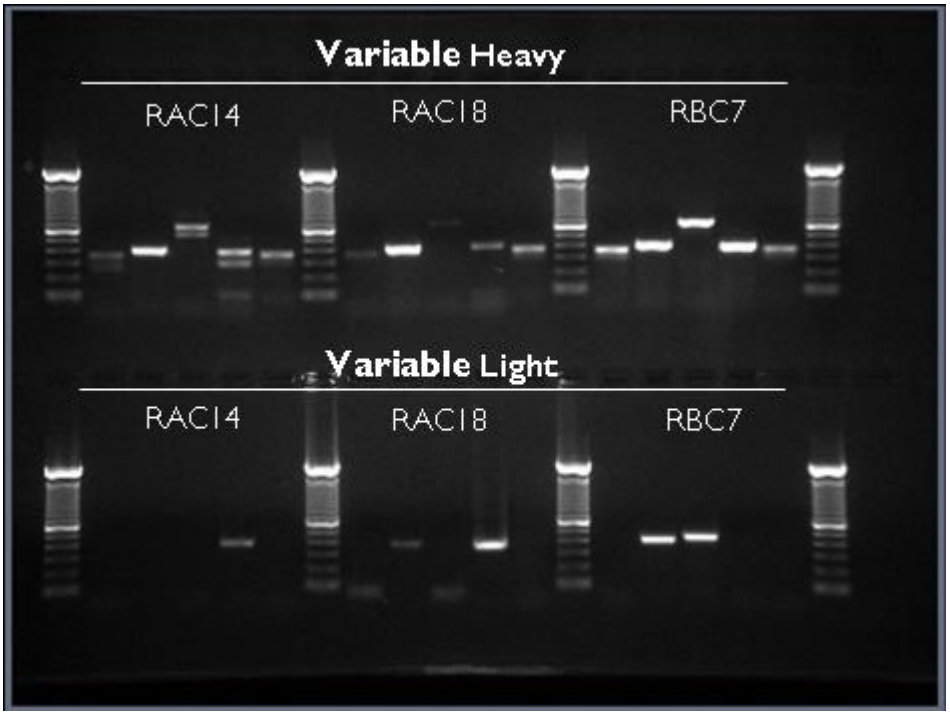

Figure 3.1: Attempted PCR amplification of RAC14, RAC18 and RBC7 mAbs variable heavy (top) and variable light (bottom) regions. The expected length of the variable regions is 350-400 nucleotides. Ladder is 100bp.

Bands in the 350-400 nucleotide region from the gel depicted in Figure 3 were excised, purified and cloned into pCR2.1 for DNA sequencing. Sequence data was analyzed by comparing the returned sequences with known mouse variable region sequences catalogued with the International Immunogenetics Information System® V-Quest. Any isolated aberrant variable regions could be discarded in this manner. The variable region sequence for RAC18 is as follows (5' – 3') (the variable region sequences of the remaining 5 mAbs can be seen in Appendix B, while the amino acid translation of RAC18 is seen in Appendix C):

RAC18
VH (1-357)
GAGGTGCAGCTGGAGGAGTCTGGACCTGTGCTGGTGAAGCCTGGGGCTTCAGTGAAGATGTCCTGTA
AGGCTTCTGGATACACGTTCACTGACTACTATGTGAACTGGGTGAAGCAGAGCCGTGGAAAGAGCCT
TGAGTGGCTTGGACTTATTATTCCTTCCAACGGTGGTACTACCTACAACCAGAAGTTCAGGGGCAAG
GCCACATTGACTGTTGACAAGTCCTCCAGCACAGCCTACATGGAACTCAACAGCCTGACATCTGAGG

```
ACTCTGCAGTCTATTACTGTGCAAGACGGGGCCTAACTGGGGCCCTCTTTGCTTACTGGGGCCAAGG
GACTCTGGTCACTGTCTCTGCA

VK (1-318)
GACATCCAGATGACACAGTCTCCATCCTCACTGTCTGCATCTCTGGGAGGCAAAGTCACCATCACTT
GCAAGGCAAGCCAAGACATTAACAAATATATAGCTTGGTACCAACACAAGGCTGGAAAAGGTCCTAG
GCTGATCATGCATTACACATCTACATTACAGCCAGGCATCCCATCAAGGTTCAGTGGAAGTGGGTCT
GGGAGAGATTATTCCTTCAGCATCATCAACCTGGAGCCTGAAGATATTGGAACTTATTATTGTCTAC
AGTATGATAATCTGTGGACGTTCGGTGGAGGCACCAAGCTGGAAATCAAA
```

The nucleotide sequences and amino acid sequences were aligned, and analyzed for any similarities/differences using MacVector software, an example of which is presented below in Figure 3.2.

```
 A.
                  <---------FR1------------>      <------FR2------>   <-
mTFTB1 VK      1 KLVMTQSPSYLAASPGETITINCRASKSINKYLAWYQEKPGKTNKLLIYSGSTL
mRBC7  VK      1 ELVMTQSPASLSASVGETVTITCRVSENIDSYLAWYQQKQGKSPQLLVYATTLL
                  *******. *.** ***.**.** *  *  ******.* **. .**.*. . *

                  ---------FR3---------------------->
mTFTB1 VK         QSGIPSRFSGSGSGTDFTLTISSLEPEDFAMYYCQQHNEYPWTFGGGTKLEIK 107
mRBC7  VK         ADGVPSRFSGSGSGTQYSLKINSLQSEDVARYFCQHYYSLPFTFGTGTKLEIK 107
                    *.*********** ..* * **. ** * *.**.    * *** *******

 B.
              <--------FR1------------>       <------FR2------->          <-----
mTFTB1 VH  1 EVQLEESGGGLVQPGGSRKLSCAASGFTFSSFGMHWVRQAPEKGLEWVAYISSGSS--TLHYADTV
mRBC7  VH  1 EVQLEESGGGLVQPGSSLSLSCAASGFTFTDYYMSWVRQPPGKALEWLGFIRNKANGYTTEYSASV
              *************** *  **********. . * **** * * ***. .*    .   *  *. .*

              -----FR3----------------------->
mTFTB1 VH    KGRFTISRDNPKNTLFLQMTSLRSEDTAMYYCAR-----WGNYPHYAMDYWGQGTSVTVSS 120
mRBC7  VH    KGRFTISRDNSQSILYLQMNALRAEDSATYYCARSASYYYGTSSYWYFDVWGTGTTVTVSS 127
              ********** .  *.***..**.**.* *****      *.      * ** **.*****
```

Figure 3.2: Amino acid sequence comparison of the (**A**.) VL regions and (**B**.) VH regions of two anti-ricin B-chain mAbs isolated from murine cDNA. Complementarity determining regions are colored, red for CDR1, blue for CDR2 and green for CDR3. As expected, framework regions exhibit similarities, while CDRs are variable. A '*****' indicates homology, '**.**' indicates a conserved substitution.

3.2 Chimeric Ab development

3.2.1 Insertion of restriction enzyme sites

The pcDNA3.1-RAC18VK vector was supplied by Dr. Seth Pincus, and upon receipt, the variable region and the constant Kappa region were sequenced and shown to be an exact match with the regions isolated in section 3.1. No further modifications were made to this vector prior to transfection.

To prepare for ligation into the p-db expression vectors, the EcoRV RE site (3') and NcoI RE site (5') were successfully introduced flanking the variable regions via PCR (see section 2.4.2 for primer sequences). The sites were introduced in such a manner as to retain the reading frame in relation to the initiation codon of the recipient vector.

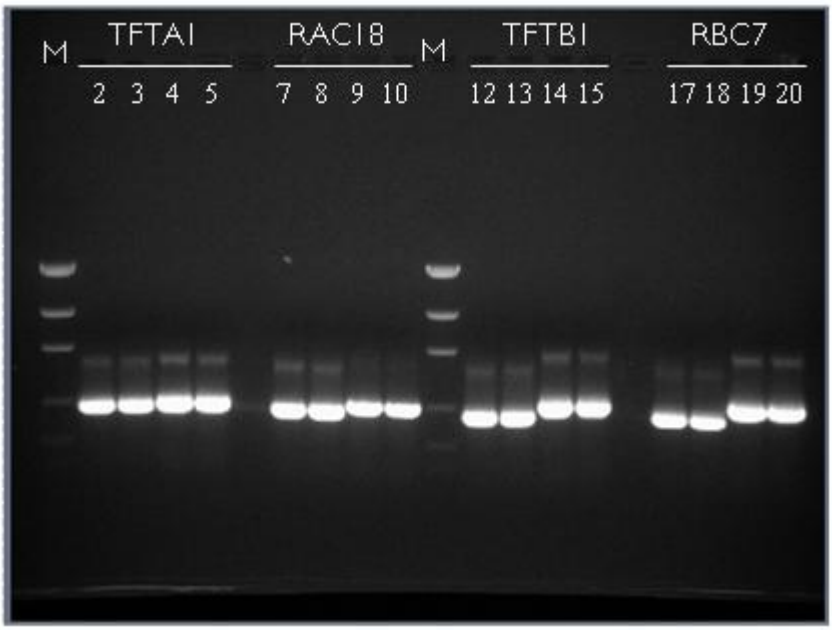

Figure 3.3: Agarose gel electrophoresed with the PCR products to insert the EcoRV and NcoI RE sites before and after the variable heavy and variable light chains. Lanes marked M are low molecular weight ladder. Variable region PCR products are seen in duplicate, starting with TFTA1 VK (lanes 2 and 3), TFTA1 VH (lanes 4 and 5), RAC18 VK (lanes 7 and 8), RAC18 VH (lanes 9 and 10), TFTB1 VK (lanes 12 and 13), TFTB1 VH (lanes 14 and 15), RBC7 VK (lanes 17 and 18), and RBC7 VH (lanes 19 and 20). The expected length of the variable domains is seen brightly at approximately 350 - 400bp. Visualization is with EtBr and UV illumination.

Once inserted into the p-db vectors, RAC18 sequences were manipulated into the IgG2 expression vectors pFUSE-CHIg-hG2 and pINFUSE-hIgG2-Fc2. Using the primers designed (section 2.4.2) and PCR, the XhoI RE site was inserted before the IL2ss and and the NheI RE sites was inserted after the VH region using p-dbIgG1-RAC18VH as the template. The XhoI site was inserted 3' of the initiation codon of IL2ss, and thus did not require additional base pair insertions to retain the reading frame. The NheI site in the pFUSE-CHIg-hG2 was already present such that there would be no alteration of the reading frame during primer design. As a result, this did not warrant the necessity for any extraneous base pair introductions. After the PCR was completed to introduce the XhoI and NheI RE sites, the reaction was visualized after running the products on a 1% agarose gel. The relevant bands (~400bp) were gel purified. If the purified PCR product exhibited low DNA concentration, the PCR products were cloned into pCR2.1, grown and purified as per section 2.3.3.

No modifications were necessary for insertion into pINFUSE-hIgG2-Fc2 from the p-dbIgG1-RAC18 template. A double digestion of EcoRV and BglII would ensure that the RAC18VH region would be inserted into the pINFUSE vector in frame immediately 5' of the IL2ss, and the CH1 region would be inserted in frame directly 5' of the hinge region.

3.2.2 Ligation into vectors

A double restriction enzyme digestion of the modified variable regions (the 'donor' region) alongside a double digestion of the recipient vector was performed as per section 2.4.4. Preparation of the variable regions for insertion into the p-db vectors was accomplished with the EcoRV and NcoI enzymes. As seen in Figure 3.2*A*, lanes 1 and 2 are the products of a double digestion of the amplified RAC18 VK with flanking RE sties, while lanes 3 and 4 are the same

double digestion of the recipient p-dbKappa vector (the 'open' vector). The variable Kappa region is seen at the expected size of approximately 350 bp, and the resident variable Kappa region that was digested out of the p-dbKappa vector is also seen at approximately 350bp.

After insertion into p-db vectors, the XhoI RE site was successfully inserted before the IL2ss, and the NheI RE site was inserted after the RAC18 variable heavy region (section 2.4.4). The PCR product seen at approximately 400bp was gel purified and tested for DNA concentration. The purified PCR product was double digested alongside the pFUSE-CHIg-hG2 with the restriction enzymes XhoI and NheI. Side-by-side double digestion (EcoRV and BglII) of the p-dbIgG1-RAC18VH vector and the pINFUSE vector is seen in Figure 3.4*B*, and the bands were gel purified in preparation for the ensuing ligation reaction.

The relevant bands seen in the agarose gel of the double restriction enzyme digestions were gel purified and tested for DNA concentration. A ligation reaction was set up according to 2.4.4. Once the ligation was precipitated, the vector was transformed into TOP10 *E. coli* cells, purified and screened for insert. Vectors that exhibited a RE double digested band of the expected length were sent for sequencing (see section 2.4.5). Figure 3.4*C* shows the screening of five p-dbKappa-RAC18VK vectors (lanes 1-5) and five p-dbIgG1-RAC18VH vectors (lanes 7-11) digested with EcoRV and NcoI, as well as undigested vectors (Kappa in lane 6 and heavy chain in lane 12).

Analysis of the sequencing data was performed to ensure that all the variable and constant regions still retained the correct sequences, in the correct direction and for reading frame.

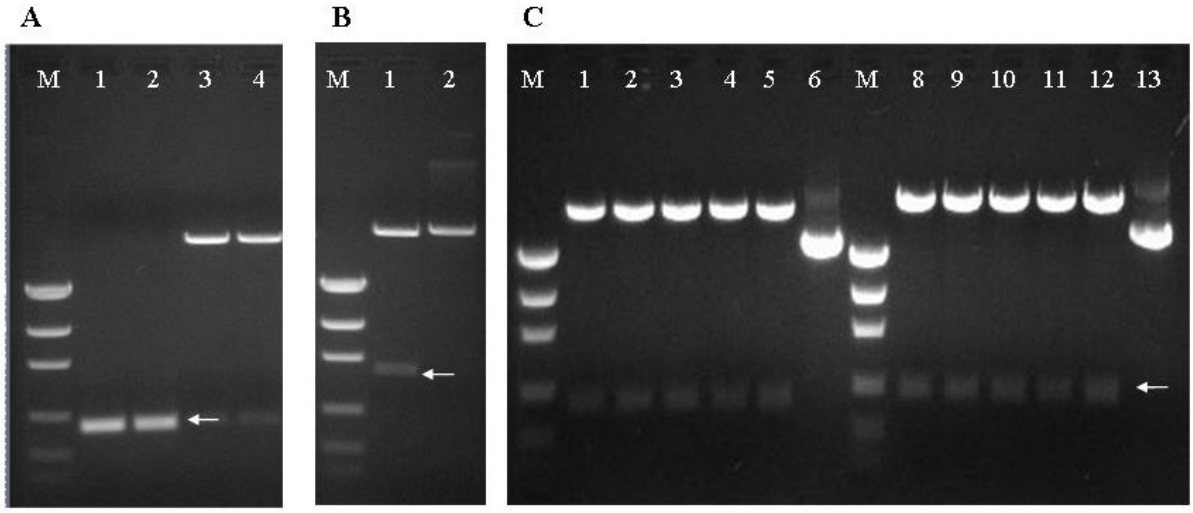

Figure 3.4: Analytical gel of V gene inserts and vectors. (**A**) In preparation for ligation, purified RAC18VK (lanes 1-2) and pdbKappa (lanes 3-4) were double digested with EcoRV and NcoI (each run in duplicate). The arrow indicates RAC18VK, which is seen next to the variable Kappa region that was digested out of pdbKappa. (**B**) Setting up a ligation to introduce the RAC18VH-CH1 sequence into pINFUSE-CHIgG2-Fc2 with an EcoRV and BglII double digestion. RAC18VH-CH1 was digested out of pdbIgG1-RAC18VH (lane 1), and pINFUSE-CHIgG2-Fc2 (lane 2) was digested in preparation to receive the RAC18VH-CH1 region. (**C**) Screening the RAC18 variable sequences in p-dbKappa (lanes 1-6) and p-dbIgG1 (lanes 7-13). Five plasmids of each were double digested with EcoRV and NcoI followed by an undigested plasmid.

3.3 Expression of rAb in HEK 293F cells

3.3.1 ELISA screening of transfection supernatant

The first tests of HEK 293F transfections were to assess the efficacy of different combinations of the vectors. The four total combinations of heavy and light chain vectors are outlined in table 2.1. The supernatant was harvested at 5 days post transfection and normalized to a total volume of 9mL. An initial screening ELISA was performed with the harvested supernatant as described in section 2.5.3, and the results are seen in Figure 3.5*A*. It was noted that the supernatants did not exhibit a very strong response against TST10114, but the response measured with Gαhu IgK-CK and Gαhu IgG-F(Ab)'2 were strong. This is likely due to the

nature of the test – the ricin analogue TST10114 offers a single epitope to the mAb, while the expression enzyme immunoassay (to detect fully formed mAbs) is based on a polyclonal capture and detection, therefore offering more epitope recognition. Another ELISA was attempted on the collected fractions and the results of this second ELISA are presented in Figure 3.5*B*. The addition of ricin toxin A-chain (RTA) was another control to monitor the binding of the chimeric antibodies to the intact toxic A-chain. The results demonstrate that both VH and VL are expressed and the resulting Abs have the ability to bind to the TST10114 surrogate ricin.

A

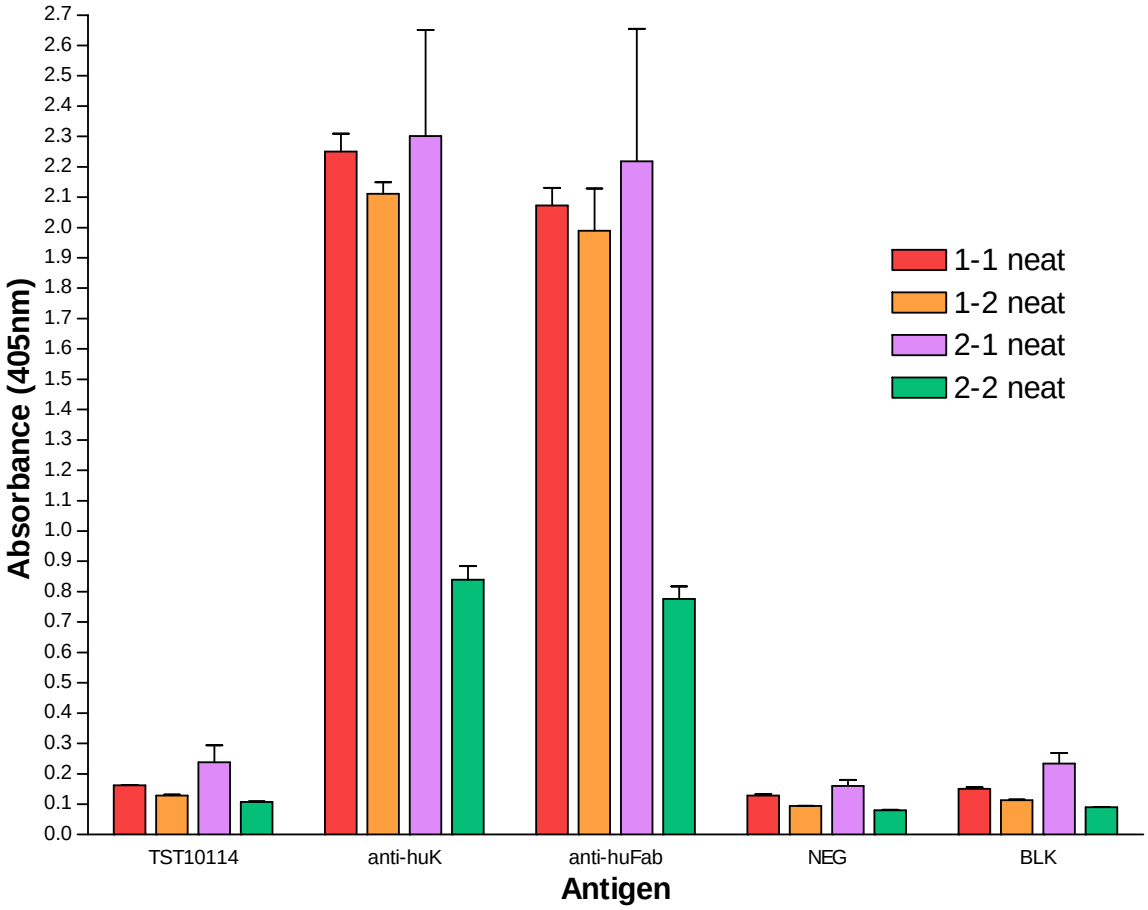

(see description on next page)

B

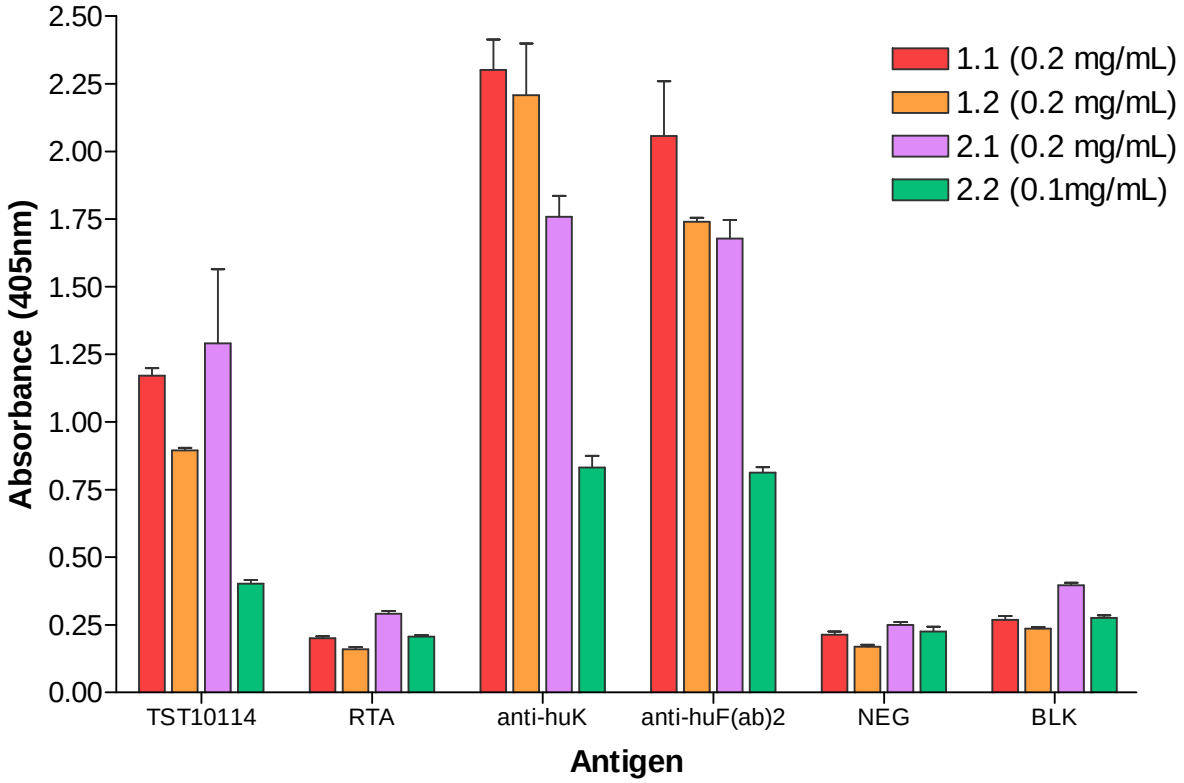

Figure 3.5: (**A.**) ELISA screening for recombinant mAbs of the supernatants from 293 transfections (neat). (**B.**) ELISA screening of the four transfection supernatants (normalized total protein concentrations). RTA is Ricin toxin A-chain; negative is 0.4% BSA:PBS; blank is PBS. Transfection combinations of VH and VL (respectively) as follows (see also section 2.5.2 and 2.5.3)
1.1 pFUSE-CHIg-hG2-RAC18VH and pcDNA3.1-RAC18VK
1.2 pFUSE-CHIg-hG2-RAC18VH and p-dbKappa-RAC18VK
2.1 pINFUSE-hIgG2-Fc2-RAC18VH and pcDNA3.1-RAC18VK
2.2 pINFUSE-hIgG2-Fc2-RAC18VH and p-dbKappa-RAC18VK

3.3.2 Large scale transfection for chimeric Ab expression

Based on ELISA data obtained in section 3.3.1, the transfection combination 2.1 was chosen for large scale transfection, with the heavy chain vector pINFUSE-hIgG2-Fc2-RAC18VH and the light chain vector pcDNA3.1-RAC18VK (see section 2.5.2 and 2.5.4).

3.4 Antibody purification

3.4.1 Chimeric antibody purification

The supernatant was concentrated as described in section 2.6.1. Aliquots taken at each step demonstrated that the chimeric Ab was not lost during these processes (data not presented).

In the purification of the chimeric antibody, five different buffer sets were tested (as described in Table 2.2 (section 2.6.3). Following a buffer exchange step, the concentration of purified chimeric Ab was determined by a microBCA analysis, and is presented in Table 3.2.

Table 3.2: Concentration of purified antibody achieved through five different purification trials. Known volumes of concentrated supernatant (6 or 8mLs) were purified. Collected volume was recorded and compared to the concentration of purified mAb (determined by microBCA) to determine the overall amount of mAb that was purified based on the starting volume.

Trial	Column	Binding Buffer	Elution Buffer	Purified Ab (per starting volume)
1	Protein A	PBS pH7.2	0.5M Acetic Acid pH3.0	18.4ug/mL
2	Protein A	Pierce Binding Buffer	Pierce Elution Buffer	1.55ug/mL
3	Protein A	PBS pH7.2	Pierce Elution Buffer	1.24ug/mL
4	Protein G	PBS pH7.2	0.01M glycine-HCl pH1.7	1.28ug/mL
5	Protein G	Pierce Binding Buffer	Pierce Elution Buffer	11.4ug/mL

Although it is evident that the total amount of antibody purified was less than ideal, trial 1 and trial 5 proved to be the most efficient in terms of quantity obtained. The purified mAb was compared by PAGE, as described in 2.7.1, and the results are presented below in Figure 3.6.

3.5 Antibody characterization

3.5.1 Denaturing protein gel (SDS-PAGE)

Purified murine and chimeric mAbs were analyzed by PAGE, and stained with Bio-Safe Coomassie. In the case of murine antibodies, 5ug of purified mAb was denatured and applied per lane.

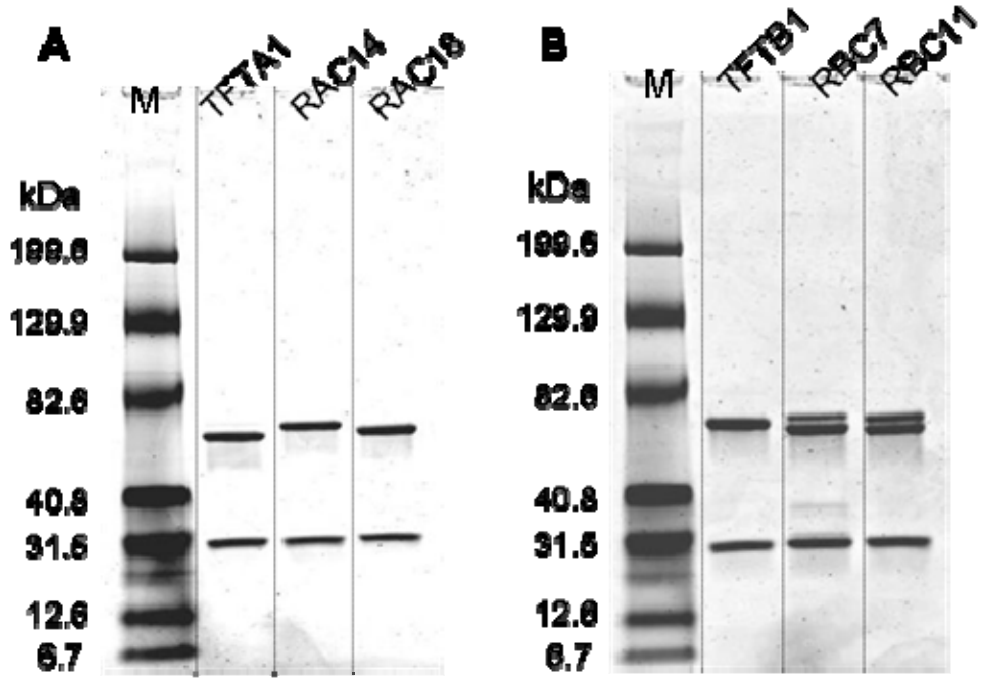

Figure 3.6: SDS-PAGE analysis of purified murine anti-ricin mAbs. Antibodies were processed and analyzed under denaturing conditions (5µg/lane). (**A**.) Shows the anti-RTA mAbs, and (**B**.) represents the anti-RTB mAbs.

During the purification trials, Trial 1 and Trial 5 purified mAbs were analyzed by SDS-PAGE (the mAb yield from Trials 2, 3 and 4 were too low for analysis, and SDS-Page analysis was not completed for these three trials). The purified concentrations were much lower in the chimeric mAb preparations compared to hybridoma yields (750ng of purified chRAC18-huG2 as opposed to 5µg in the murine analysis). The results in Figure 3.7 show the comparison of the

chimeric mAbs in trials 1 and 5. The gel clearly shows both an antibody light chain (~25kDa) and heavy chain (~50kDa), with some non-specific contaminating proteins. The mAb from Trial 1 showed the least contamination and higher yield, and this purification method was chosen to purify the remainder of the supernatant.

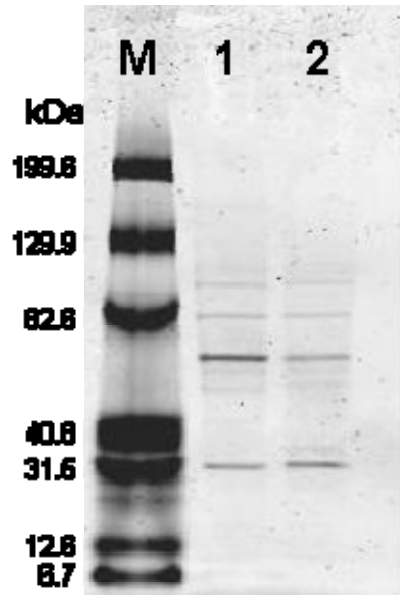

Figure 3.7: Denaturing SDS-PAGE of the chimeric mAb purified by trial 1 (lane 1) or trial 5 (lane 2) as described in table 2 (section 2.6.3). A total of 750ng of rAb was loaded per lane. Trials 2, 3, and 4 not analyzed.

3.5.2 Western Immunoblot

The Western blots presented in Figure 3.8 clearly support the statement that TST10114 is a good surrogate antigen for ricin as it is recognized by anti-ricin A-chain mAbs as well as anti-ricin B-chain mAbs.

The low yield of the purification trials made it necessary to use supernatant from 293 transfected cells with chRAC18-huG2 to perform a Western analysis (Figure 3.9). The chimeric mAb was tested for binding to TST10114, a negative (0.4% BSA) and a blank (PBS).

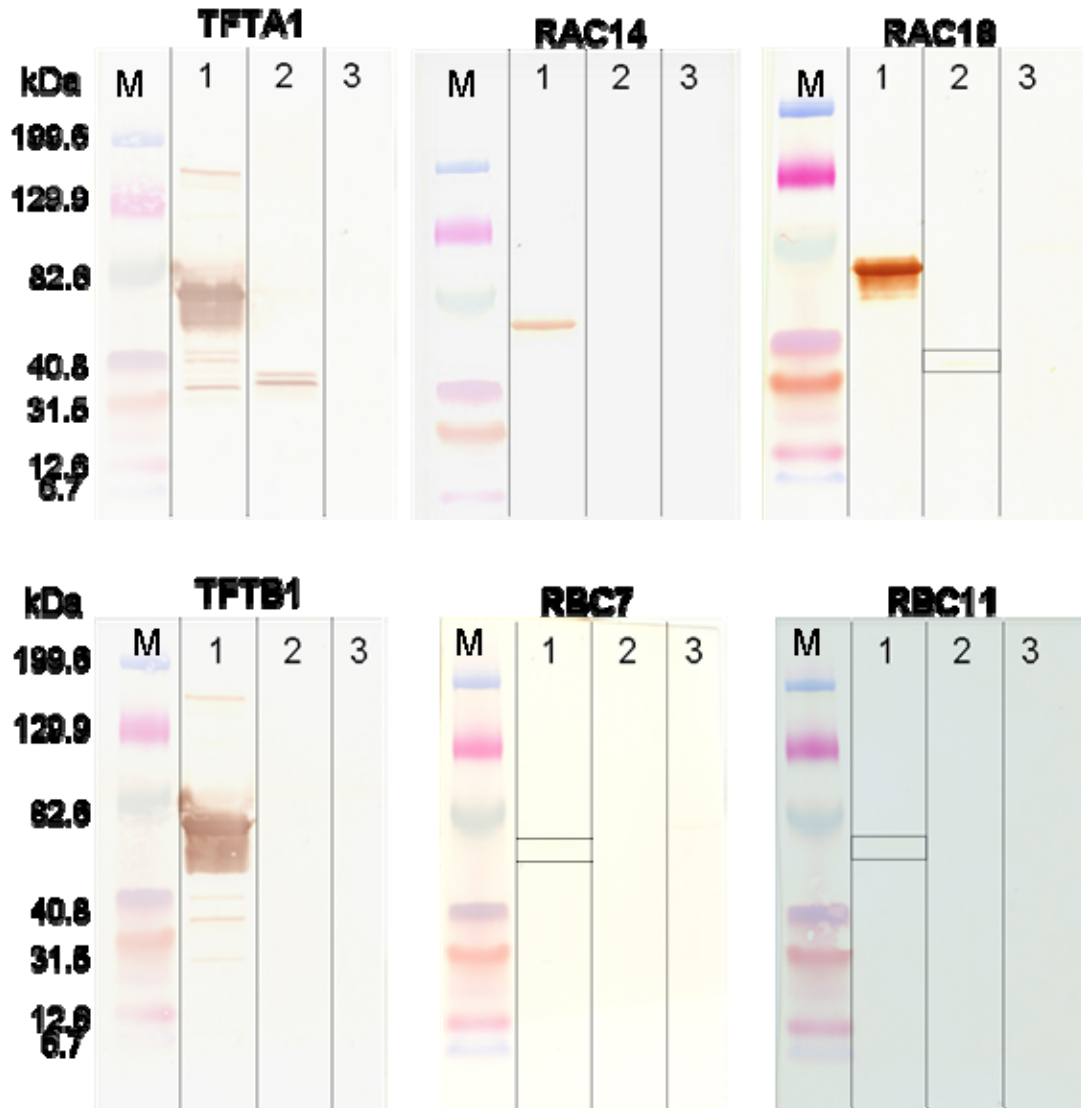

Figure 3.8: Western immunoblot testing the murine mAbs for binding activity against TST10114 (lane 1), RTA (lane 2) and a BSA negative (lane 3) boiled at 95°C for 5 minutes with β-mercaptoethanol. Starting from a 1mg/mL stock, purified murine mAbs were diluted 1:1,000 into 10mls skim milk. The PVDF membrane was allowed to incubate in the diluted mAb (primary antibody) for 1 hour. Detection of mAb binding was visualized with anti-mouseIgGFcγ and developed with DAB Metal substrate. 'M' represents a prestained ladder. Boxes indicate colorimetric devlopment that either faded quickly or were not captured electronically.

Testing the chimeric chRAC18-huG2 by immunoblot yielded similar results, with binding evident against TST10114 (Figure 3.9). The band indicating chRAC18-G2 binding to TST10114 was less intense than the signal seen from the murine RAC18. This disparity between

detection from the murine and chimeric mAbs was also evident from the ELISA on the supernatant harvest of the HEK293F transfections (Figure 3.12). It is not entirely clear why the signal responses were weaker, however it may be due to the binding nature of the anti-huIgG2-HRP secondary. The response from anti-huIgGFcγ-HRP seen in Figure 3.12(A.) is much greater than the response from the IgG2-specific secondary, leading to the indication the anti-huIgG2-HRP is a weakly performing detection antibody.

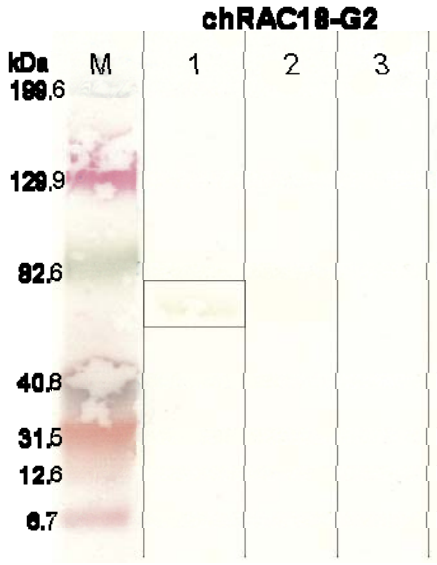

Figure 3.9: Western Immunoassay. The chimeric RAC18-G2 was tested for binding to TST10114 (lane 1), a BSA negative (lane 2) and a PBS blank (lane 3) (boiled at 95°C for 5 minutes with β-mercaptoethanol) by allowing the PVDF to incubate in transfection supernatant for 1 hour. Detection was with anti-huIgG2-HRP. 'M' represents a prestained ladder. The boxed area indicates a colorimetric development that was not captured electronically.

3.5.3 ELISA

The murine anti-ricin mAbs were tested for relative binding to both TST10114 and, in the case of anti-ricin A-chain mAbs, binding to ricin toxin A-chain (RTA) as well. The chimeric chRAC18-huG2 was tested against TST10114, anti-huκ, anti-huFcγ, a 0.4% BSA negative and a

PBS blank. Detection of the chimeric antibody was accomplished with both anti-huIgGFcγ-HRP and the human IgG2 isotype specific anti-huIgG2-HRP.

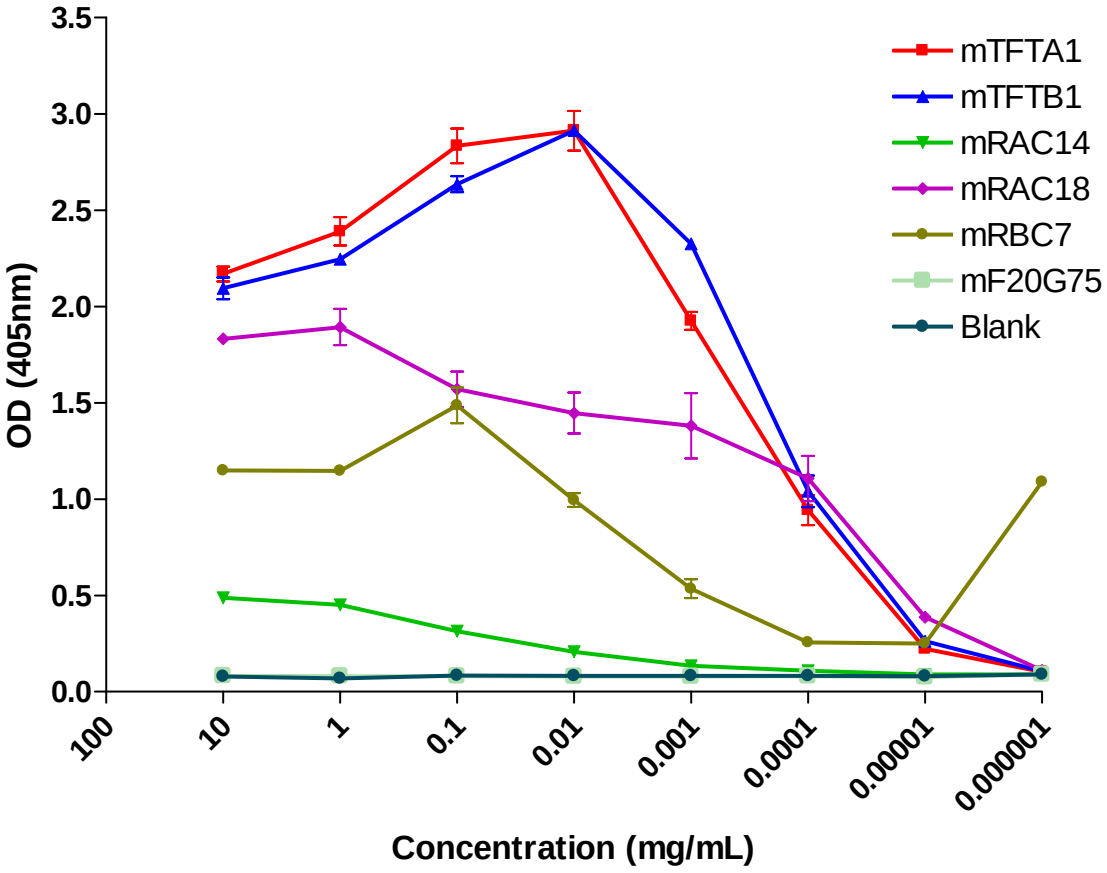

Figure 3.10: Reactivity of murine mAbs with TST10114 via ELISA. Binding is demonstrated to be concentration dependant. TST10114 was coated on a 96-well plate, and detection was achieved with goat anti-mouse IgG-HRP. Data represents trends seen in triplicate analysis.

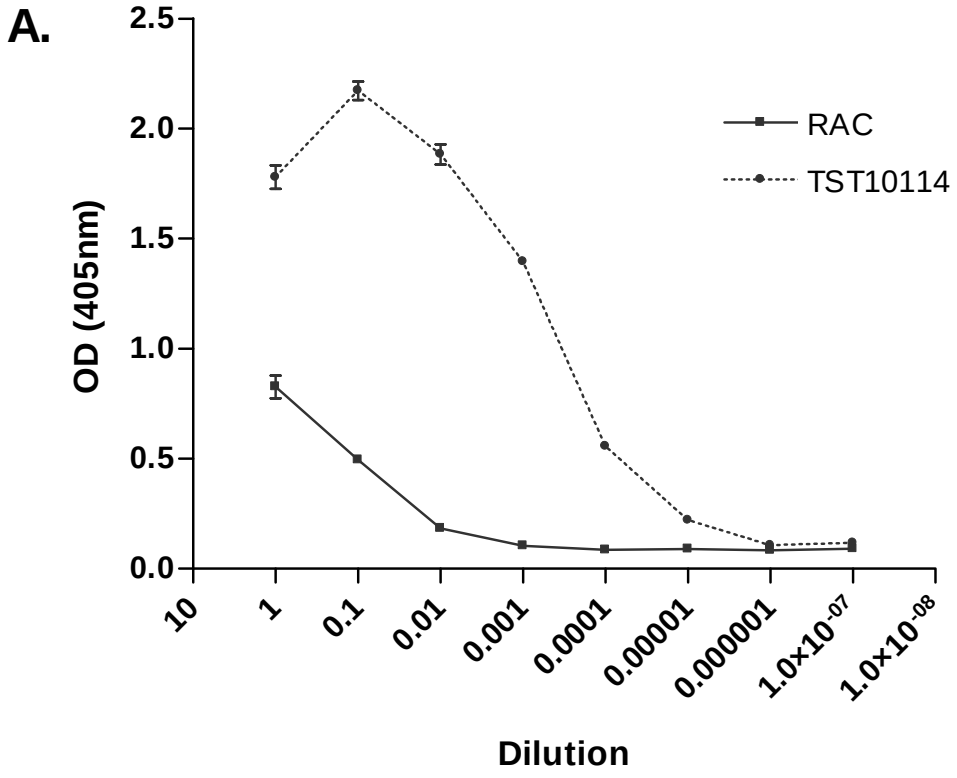
A.
2.5
2.0
1.5
1.0
0.5
0.0
OD (405nm)
RAC
TST10114
10
1
0.1
0.01
0.001
0.0001
0.00001
0.000001
1.0×10-07
1.0×10-08
Dilution

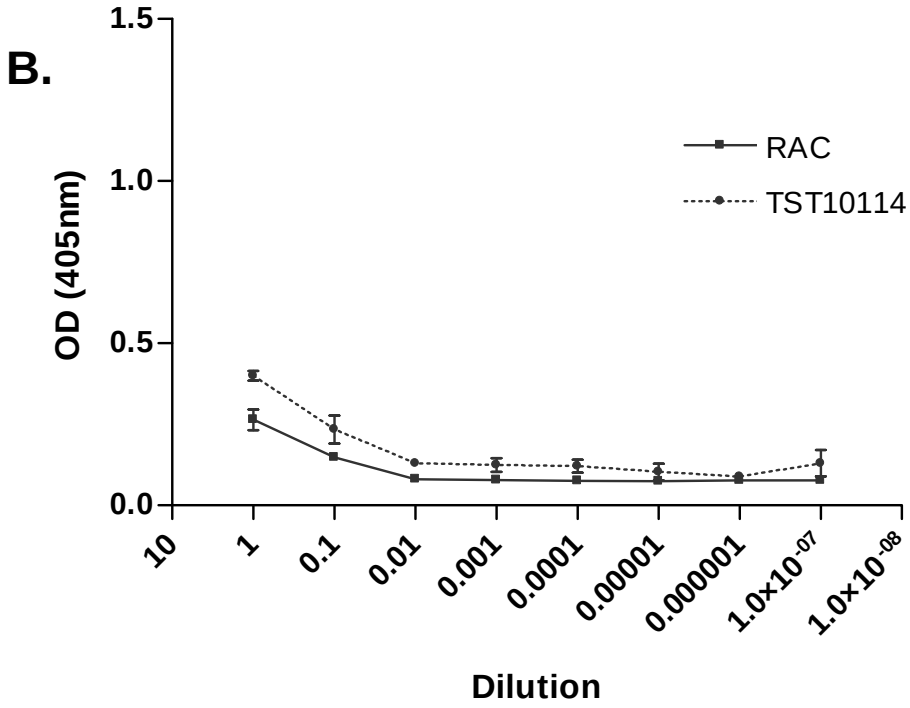
B.
1.5
1.0
0.5
0.0
OD (405nm)
RAC
TST10114
10
1
0.1
0.01
0.001
0.0001
0.00001
0.000001
1.0×10-07
1.0×10-08
Dilution

(continues)

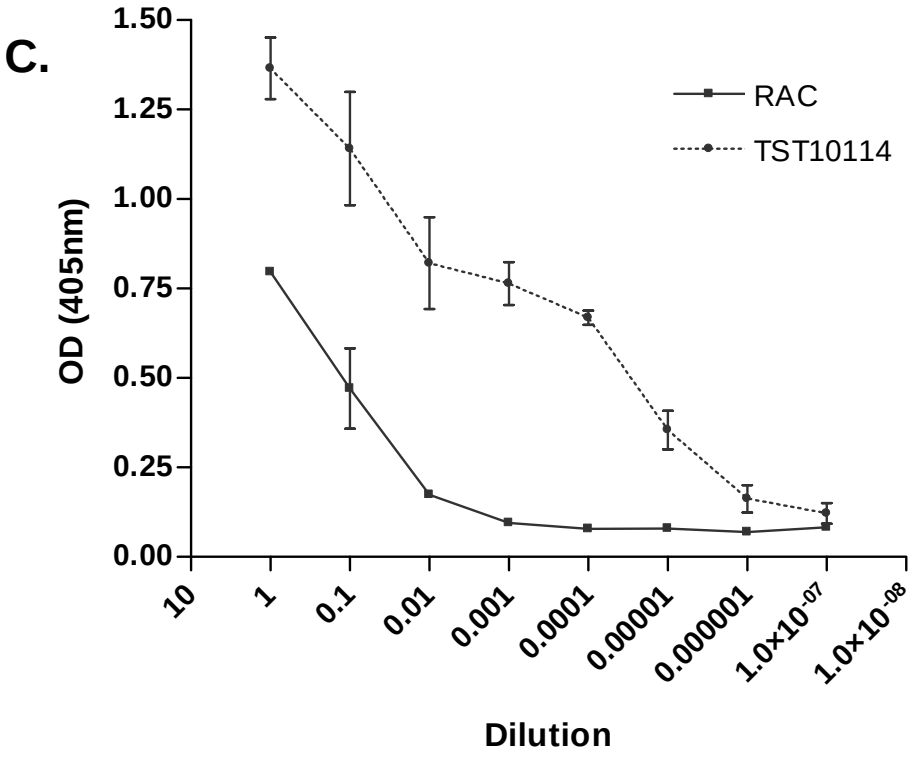

Figure 3.11: Reactivity of murine anti-ricin A-chain mAbs with ricin A-chain (RAC) and TST10114 via ELISA. The three mAbs, **(A)** TFTA1; **(B)** RAC14; and **(C)** RAC18 were assayed in a dilution series. Detection was achieved with goat anti-mouse IgG-HRP. Solid line depicts binding response againse ricin A-chain; dashed line depicts binding response against TST10114. Data represents trends seen in duplicate analysis.

A.

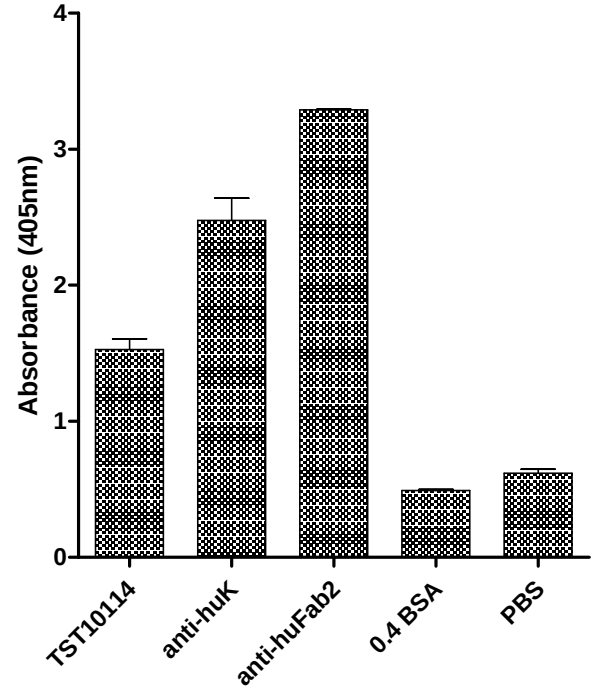

B.

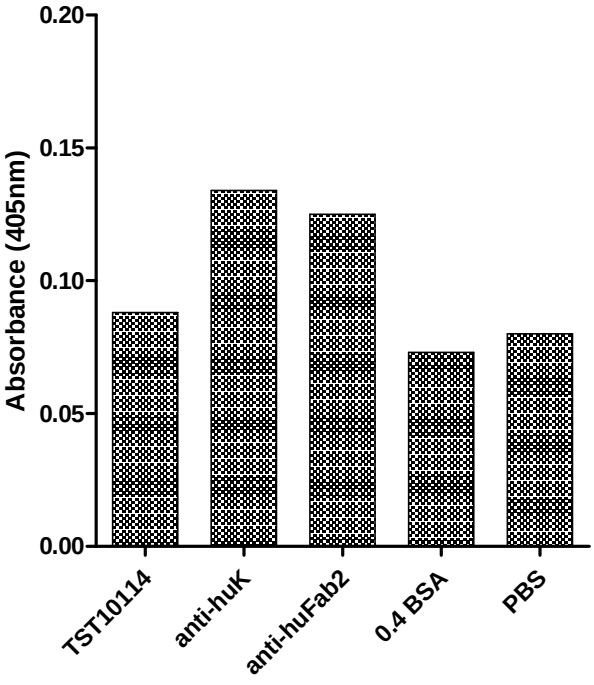

Figure 3.12: ELISA on the mAb supernatant harvested at 5 days post transfection. Detection (secondary antibody) is (**A**.) anti-huIgGFcγ-HRP and (**B**.) anti-huIgG2-HRP.

3.5.4 Affinity determination (BIAcore)

The use of the BIACore-2000 was invaluable in the determination of the individual affinities of the mAbs against the ricin surrogate TST10114. Coating TST10114 onto the surface of the CM5-chip involves four steps as seen in Figure 3.13. First, the flow cell needs to be activated which allows the covalent binding of the Ag to the carboxymethylated dextran surface. Once the Ag is bound, any open binding sites need to be blocked to prevent non-specific interactions, followed by scrubbing of the surface to remove any excesses.

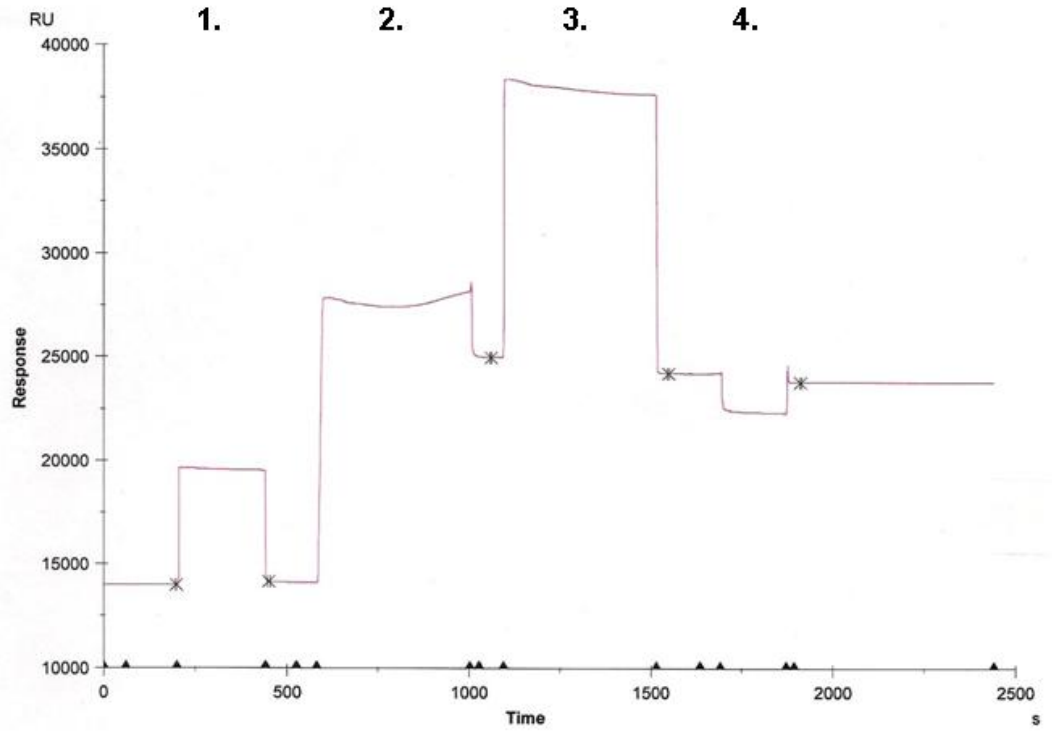

Figure 3.13: Coating a flow cell of a CM5 chip with TST10114. The four steps involved in the coating process are decribed in detail in section 2.7.4, and include: (1) activation of the cell to allow the binding of TST10114 to the cell; (2) coating the Ag TST10114; (3) blocking of any unbound sites; and (4) scrubbing away any unbound proteins.

Once the flow cell has been coated, the interactions of the Ab and the Ag can be measured. A known starting concentration of mAb was diluted in the running buffer to a series of

concentrations (5-8 runs). The program described in section 2.7.4 was then executed to achieve the sensorgrams seen in Figure 3.14.

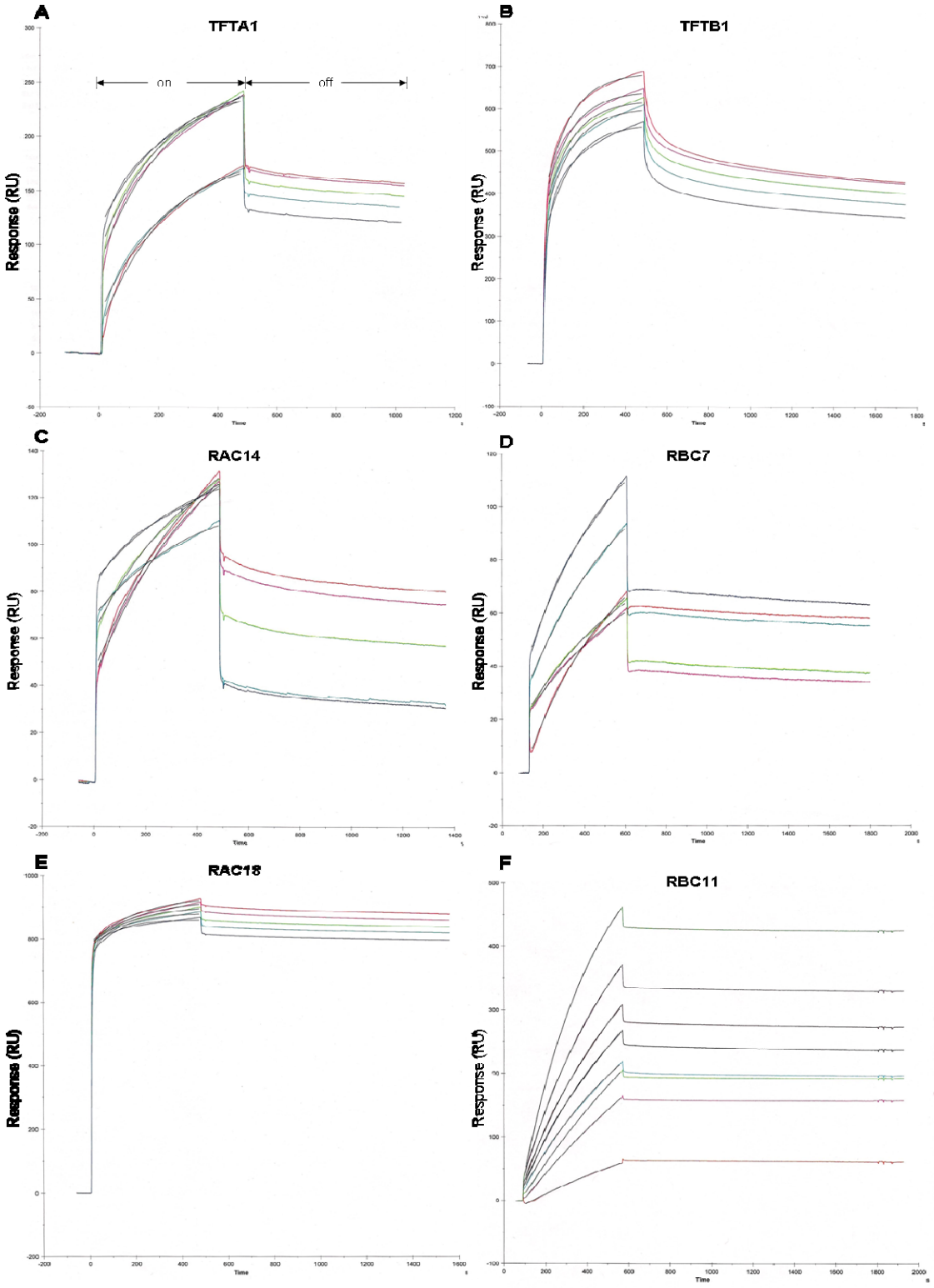

Figure 3.14: Surface plasmon resonance sensorgrams attained from a flow of murine mAb over a flow cell coated with TST10114. Sensorgrams on the left are representative of anti-RTA mAbs: (**A**) TFTA1, (**C**) RAC14 and (**E**) RAC18, while the right shows the sensorgrams from anti-RTB mAbs: (**B**) TFTB1, (**D**) RBC7 and (**F**) RBC11. The "on" rate is used to calculate the

affinity constant (ka), while the "off" rate calculates the dissociation constant (kd). The affinity constant (KD) is calculated from kd/ka.

BIAevaluation software was used for the determination of the association (ka) and dissociation (kd) constants obtained from the sensorgrams in Figure 3.14. The affinity constant KD was calculated from the individual sensorgrams, and averaged to achieve the final affinity constant for each mAb, as reported in Table 3.3.

Table 3.3: Brief summary of the activities and affinities of murine mAbs to TST10114.

mAb	Chain Specificity	Neutralizing Ability? *	ka(1/Ms)	kd (1/s)	KD (nM)	Immunoblot Reactivity
mTFTA1	A	N	4.02e3	1.47e-4	43.3 +/- 16.5	+
mRAC14	A	N	2.22e3	2.03e-4	102.0 +/- 24.3	+
mRAC18	A	**Y**	6.72e3	2.16e-5	9.84 +/- 7.88	+
mTFTB1	B	N	6.06e3	1.50e-4	25.9 +/- 5.08	+
mRBC7	B	N	1.11e3	8.43e-5	76.6 +/- 2.61	+
mRBC11	B	**Y**	1.08e5	9.59e-6	0.160 +/- 0.096	+

* Neutralizing data obtained from Maddaloni *et al.*, 2004.

The chimeric chRAC18-huG2 was also analyzed by the BIACore-2000. The results, however, were not representative of a typical sensorgram. Specifically, the binding signal continued to rise after the flow of chRAC18-huG2 was terminated. The calculated value of KD for chRAC18-huG2 was 6.04pM, a full 3 orders of magnitude lower than the parental murine mAb.

3.5.5 Determination of epitope specificity inferred via cELISA

A competitive ELISA was used to test if epitope recognition was retained during the chimerization process. A 96-well ELISA plate was coated with TST10114, and varying ratios of

competing mAbs were added to the wells, and detected with mouse specific or human specific secondary antibodies. In the chimeric competition, chRAC18-huG2 was assessed for its ability to compete for the binding site by increasing its concentration against the murine RAC18. A increase in signal from the chimeric mAb is indicative of chimeric competition, demonstrating that the two mAbs are binding the same epitope. Next, the murine competition was assessed by increased concentrations of murine RAC18 competing against a constant level of chRAC18-huG2.

A.

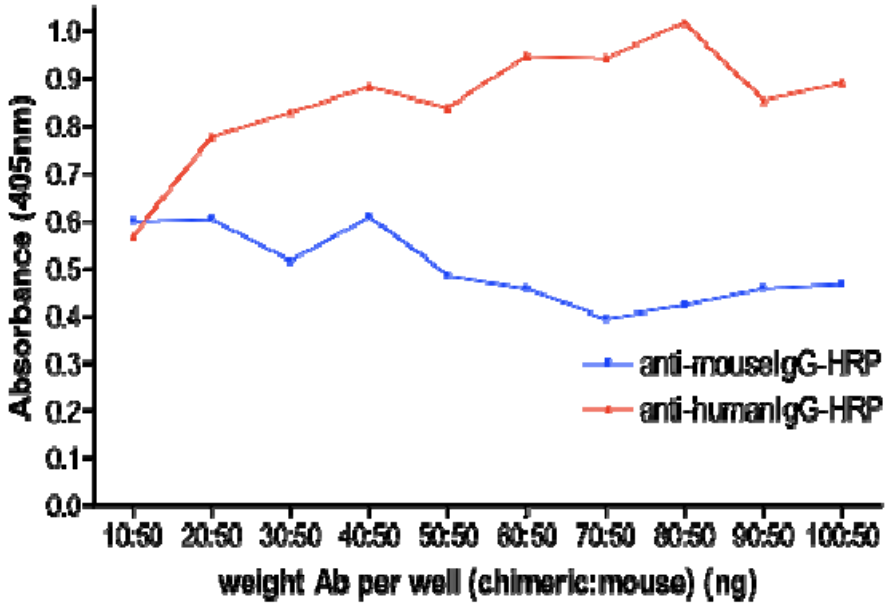

B.

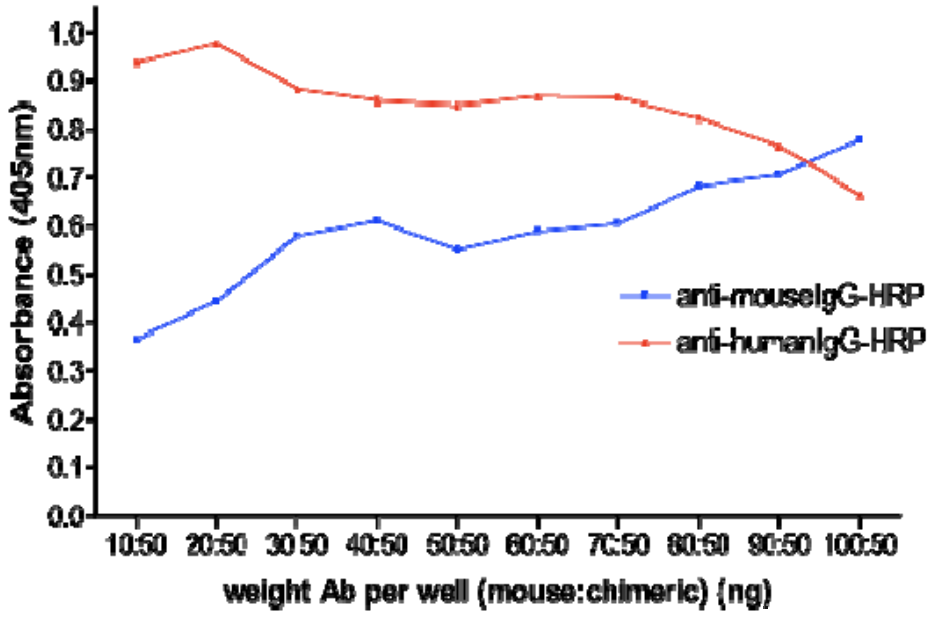

Figure 3.15: cELISA, the ability of chRAC18-huG2 to recognize the same epitope as the parental RAC18 was assessed by competition ELISA. In the chimeric competition (**A**), the amount of murine mAb was constant, while the amount of the competing chRAC18-huG2 was increased. Meanwhile, in the murine Competition (**B**) a constant amount of chRAC18-huG2 was competed against by the increasing levels of the murine RAC18.

4.0 Discussion

4.1 Selection of RAC18 anti-ricin mAb for IgG2 chimerization

This project initially started with six murine hybridomas produced in mice immunized with purified ricin. Two of the previously characterized mAbs (TFTA1 and TFTB1) were used as controls to which the mAbs provided from Dr. Pincus' lab were compared. Dr. Seth Pincus (Research Institute for Children, Children's Hospital, Louisiana State University Health Sciences Center, New Orleans, LA, USA), kindly shared these hybridomas with Dr. Berry, two of which produce mAbs with binding activity against the ricin toxin A-chain (RAC14 and RAC18), and two with binding activity against the ricin B-chain (RBC7 and RBC11). Ricin toxin is a highly regulated substance, and it was necessary to procure an analogue that could be used in a general laboratory setting. To this end, a non-toxic ricin analogue, TST10114 was obtained from Twinstrand Therapeutics, which served as a substitute for intact ricin in the characterization experiments. A deactivated ricin A-chain was also used in select experiments, but was shown to be a weaker control, likely due to the extensive denaturation processes involved in its deactivation.

The variable region gene cDNA of all six anti-ricin mAbs were successfully sequenced, and the sequences of the variable regions of RAC14, RAC18, RBC7 and RBC11 are reported here for the first time (see Appendix B). None of the mAbs had identical VH or VL genes and all were unique. Comparisons between the amino acid sequences of the individual variable heavy and variable light regions yielded expected results, with the majority of differences occurring in the CDRs, specifically CDR3. The surrounding framework regions exhibited slight

differences, but were mostly conserved. It is an important aspect of the chimerization process that the framework regions remain unaltered from the murine mAbs.

One important discovery from this research is that the TST10114 protein was determined to be a good surrogate antigen for native ricin. The murine hybridomas that were used had been derived from mice that were immunized with ricin toxin. As such, it was necessary to determine if the isolated mAbs would also recognize the nontoxic analogue, TST10114 (Figure 3.10). Initial ELISA results demonstrated that all six anti-ricin mAbs bound TST10114, and that a non-specific anti-anthrax mAb (F20G75) had no reactivity against the ricin analogue. The anti-RTA mAbs were also tested by ELISA for binding against the deactivated RTA. The responses against deactivated RTA were greatly reduced when analyzed side-by-side with TST10114. This was the first indication that the deactivated RTA might not be as ideal compared to the TST10114. It is likely that the method of formalin deactivation (which methylates cysteine residues) lowered the ability for the anti-RTA mAbs to recognize the molecule. Western immunoblot further demonstrated specific binding of murine mAbs to TST10114, compared to a BSA negative control protein (Figure 3.8). This was in agreement with the literature that state that RAC14, RAC18, RBC7 and RBC11 react specifically with ricin the Western immunoblot (Maddaloni *et al.* 2007). This clearly shows that the epitopes in ricin are portrayed in TST10114 for this panel of mAbs. Basically, this allows for the creation of serological tests for ricin exposure that may be executed in a lower containment level laboratory, greatly increasing the availability of the deployment of such an assay. Ricin toxin itself is a highly regulated molecule, and requires high containment level facilities for its use, however, the identification of a suitable non-toxic substitute (TST10114) leads to the opportunity of basic laboratories to test for ricin

antibodies. In the case of RAC18, binding in Western immunoblot was a slightly unexpected reactivity. In contrast, in the original article by Maddaloni *et al*., the binding site of RAC18 is reported to be a three-dimensional area inside the ricin A-chain's active site with the motif QXXWXXA and corresponding to glutamine 173 (Q173), tryptophan 211 (W211) and alanine 178 (A178). Upon denaturing, the TST10114 analogue should be linearized, which would separate these specific residues, however, as can be seen in Figure 3.8, there is reactivity of RAC18 mAb against the denatured TST10114. The fact that RAC18 mAb also bound to denatured ricin toxin A-chain in Western immunoblot analysis supports the theory that it is not an artifact of the preparation of the reagent, but that there is actual binding of the anti-ricin mAb to the denatured protein (Figure 3.8). While migrating through the matrix of the polyacrylamide gel, perhaps the epitope was brought together close enough that the RAC18 mAb was able to recognize the necessary amino acids. It is unlikely that the denaturing process failed to fully denature the TST10014, as the anti ricin A-chain mAbs are seen to bind to it near 65kDa – which is the approximate size of a full length ricin molecule.

It is also evident in the Western analysis that the binding of both anti RTA and anti RTB mAbs occurred at approximately the same weight - 65-70kDa. While RTA and RTB are close in size (~34 and 32 kDa respectively), they are slightly different, which is not reflected in the results of the Western. This phenomenon is due to the fact that the denaturing process used to prepare the TST10114 reagent did not cleave the two chains from each other. Binding of RAC18 mAb to the deactivated and denatured RTA was visualized closer to the expected RTA size of 34kDa, which further supports the fact that the TST10114 is covalently bound, and not cleaved under denaturing conditions.

In order to quantify the binding abilities of the murine anti-ricin mAbs, surface plasmon resonance was measured using the BIACore-2000. This apparatus allows the recording and measurement of molecular binding events between the Ab and its Ag. In this case, the Ag, TST10114 was coated on a carboxymethyl cellulose chip, and the anti-ricin mAbs were flowed over the chip to measure real time binding. As shown in Table 3.3, the binding affinities of the anti-ricin mAbs varied between the mAbs, with RBC11 having the highest affinity overall, and RAC18 had the highest affinity of the anti-RTA mAbs. While it is not an exhaustive comparison, the data and published neutralization information suggest that toxin neutralizing mAbs exhibit high affinity.

The fact that RAC18 mAb has a strong affinity for TST10114, is a neutralizing Ab (Maddaloni *et al.* 2007), and that it binds to the enzymatic (or toxic) chain contribute to the choice of this mAb to be chimerized. Previous authors have stated that anti-RTA Abs are generally more protective than anti-RTB Abs. Interestingly, the binding affinity K_D of RAC18 was much lower than that of RAC14 (by a full order of magnitude – lower K_D correlates to stronger affinity). It is also known that Type II RIPs have the same method of action – which is to cleave A_{4324} from the GAGA tetraloop of 28S rRNA. Knowing these facts, amino acid comparisons have been made between different Type II RIPs, and it seen that the glutamine, tryptophan and alanine residues previously mentioned are conserved in the active site of these different molecules.

4.2 Construction of expression system for chRAC18-huG2

For the chimerization process and expression of a chimeric RAC18 mAb, an IgG2 isotype was chosen. Human IgG2 has a higher avidity than IgG1 due to its ability to form covalent dimers (Yoo *et al.*, 2003). The ability of IgG2 to dimerize is thought to be due to the differences in the hinge region of IgG1 and IgG2. IgG2 has a shorter, 12 amino acid long hinge, with more cysteine residues, as opposed to IgG1s 15 amino acid hinge region (Salfeld, 2007). The increase in the number of cysteines is thought to encourage more disulfide bonds between separate IgG2 molecules. IgG2 also has lowered effector functions (Salfeld, 2007). If the target of a therapeutic IgG is a cell (cancer cell for example), it is necessary for that Ab to be able to recognize the cell, and recruit aspects of the immune system to kill that cell, including complement activation, or antibody-dependant cell-mediated cytotoxicity. However, if the desired result is merely to neutralize a target, such as a toxin, then a so-called inactive isotype may be preferred. IgG2 was chosen in this project due to its decreased activation of complement proteins, and lowered recognition from cellular Fc receptors – basically, there would not be any extra accumulation of immune proteins unnecessarily. IgG2 also has a long serum half life at 37.1 +/- 13.9 days – comparable to IgG1 with 36.3 +/- 9.2 days (Salfeld, 2007). All these factors make IgG2 a desirable isotype – the Abs remain in serum for long periods of time, have tetravalent avidity, and are good at neutralizing toxins.

A dual vector system was chosen for expression of the recombinant mAb due to the availability of commercial and in-house made vectors. A dual vector expression system was constructed in Dr. Berry's lab previously. The vectors had been prepared with common restriction enzyme sites flanking the variable regions so that insertion of the anti-ricin variable region sequences would still be read in frame as soon as the RE sites were introduced into their

respective sequences. Once in the pdIgG1 vector, a simple double RE digestion followed by ligation was accomplished to insert the variable heavy region of RAC18 into pFUSE-CHIg-hG2. One minor modification had to be made to the p-dbIgG1 vector before the ligation into the second vector, pINFUSE-hIgG2-Fc2, which lacked the IL2ss and constant heavy 1 (CH1) region. In the creation of the p-dbIgG1 vector, the BglII RE site had already been introduced in frame at the end of CH1, and by examining the multiple cloning site of pINFUSE-hIgG2-Fc2, the XhoI RE site was inserted into p-dbIgG1 immediately prior to the IL2ss. This allowed for a RE double digestion, and isolation of the entire IL2ss-RAC18VH-CH1 region from the modified p-dbIgG1, and ligation into the pINFUSE-hIgG2-Fc2 vector. The CH1 region is extremely similar between IgG1 and IgG2, and the use of the IgG1 CH1 region was not anticipated to alter the functionality of the IgG2 chimeric. The use of a vector containing (pINFUSE-hIgG2-Fc2) was one method of assessing and optimizing the expression of chRAC18-huG2, as the presence or absence of introns may affect recombinant expression (Kalwy *et al.*, 2006). The two light chain vectors (p-dbKappa and pcDNA3.1) had different promoters for expression, and they were transfected in combinations as well for optimization. The p-dbKappa vector has a composite promoter with the human Elongation Factor-1a core promoter, with components of the Human T-Cell Leukemia Virus Type 1 Long Terminal Repeat and a part of the U5 sequence. On the other hand, the pcDNA3.1 vector has a promoter from cytomegalovirus (pCMV).

HEK cells were chosen due to the fact that they are derived from human tissue, and any modifications made would be reflective of a human system.

4.3 Optimization of expression system and purification

A number of approaches were taken in regards to the expression of chRAC18-huG2 (see Table 2.1). Based on ELISA and PAGE data, expression system 2.1 was chosen, which consisted of pINFUSE-hIgG2-Fc2-RAC18VH as the heavy chain vector, and pcDNA3.1-RAC18VK as the light chain vector.

Multiple buffers and columns were available for the chromatographic purification of the chimeric mAb. Commercial buffers and columns were available from GE Healthcare and Pierce (Thermo Scientific), and numerous buffers were also tested that had been prepared in lab or purchased (listed in Table 3.2). The nature of the Protein A or G columns allow for binding of the Fc portion of an IgG molecule, and running an acidic solution (high positive ion concentration) through the column displaces the IgG from its binding spots in the column. The results of the purification trials are seen in Table 3.2, and the chosen method for purification of chRAC18-huG2 was method 1, with a Protein A column, PBS (pH7.2) as the binding buffer, 0.5M acetic acid (pH3.0) as the elution buffer and 1.0M Tris-HCl (pH8.0) as the neutralization buffer. This yielded the highest concentration of purified mAb, which was also quite pure.

4.4 Characterization of chRAC18-huG2

Once the chRAC18-huG2 mAb was expressed and purified, it was subjected to similar tests and assays as the parental murine RAC18 mAb, including an ELISA to test its specificity, a Western immunoblot, SDS-PAGE analysis, and a competition ELISA to determine if the chimeric mAb retained the same epitope recognition. The BIACore results from the chimeric

were dismissed due to inconsistencies in the sensorgrams. During the analysis, there was an unexplainable increasing signal after the antibody had stopped flowing over the flow cell (indicating increasing ligand interactions). One factor that could have led to the results seen may have been the inherent ability of human IgG2 to form covalent dimers, or simply an instrumentation malfunction. An alternate method that may have alleviated this problem would have been to coat the flow cell with chRAC18-huG2, and monitor the flow of TST10114 over the antibody.

During the characterization process, it was first necessary to test the chimeric by an antibody capture ELISA to ensure that a full length recombinant mAb was being expressed by the 293F cells. An ELISA plate was coated with anti-huκ and detected with anti-huIgFcγ. If a full length chimeric mAb was present, the light chain would be caught by the anti-huκ, and the heavy chain would be detected with the anti-huIgFcγ. The assay shows if an intact antibody possesses both a heavy chain and co-folded light chain is present as a fully assembled mAb. The ELISA data demonstrated that chRAC18-huG2 still had strong binding to TST10114, without any non-specific binding. The chimeric was also recognized by an anti-humanIgG2 antibody, confirming its IgG2 isotype. This specific reagent was not used extensively though - initial results indicated it was not very robust, and its optimization or use was not pursued. Western analysis further demonstrated binding to TST10114, however, this could not be directly compared to the binding by murine RAC18, due to the differences in concentrations applied to the PVDF membrane. PAGE analysis demonstrated the strong bands reflective of the antibody light chain (~25kDa) and the heavy chain (~50kDa) however, two further bands were present near 82kDa and 100kDa. This could have been an artifact by inadequately denaturing the

antibody. For example, two bound heavy chains would be expected to appear close to 100kDa, while a heavy-light chain dimer may be near 75kDa. Further, the bands appear on both purification trials, which were processed for PAGE analysis at the same time. It is unclear if the bands are as described above or perhaps extraneous proteins or protein fragments that were purified from the supernatant.

The final analysis completed was a competition ELISA. The results obtained in Figure 3.14 indicate that the parental murine RAC18 mAb and the chRAC18-huG2 recognize and bind to the same epitope. In the chimeric competition, the signal from the anti-humanIgG-HRP secondary antibody increases as the concentration of chRAC18-huG2 increases, while the signal from the anti-mouseIgG-HRP secondary decreases as the amount or murine antibody remains constant. Essentially, the increasing amount of chRAC18-huG2 is displacing the bound murine RAC18. In the murine competition, similar results were recorded – increasing the amount of murine RAC18 against a constant chRAC18-huG2 demonstrated an increase in murine signal alongside a decrease in chimeric signal. These trends would begin to indicate that there is actual competition for the epitope, however this can not be decisively concluded without the analysis of irrelevant antibodies. A repeat of the competitive ELISA with mF20G75 (used as a negative control in Figure 3.10) as a competing antibody would be prudent.

4.5 Summary and future directions

A chimeric anti-ricin antibody was successfully constructed and expressed. The chRAC18-huG2 was shown to bind to the surrogate nontoxic TST10114, and was expressed as an IgG2 isoform.

The logical next step of this project would be to test if the newly synthesized recombinant chRAC18-huG2 offers protection to ribosomes through any neutralizing properties. The murine mAb RAC18 has been previously reported as having neutralizing capabilities (Maddaloni *et al.*, 2004) however it is unknown if this trait has been conserved during the construction of the chimeric. Cell-free systems to monitor ribosome activity are fairly easy to acquire, and usually rely on the ability of ribosomes to translate a reporter gene. If chRAC18-huG2 is able to neutralize intact toxic RTA in a system such as this, a move into *in vitro* cellular systems would be ideal, followed by animal studies. The potential toxicity of the chimeric would need to be determined, as well as administration routes for maximum efficacy.

In terms of the characterization of chRAC18-huG2, an affinity determination would also be recommended. Recording the interactions of the antigen TST10114 over a flow cell that had been coated with chRAC18-huG2 may have helped abrogate the problems encountered earlier. Epitope mapping would also be recommended to provide further proof that the chimeric binds the same area as the murine.

Examining any cross reactivity with other ribosome inactivating proteins could lead to possible broad spectrum applications. It is well known that the active sites are fairly conserved between the different RIPs, and sequence comparisons indicate that the residues recognized by murine RAC18 (Q173, W211, A178) may also be present in the correct orientation in other RIPs.

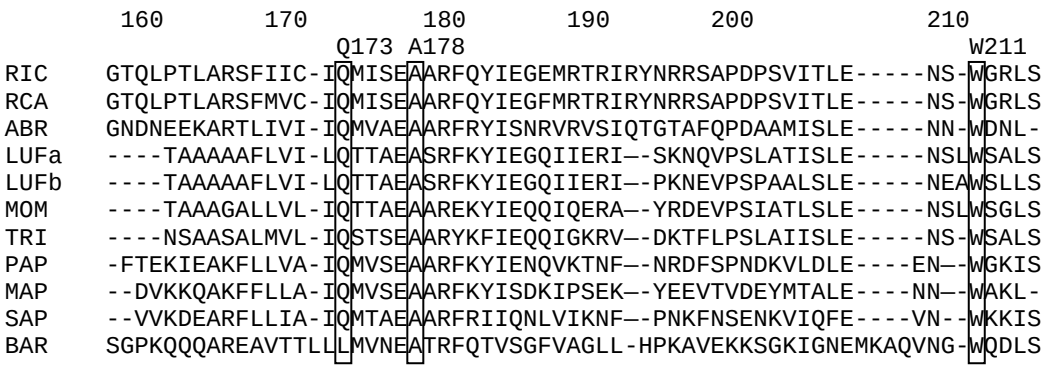

Figure 4.1: Comparison of the sequences of 11 different A-chains from various ribosome inactivating proteins. Residues corresponding to Q173, W211 and A178 are highlighted. The proteins are ricin A-chain (RIC), *Ricinus communis* agglutin (RCA), abrin A-chain (ABR), luffin-a (LUFa), luffin-b (LUFb), momordin (MOM), trichosanthin (TRI), PAP-S (PAP), MAP, saporin (SAP) and barley translation inhibitor (BAR) [Adapted from Funatsu *et al.* (1991)].

A recent *in vitro* assay which analyzed ricin toxin A-chain inhibitors also demonstrated inhibition of Shiga toxin A-chain (Bai *et al.* 2010), lending further support to the search for toxin inhibitors with broad spectrum activity.

It was also determined from this thesis that the non-toxic ricin surrogate TST10114 is a suitable replacement for actual ricin toxin in the general laboratory. It would be interesting to know if TST10114 can illicit an immune response to produce antibodies against intact ricin toxin. This may be an effective and easy way of creating and screening for mAbs that block binding of ricin to cellular surfaces via the ricin B-chain, or even to create detection Abs that may be used in immunological assays. It might not be as good at finding Abs that are effective at abrogating the toxic effects of ricin though, because in the TST10114 molecule, the toxic A-chain is never cleaved from the B-chain, thus the active site is not exposed for the host to create

an antibody response against the active site. This is worth considering as it has been reported that Abs targeting the A-chain of ricin are more effective at blocking toxicity.

Appendix A: Expression system coding sequences and Cloning Sites:

p-dbKappa-RAC18VK cloning site with insert:

```
                                EcoRV
615- GCA CTT GTC ACG AAT TCG ATA TCT GAT GTT TTG ATG ACC CAA -656
      A   L   V   T   N   S   I   S   D   V   L   M   T   Q
     ------ IL2ss --------->         <------ RAC18VK -------


                                    NcoI
975- ACC AAG CTG GAG CTG AAA GCC ATG GGT ACT GTG GCT GCA CCA -996
      T   K   L   E   L   K   A   M   G   T   V   A   A   P
```

Entire Region: Coding region in bold (including IL2 signal sequence (Black), Vk (Blue), Constant Kappa (Red))

539–
GCCTACCTGAGATCACCGGcGAAGGAGGGCCACC**ATGTACAGGATGCAACTCCTGTCTTGCATTGCA**
CTAAGTCTTGCACTTGTCACGAATTC*GATATC*TGATGTTTTGATGACCCAAACTCCACTCTCCCTGC
CTGTCAGTCTTGGAGATCAAGCCTCCATCTCTTGTAGATCTAGTCAGAGCATTATACATAGTAATGG
AGACACCTTTTTAGAATGGTTCCTGCAGAAACCAGGCCAGTCTCCAAAGCTCCTGATCTACAAAGTT
TCCAACCGATTTTCTGGGGTCCCAGACAGGTTCAGTGGCAGTGGATCAGGGACAGATTTCACACTCA
AGATCAGCAGAGTGGAGGCTGAGGATCTGGGAGTTTATTACTGCTTTCAAGGTTCACATGTTCCGCT
CACGTTCGGTGCTGGGACCAAGCTGGAGCTGAAAG*CCATG*GTACTGTGGCTGCACCATCTGTCTTC
ATCTTCCCGCCATCTGATGAGCAGTTGAAATCTGGAACTGCCTCTGTTGTGTGCCTGCTGAATAACT
TCTATCCCAGAGAGGCCAAAGTACAGTGGAAGGTGGATAACGCCCTCCAATCGGGTAACTCCCAGGA
GAGTGTCACAGAGCAGGACAGCAAGGACAGCACCTACAGCCTCAGCAGCACCCTGACGCTGAGCAAA
GCAGACTACGAGAAACACAAAGTCTACGCCTGCGAAGTCACCCATCAGGGCCTGAGCTTGCCCGTCA
CAAAGAGCTTCAACAGGGGAGAGTGTTAG*GCTAGC*TGGCCAGACATGATAAGATACATTGATGAGTT
T
-1343

p-dbIgG1-RAC18VH cloning site with insert:

```
                          EcoRV
618- CTT GTC ACG AAT TCG ATA TCG GAG GTG CAG CTG GAG -656
      L   V   T   N   S   I   S   E   V   Q   L   E
     ----- IL2ss ------>         <---- RAC18VH -----


                                  NcoI                ApaI
978- CTG GTC ACT GTC TCT GCA GCC ATG GCC TCC ACC AAG GGC CCA -1020
      L   V   T   V   S   A   A   M   A   S   T   K   G   P
     ------ RAC18VH ------->          <------ hIgG1 Fc ------
```

Entire Region: Coding region in bold (including IL2 signal sequence (Black), VH (Blue), CH1 – CH3 (Red))

539 –
GCCTACCTGAGATCACCGGCGAAGGAGGGCCACC**ATGTACAGGATGCAACTCCTGTCTTGCATTGCA**
CTAAGTCTTGCACTTGTCACGAATTCGATATCGGAGGTGCAGCTGGAGGAGTCTGGACCTGTGCTGG
TGAAGCCTGGGGCTTCAGTGAAGATGTCCTGTAAGGCTTCTGGATACACGTTCACTGACTACTATGT
GAACTGGGTGAAGCAGAGCCGTGGAAAGAGCCTTGAGTGGCTTGGACTTATTATTCCTTCCAACGGT
GGTACTACCTACAACCAGAAGTTCAGGGGCAAGGCCACATTGACTGTTGACAAGTCCTCCAGCACAG
CCTACATGGAACTCAACAGCCTGACATCTGAGGACTCTGCAGTCTATTACTGTGCAAGACGGGGCCT
AACTGGGGCCCTCTTTGCTTACTGGGGCCAAGGGACTCTGGTCACTGTCTCTGCAGCCATG**GCCTCC**
ACCAAGGGCCCATCGGTCTTCCCCCTGGCACCCTCCTCCAAGAGCACCTCTGGGGGCACAGCGGCCC
TGGGCTGCCTGGTCAAGGACTACTTCCCCGAACCGGTGACGGTGTCGTGGAACTCAGGCGCCCTGAC
CAGCGGCGTGCACACCTTCCCGGCTGTCCTACAGTCCTCAGGACTCTACTCCCTCAGCAGCGTGGTG
ACCGTGCCCTCCAGCAGCTTGGGCACCCAGACCTACATCTGCAACGTGAATCACAAGCCCAGCAACA
CCAAGGTGGACAAGAAAGCAGAGCCCAAATCT*AGATCT*GACAAAACTCACACATGCCCACCGTGCCC
AGCACCTGAACTCCTGGGGGGACCGTCAGTCTTCCTCTTCCCCCCAAAACCCAAGGACACCCTCATG
ATCTCCCGGACCCCTGAGGTCACATGCGTGGTGGTGGACGTGAGCCACGAAGACCCTGAGGTCAAGT
TCAACTGGTACGTGGACGGCGTGGAGGTGCATAATGCCAAGACAAAGCCGCGGGAGGAGCAGTACAA
CAGCACGTACCGTGTGGTCAGCGTCCTCACCGTCCTGCACCAGGACTGGCTGAATGGCAAGGAGTAC
AAGTGCAAGGTCTCCAACAAAGCCCTCCCAGCCCCCATCGAGAAAACCATCTCCAAAGCCAAAGGGC
AGCCCCGAGAACCACAGGTGTACACCCTGCCCCCATCCCGGGAGGAGATGACCAAGAACCAGGTCAG
CCTGACCTGCCTGGTCAAAGGCTTCTATCCCAGCGACATCGCCGTGGAGTGGGAGAGCAATGGGCAG
CCGGAGAACAACTACAAGACCACGCCTCCCGTGCTGGACTCCGACGGCTCCTTCTTCCTCTACAGCA
AGCTCACCGTGGACAAGAGCAGGTGGCAGCAGGGGAACGTCTTCTCATGCTCCGTGATGCATGAGGG
TCTGCACAACCACTACACGCAGAAGAGCCTCTCCCTGTCTCCGGGTAAATGAGT***GCTAGC***TGGCCAG**
ACATGATAAGATACATTGATGAGTTT - 2020

pINFUSE-hIgG2-Fc2-RAC18VH cloning site with insert:

```
                              EcoRV
615-GCA CTT GTC ACG AAT TCG ATA TCG GAG GTC CAA CTA GAG -653
     A   L   V   T   N   S   I   S   E   V   Q   L   E
    ------ IL2ss --------->         <---- RAC18VH -----


                              BglII
1290-AAA GCA GAG CCC AAA TCT AGA TCT GTG GAG TGC CCA CCG TGC-1331
      K   A   E   P   K   S   R   S   V   E   C   P   P   C
     ------- huCH1 -------->         <---- huIgG2 hinge ----
```

Entire region: Coding region in bold (including IL2 signal sequence (Black), RAC18VH (Blue) and human Constant Heavy (Red))

539–
GCCTACCTGAGATCACCGGcGAAGGAGGGCCACC**ATGTACAGGATGCAACTCCTGTCTTGCATTGCA**
CTAAGTCTTGCACTTGTCACGAATTC*GATATC*GGAGGTCCAACTAGAGGAGTCTGGACCTGTGCTGG
TGAAGCCTGGGGCTTCAGTGAAGATGTCCTGTAAGGCTTCTGGATACACGTTCACTGACTACTATGT
GAACTGGGTGAAGCAGAGCCGTGGAAAGAGCCTTGAGTGGCTTGGACTTATTATTCCTTCCAACGGT
GGTACTACCTACAACCAGAAGTTCAGGGGCAAGGCCACATTGACTGTTGACAAGTCCTCCAGCACAG
CCTACATGGAACTCAACAGCCTGACATCTGAGGACTCTGCAGTCTATTACTGTGCAAGACGGGGCCT
AACTGGGGCCCTCTTTGCTTACTGGGGCCAAGGGACTCTGGTCACTGTCTCTGCAGCCATG**GCCTCC**
ACCAAGGGCCCATCGGTCTTCCCCCTGGCAcCCTCCTCCAAGAGCACCTCTgGGGGCACAGCGGCCC
TGGGCTGCCTGGTCAAGGACTACTTCCCCGAACCGGTGACGGTGTCGTGGAACTCAGGCGCCCTGAC
CAGCGGCGTGCACACCTTCCCGGCTGTCCTACAGTCCTCAGGACTCTACTCCCTCAGCAGCGTGGTG
ACCGTGCCCTCCAGCAGCTTGGGCACCCAGACCTACATCTGCAACGTGAATCACAAGCCCAGCAACA
CCAAGGTGGACAAGAAAGCAGAGCCCAAATCT*AGATCT*GTGGAGTGCCCACCGTGCCCAGgtaagcc
agcccaggcctcgccctccagctcaaggcgggacaggtgccctagagtagcctgcatccagggacag
gccccagctgggtgctgacacgtccacctccatctcttcctcagCACCACCTGTGGCAGGACCGTCA
GTCTTCCTCTTCCCCCCAAAACCCAAGGACACCCTCATGATCTCCCGGACCCCTGAGGTCACGTGCG
TGGTGGTGGACGTGAGCCACGAAGACCCCGAGGTCCAGTTCAACTGGTACGTGGACGGCGTGGAGGT
GCATAATGCCAAGACAAAGCCACGGGAGGAGCAGTTCAACAGCACGTTCCGTGTGGTCAGCGTCCTC
ACCGTTGTGCACCAGGACTGGCTGAACGGCAAGGAGTACAAGTGCAAGGTCTCCAACAAAGGCCTCC
CAGCCCCCATCGAGAAAACCATCTCCAAAACCAAAGgtgggacccgcggggtatgagggccacatgg
acagaggccggctcggcccaccctctgccctgggagtgaccgctgtgccaacctctgtccctacagG
GCAGCCCCGAGAACCACAGGTGTACACCCTGCCCCCATCCCGGGAGGAGATGACCAAGAACCAGGTC
AGCCTGACCTGCCTGGTCAAAGGCTTCTACCCCAGCGACATCGCCGTGGAGTGGGAGAGCAATGGGC
AGCCGGAGAACAACTACAAGACCACACCTCCCATGCTGGACTCCGACGGCTCCTTCTTCCTCTACAG
CAAGCTCACCGTGGACAAGAGCAGGTGGCAGCAGGGGAACGTCTTCTCATGCTCCGTGATGCATGAG
GCTCTGCACAACCACTACACGCAGAAGAGCCTCTCCCTGTCTCCGGGTAAATGAGT*GCTAGC*TGGCC
A
-2214

pFUSE-CHIg-hG2-RAC18VH cloning site with insert:

```
                         XhoI
558- TGA ATT CGA TAT CTC GAG ATG TAC AGG ATG CAA -590
                           E   M   Y   R   M   Q
     ---- Vector ------> <------ IL2ss ---------

                              NheI
984- GTC ACT GTC TCT GCA GCT AGC ACC AAG GGC CCA TCG -1019
      V   T   V   S   A   A   S   T   K   G   P   S
     ----- RAC18VH --------> <------- huCH1---------
```

Entire region: Coding region in bold (including IL2 signal sequence (Black), RAC18VH (Blue) and human Constant Heavy (Red))

550-
ATCACCGGTGAATTCGATATCTCGAG**ATGTACAGGATGCAACTCCTGTCTTGCATTGCACTAAGTCT**
TGCACTTGTCACGAATTCGATATCGGAGGTCCAACTACAGCAGTCTGGACCTGTGCTGGTGAAGCCT
GGGGCTTCAGTGAAGATGTCCTGTAAGGCTTCTGGATACACGTTCACTGACTACTATGTGAACTGGG
TGAAGCAGAGCCGTGGAAAGAGCCTTGAGTGGCTTGGACTTATTATTCCTTCCAACGGTGGTACTAC
CTACAACCAGAAGTTCAGGGGCAAGGCCACATTGACTGTTGACAAGTCCTCCAGCACAGCCTACATG
GAACTCAACAGCCTGACATCTGAGGACTCTGCAGTCTATTACTGTGCAAGACGGGGCCTAACTGGGG
CCCTCTTTGCTTACTGGGGCCAAGGGACTCTGGTCACTGTCTCTGCAGCTAGCACCAAGGGCCCATC
GGTCTTCCCCCTGGCGCCCTGCTCCAGGAGCACCTCCGAGAGCACAGCGGCCCTGGGCTGCCTGGTC
AAGGACTACTTCCCCGAACCGGTGACGGTGTCGTGGAACTCAGGCGCTCTGACCAGCGGCGTGCACA
CCTTCCCAGCTGTCCTACAGTCCTCAGGACTCTACTCCCTCAGCAGCGTGGTGACCGTGCCCTCCAG
CAACTTCGGCACCCAGACCTACACCTGCAACGTAGATCACAAGCCCAGCAACACCAAGGTGGACAAG
ACAGTTGAGCGCAAATGTTGTGTCGAGTGCCCACCGTGCCCAGCACCACCTGTGGCAGGACCGTCAG
TCTTCCTCTTCCCCCCAAAACCCAAGGACACCCTCATGATCTCCCGGACCCCTGAGGTCACGTGCGT
GGTGGTGGACGTGAGCCACGAAGACCCCGAGGTCCAGTTCAACTGGTACGTGGACGGCGTGGAGGTG
CATAATGCCAAGACAAAGCCACGGGAGGAGCAGTTCAACAGCACGTTCCGTGTGGTCAGCGTCCTCA
CCGTTGTGCACCAGGACTGGCTGAACGGCAAGGAGTACAAGTGCAAGGTCTCCAACAAAGGCCTCCC
AGCCCCCATCGAGAAAACCATCTCCAAAACCAAAGGGCAGCCCCGAGAACCACAGGTGTACACCCTG
CCCCCATCCCGGGAGGAGATGACCAAGAACCAGGTCAGCCTGACCTGCCTGGTCAAAGGCTTCTACC
CCAGCGACATCGCCGTGGAGTGGGAGAGCAATGGGCAGCCGGAGAACAACTACAAGACCACGCCTCC
CATGCTGGACTCCGACGGCTCCTTCTTCCTCTACAGCAAGCTCACCGTGGACAAGAGCAGGTGGCAG
CAGGGGAACGTCTTCTCATGCTCCGTGATGCATGAGGCTCTGCACAACCACTACACGCAGAAGAGCC
TCTCCCTGTCTCCGGGTAAATGAGTCCTAGCTGGCCAGACATG
-2000

Appendix B: Variable region Sequences of the 6 mAbs provided in this thesis:

TFTA1

VH (1-339)

CAGCTCCAGCTTCAGGAGTCAGGGCCTGGCCTGGTGAAGCCTTCTGAGTCAGTTTCACTCACCTGCA
CTGTCACTGGCTACTCCATCACCAGTGGTTTTAGCTGGCACTGGGTCCGGCAGTTTCCAGGAAACAA
ACTGGAATGGATGGCCTACATACACTACAGTGGTAGTACTGACTGCAACCCATCTCTCAAAAGTCGG
ATCTCTATCACTCGAAACACATCCAAGAACCAATTCTTCCTGCATCTGAAATCTGTGACCACTGAAG
ACTCAGCCACATATTACTGTTTAAGAATGCCTGATTCTTGGGGGCCAGGCACCACTCTCACAGTCTC
CTCA

VK (1-336)

GATGTTGTGATGACCCAGACTCCACTCACTTTGTCGGTTATCATTGGACAACCAGCCTCCATCTCTT
GCAAGTCAAGTCAGAGCCTCTTAGATAGCGATGGAAAGACATTTTTGAATTGGTCGTTGCAGAGGCC
AGGCCAGTCTCCAAAGCGCCTAATCTATCTGGTGTCTAAGCTGGACTCTGGAGTCCCTGACAGGTTC
ACTGGCAGTGGGTCAGGGACAGATTTCACACTGAAAATCAGCAGAGTGGAGGCTGAGGATTTGGGAG
TTTATTATTGCTGGCAAGGAACACATTTTCCGTACACGTTCGGAGGGGGGACCAAGCTGGAAATAAA
A

RAC14

VH (1-357)

GAGGTCCAGCTCGTGCAGTCTGGACCTGAGCTGGTGAAGCCTGGGGCTTCAGTGAAGATAACCTGTA
AGGCTTCTGGATACACGTTCACTGACTACTACATGAGCTGGTTGAAGCTGAGCCATGGAAAGAGCCT
TGAGTGGATTGGAGAAATCAATCCTAAAAATGGTGGTTCTAGTAACAACCAGAGATTCAGGGACAAG
GCCACATTGACTGTAGACACGTCCTCCAGCACAGCCTACATGGAGCTCCGCAGCCTGACATCTGAGG
ACTCTGCAGTCTATTTCTGTGCAAGAGAAGAAGAATATGGTTCCGTCGGGGATTATTACTATGCTAT
GGACTACTGGGGTCAAGGAACCTCAGTCACCGTCTCCTCA

VK (1-321)

GACATTGTGATGACCCAGTCTCACAAATTCATGTCCACATCAGTAGGAGACAGGGTCAGCATCACCT
GCAAGGCCAGTCAGGATGTGACTTCTGCTGTTGCCTGGTTTCAACAGAAACCAGGACAATCTCCTAA
ACTACTGATTTATTCGGCATCCTACCGGTACACTGGAGTCCCTGATCGCTTCACTGGCAGTGGATCT
GGGACGGATTTCACTTTCACCATCAGCAGTGTGCAGGCTGAAGACCTGGCAGTTTATTACTGTCAGC
AGCATTATGGTACTCCGCTCACGTTCGGTGCTGGGACCAAGCTGGAGCTGAAA

RAC18

VH (1-357)

GAGGTGCAGCTGGAGGAGTCTGGACCTGTGCTGGTGAAGCCTGGGGCTTCAGTGAAGATGTCCTGTA
AGGCTTCTGGATACACGTTCACTGACTACTATGTGAACTGGGTGAAGCAGAGCCGTGGAAAGAGCCT
TGAGTGGCTTGGACTTATTATTCCTTCCAACGGTGGTACTACCTACAACCAGAAGTTCAGGGGCAAG
GCCACATTGACTGTTGACAAGTCCTCCAGCACAGCCTACATGGAACTCAACAGCCTGACATCTGAGG
ACTCTGCAGTCTATTACTGTGCAAGACGGGGCCTAACTGGGGCCCTCTTTGCTTACTGGGGCCAAGG
GACTCTGGTCACTGTCTCTGCA

VK (1-318)

GACATCCAGATGACACAGTCTCCATCCTCACTGTCTGCATCTCTGGGAGGCAAAGTCACCATCACTT
GCAAGGCAAGCCAAGACATTAACAAATATATAGCTTGGTACCAACACAAGGCTGGAAAAGGTCCTAG
GCTGATCATGCATTACACATCTACATTACAGCCAGGCATCCCATCAAGGTTCAGTGGAAGTGGGTCT
GGGAGAGATTATTCCTTCAGCATCATCAACCTGGAGCCTGAAGATATTGGAACTTATTATTGTCTAC
AGTATGATAATCTGTGGACGTTCGGTGGAGGCACCAAGCTGGAAATCAAA

TFTB1

VH (1-360)

GAGGTGCAGCTGGAGGAGTCTGGGGGAGGCTTAGTGCAGCCTGGAGGGTCCCGGAAACTCTCCTGTG
CAGCCTCTGGATTCACTTTCAGTAGCTTTGGAATGCACTGGGTTCGTCAGGCTCCAGAGAAGGGGCT
GGAGTGGGTCGCATACATTAGTAGTGGCAGTAGTACCCTCCACTATGCAGACACAGTGAAGGGCCGA
TTCACCATCTCCAGAGACAATCCCAAGAACACCCTGTTCCTGCAAATGACCAGTCTAAGGTCTGAGG
ACACGGCCATGTATTACTGTGCAAGATGGGGTAACTACCCTCACTATGCTATGGACTACTGGGGTCA
AGGAACCTCAGTCACCGTCTCCTCA

VK (1-321)

AAGCTCGTGATGACCCAGTCTCCATCTTATCTTGCTGCATCTCCTGGAGAAACCATTACTATTAATT
GCAGGGCAAGTAAGAGCATTAACAAATATTTAGCCTGGTATCAAGAGAAACCTGGGAAAACTAATAA
GCTTCTTATCTACTCTGGATCCACTTTGCAATCTGGAATTCCATCAAGGTTCAGTGGCAGTGGATCT
GGTACAGATTTCACTCTCACCATCAGTAGCCTGGAGCCTGAAGATTTTGCAATGTATTACTGTCAAC
AGCATAATGAATACCCGTGGACGTTCGGTGGAGGCACCAAGCTGGAAATCAAA

RBC7

VH (1-381)

GAGGTGCAGCTGGAGGAGTCTGGAGGAGGCTTGGTACAGCCTGGGAGTTCTCTGAGTCTCTCCTGTG
CAGCTTCTGGATTCACCTTTACTGATTACTACATGAGCTGGGTCCGCCAGCCTCCAGGGAAGGCACT
TGAGTGGTTGGGTTTTATTAGAAACAAAGCTAATGGTTACACAACAGAATACAGTGCATCTGTGAAG
GGTCGGTTCACCATCTCCAGAGATAATTCCCAAAGCATCCTCTATCTTCAAATGAATGCCCTGAGAG
CTGAGGACAGTGCCACTTATTACTGTGCAAGATCCGCCTCTTATTACTACGGTACGAGCTCATACTG
GTACTTCGATGTCTGGGGCACAGGGACCACGGTCACCGTCTCCTCA

VK (1-321)

GAGCTCGTGATGACCCAGTCTCCAGCTTCCCTGTCTGCATCTGTGGGAGAAACTGTCACCATCACAT
GTCGAGTGAGTGAGAATATTGACAGTTATTTAGCATGGTATCAGCAGAAACAGGGAAAATCTCCTCA
GCTCCTAGTCTATGCTACAACACTCTTAGCAGATGGTGTGCCATCAAGGTTCAGTGGCAGTGGATCA
GGCACACAGTATTCTCTCAAGATCAATAGCCTGCAGTCTGAAGATGTTGCGAGATATTTCTGTCAAC
ATTATTATAGTCTTCCATTCACGTTCGGCACGGGGACAAAATTGGAAATAAAA

RBC11

VH

GAGGTGCAGCTGGAGGAGTCTGGACCTGAGCTGGTGAAGCCTGGGGCTTCAGTGAAGGTATCCTGCA
AGGCTTCTGGTTACTCATTCACTGACTACAACATGTACTGGGTGAAGCAGAGCCATGGAACGAGCCT
TGAATGGATTGGCGTTATTGATCCTAACAATGGTGTTACTAGCTACAACCAGAAGTTCAAGGACAAG
GCCACATTGACTGCTGACAAGTCCTCCAGTACAGCCTTCATGCATCTCAACAGCCTGACATCTGAGG
ACTCTGCAGTCTATCATTGTTCAAGAGGGGGTCTTGACTACTGGGGCCAGGGCACCACTCTCACAGT
CTCCTCA

VK

GAGCTCGTGATGACCCAGTCTCCATCCTCACTGTCTGCATCTCTGGGAGGCAAAGTCACCATCACTTGCA
AGGCAAGCCAAGACATTAACAAGTATATAGCTTGGTACCAAAACAAGCCTGGAAAAGGTCCTAGGCTGAT
CATACATTACACATCTACATTACAGCCAGACATCCCATCAAGGTTCAGTGGAAGTGGGTCTGGGAAAGAT
TATTCCTTCAGCATCAGCAACCTGGAGCCAGAAGATATTGCAACTTATTATTGTCTACAGTATGATAATC
TGTGGACGTTCGGTGGAGGCACCAAGCTGGAAATCAAA

Appendix C: IMGT/V-Quest search of the RAC18 variable regions:

RAC18 Variable Heavy region:

```
A. Detailed results for the IMGT/V-QUEST analysed sequences

1 sequences have been analysed in the current run:


------------------------------


Sequence number 1 : RAC18_VH
compared with the mouse IG set from the IMGT reference directory

>RAC18_VH
gaggtgcagctggaggagtctggacctgtgctggtgaagcctggggcttcagtgaagatg
tcctgtaaggcttctggatacacgttcactgactactatgtgaactgggtgaagcagagc
cgtggaaagagccttgagtggcttggacttattattccttccaacggtggtactacctac
aaccagaagttcaggggcaaggccacattgactgttgacaagtcctccagcacagcctac
atggaactcaacagcctgacatctgaggactctgcagtctattactgtgcaagacggggc
ctaactggggccctctttgcttactggggccaagggactctggtcactgtctctgca


Result summary: ;
 Productive IGH rearranged sequence (no stop codon and in-frame junction);
V-GENE and allele;Musmus IGHV1-19*01; score = 1309; identity = 95,14% (274/288 nt);
J-GENE and allele;Musmus IGHJ3*01; score = 208; identity = 93,62% (44/47 nt);
D-GENE and allele by IMGT/JunctionAnalysis;No results;-;
FR-IMGT lengths, CDR-IMGT lengths and AA JUNCTION;[25.17.38.11];[8.8.12];CARRGLTGALFAYW;



Closest V-REGIONs (evaluated from the V-REGION first nucleotide to  the 2nd-CYS codon)
                                Score       Identity
AC073565 Musmus IGHV1-19*01     1309        95,14% (274/288 nt)
AC073565 Musmus IGHV1-26*01     1228        92,01% (265/288 nt)
L17134 Musmus IGHV1-34*02       1192        90,62% (261/288 nt)
AC073565 Musmus IGHV1-36*01     1192        90,62% (261/288 nt)
M20774 Musmus IGHV1S46*01       1183        90,28% (260/288 nt)


1. Alignment for V-GENE
                           <---------------------------------- FR1-IMGT ---------------
RAC18_VH                   gaggtgcagctggaggagtctggacct...gtgctggtgaagcctggggcttcagtgaag
AC073565 Musmus IGHV1-19*01 -----c------c-ac-----------..-----------------------------
AC073565 Musmus IGHV1-26*01 -----c------c-ac-a---------...-a---------------------------
L17134 Musmus IGHV1-34*02   -----c------c-ac-----------...-a----------------a----------
AC073565 Musmus IGHV1-36*01 -----c------c-ac-----------..------------------c-----------
M20774 Musmus IGHV1S46*01   -----c------c-ac-----------...-a---------------------------

                           -----------------> CDR1-IMGT ____________<-----
RAC18_VH                   atgtcctgtaaggcttctggatacacgttc............actgactactatgtgaac
AC073565 Musmus IGHV1-19*01 -------------------------a---.............-----------a-----
AC073565 Musmus IGHV1-26*01 --a-----------------------.............-----------ca-----
L17134 Musmus IGHV1-34*02   --------c-----------c-----a---.............-----------ca--g--
AC073565 Musmus IGHV1-36*01 --a-------------------t---a---.............-----------ca--c--
M20774 Musmus IGHV1S46*01   --a-----c-------------t---a---.............--------tgtca--c--
```

```
                                  --------------- FR2-IMGT ------------------>___________ CDR
RAC18_VH                          tgggtgaagcagagccgtggaaagagccttgagtggcttggacttattattccttcc...
AC073565 Musmus IGHV1-19*01       ----------------a------------------a-----g------a-----a-...
AC073565 Musmus IGHV1-26*01       ----------------a------------------a-----ga-----a----aa-...
L17134 Musmus IGHV1-34*02         ----------------a------------------a-----ta----ta----aa-...
AC073565 Musmus IGHV1-36*01       ----------------a------------------a--------g--ta-----a-...
M20774 Musmus IGHV1S46*01         ----------------a------------------a-----------------a-...

                                  2-IMGT ________<-------------------------------------------
RAC18_VH                          ...aacggtggtactacctacaaccagaagttcagg...ggcaaggccacattgactgtt
AC073565 Musmus IGHV1-19*01       ...-------------g-----------------a-...--------------------
AC073565 Musmus IGHV1-26*01       ...--t----------g-----------------a-...--------------------a
L17134 Musmus IGHV1-34*02         ...--t----------g------t----------a-...--------------------a
AC073565 Musmus IGHV1-36*01       ...--t----------g-----------------a-...--------------------a
M20774 Musmus IGHV1S46*01         ...--t----a----tt-----------------a-...--------------------a

                                  --------- FR3-IMGT ----------------------------------------
RAC18_VH                          gacaagtcctccagcacagcctacatggaactcaacagcctgacatctgaggactctgca
AC073565 Musmus IGHV1-19*01       ----------------------------g-----------------------------
AC073565 Musmus IGHV1-26*01       ----------------------------g---cg-------------------------
L17134 Musmus IGHV1-34*02         ----------------------------g---c--------------------------
AC073565 Musmus IGHV1-36*01       ----ca----------------------g--a-----------t--------------g
M20774 Musmus IGHV1S46*01         ----ca----------------------g-------------------------t----

                                  ----------->_____________ CDR3-IMGT ____________
RAC18_VH                          gtctattactgtgcaagacggggcctaactggggccctctttgcttactggggccaaggg
AC073565 Musmus IGHV1-19*01       ------------------
AC073565 Musmus IGHV1-26*01       ------------------
L17134 Musmus IGHV1-34*02         ------------------
AC073565 Musmus IGHV1-36*01       ------------------
M20774 Musmus IGHV1S46*01         ------------------t


RAC18_VH                          actctggtcactgtctctgca
AC073565 Musmus IGHV1-19*01
AC073565 Musmus IGHV1-26*01
L17134 Musmus IGHV1-34*02
AC073565 Musmus IGHV1-36*01
M20774 Musmus IGHV1S46*01
```

2. Alignment for D-GENE

	Score	Identity
L32868 Musmus IGHD4-1*01	45	100,00% (9/9 nt)
J00440 Musmus IGHD4-1*02	31	87,50% (7/8 nt)
J00433 Musmus IGHD2-9*01	14	60,00% (6/10 nt)
M23243 Musmus IGHD3-2*01	14	60,00% (6/10 nt)
AC073553 Musmus IGHD5-5*01	14	60,00% (6/10 nt)

```
RAC18 VH                          cggggcctaactggg
L32868 Musmus IGHD4-1*01          .....---------ac
J00440 Musmus IGHD4-1*02          .......c-------ac
J00433 Musmus IGHD2-9*01          .........----ctat--ttacgac
M23243 Musmus IGHD3-2*01          -tc--g---c
AC073553 Musmus IGHD5-5*01        ....-a---c--ac
```

3. Alignment for J-GENE

```
                                    Score       Identity
V00770 Musmus IGHJ3*01              208         93,62% (44/47 nt)
S73821 Musmus IGHJ3*02              190         89,36% (42/47 nt)
V00770 Musmus IGHJ2*01              109         70,21% (33/47 nt)
S77041 Musmus IGHJ2*02              108         71,11% (32/45 nt)

RAC18 VH                        cggggcctaactggggccctctttgcttactggggccaagggactctggtcactgtctct
V00770 Musmus IGHJ3*01          .................--tgg---------------------------------------
S73821 Musmus IGHJ3*02          .................--tgg----g---g-------------------------------
V00770 Musmus IGHJ2*01          .................a-ta-----ac--------------c--cactc----a-----c
S77041 Musmus IGHJ2*02          ..................ta-----ac--------------c--cagtc----a-----c

RAC18 VH                        gca
V00770 Musmus IGHJ3*01          ---g
S73821 Musmus IGHJ3*02          ---g
V00770 Musmus IGHJ2*01          t--g
S77041 Musmus IGHJ2*02          t--g
```

7. V-REGION translation

```
                                <-------------------------------------------  FR1 - IMGT
                                1               5                   10                  15
                                 E   V   Q   L   E   E   S   G   P       V   L   V   K   P
RAC18_VH                        gag gtg cag ctg gag gag tct gga cct ... gtg ctg gtg aag cct
                                                 Q   Q
AC073565 Musmus IGHV1-19*01     --- --c --- --- c-a c-- --- --- --- ... --- --- --- --- ---

                                ----------------------------------------> _________________
                                                20                  25                  30
                                 G   A   S   V   K   M   S   C   K   A   S   G   Y   T   F
RAC18_VH                        ggg gct tca gtg aag atg tcc tgt aag gct tct gga tac acg ttc

AC073565 Musmus IGHV1-19*01     --- --- --- --- --- --- --- --- --- --- --- --- --- --a ---

                                __  CDR1 - IMGT  _______________ <--------------------------
                                                35                  40                  45
                                                 T   D   Y   Y   V   N   W   V   K   Q   S
RAC18_VH                        ... ... ... ... act gac tac tat gtg aac tgg gtg aag cag agc
                                                                 M
AC073565 Musmus IGHV1-19*01     ... ... ... ... --- --- --- --- a-- --- --- --- --- --- ---

                                 FR2 - IMGT  -------------------------> _______________  CDR2
                                                        50                  55
60
                                 R   G   K   S   L   E   W   L   G   L   I   I   P   S
RAC18_VH                        cgt gga aag agc ctt gag tgg ctt gga ctt att att cct tcc ...
                                 H                           I       V       N       Y
AC073565 Musmus IGHV1-19*01     -a- --- --- --- --- --- --- a-- --- g-- --- -a- --- -a- ...

                                 - IMGT  __________ <-----------------------------------------
                                                65                  70                  75
                                     N   G   G   T   T   Y   N   Q   K   F   R       G   K
RAC18_VH                        ... aac ggt ggt act acc tac aac cag aag ttc agg ... ggc aag
                                                        S                       K
AC073565 Musmus IGHV1-19*01     ... --- --- --- --- -g- --- --- --- --- --- -a- ... --- ---
```

```
                                ------------------------------  FR3 - IMGT  ---------------
                                                80                  85                  90
                                 A   T   L   T   V   D   K   S   S   S   T   A   Y   M   E
RAC18_VH                        gcc aca ttg act gtt gac aag tcc tcc agc aca gcc tac atg gaa

AC073565 Musmus IGHV1-19*01     --- --- --- --- --- --- --- --- --- --- --- --- --- --- --g

                                ----------------------------------------------------> ____
                                                95                  100             104
                                 L   N   S   L   T   S   E   D   S   A   V   Y   Y   C   A
RAC18_VH                        ctc aac agc ctg aca tct gag gac tct gca gtc tat tac tgt gca

AC073565 Musmus IGHV1-19*01     --- --- --- --- --- --- --- --- --- --- --- --- --- --- ---

                                _______________  CDR3 - IMGT  _______________

                                 R   R   G   L   T   G   A   L   F   A   Y   W   G   Q   G
RAC18_VH                        aga cgg ggc cta act ggg gcc ctc ttt gct tac tgg ggc caa ggg

AC073565 Musmus IGHV1-19*01     ---



                                 T   L   V   T   V   S   A
RAC18_VH                        act ctg gtc act gtc tct gca

AC073565 Musmus IGHV1-19*01
```

RAC18 Variable Kappa region:

```
A. Detailed results for the IMGT/V-QUEST analysed sequences

1 sequences have been analysed in the current run:


------------------------------


Sequence number 1 : RAC18_VK
compared with the mouse IG set from the IMGT reference directory

>RAC18_VK
gacatccagatgacacagtctccatcctcactgtctgcatctctgggaggcaaagtcacc
atcacttgcaaggcaagccaagacattaacaaatatatagcttggtaccaacacaaggct
ggaaaaggtcctaggctgatcatgcattacacatctacattacagccaggcatcccatca
aggttcagtggaagtgggtctgggagagattattccttcagcatcatcaacctggagcct
gaagatattggaacttattattgtctacagtatgataatctgtggacgttcggtggaggc
accaagctggaaatcaaa


Result summary: ;
 Productive IGK rearranged sequence (no stop codon and in-frame junction);
V-GENE and allele;Musmus IGKV19-93*01; score = 1336; identity = 97,85% (273/279 nt);
J-GENE and allele;Musmus IGKJ1*01; score = 185; identity = 100,00% (37/37 nt);
FR-IMGT lengths, CDR-IMGT lengths and AA JUNCTION;[26.17.36.10];[6.3.8];CLQYDNLWTF;



Closest V-REGIONs (evaluated from the V-REGION first nucleotide to the 2nd-CYS codon plus 15
nt of the CDR3-IMGT)
                                  Score       Identity
AJ235935 Musmus IGKV19-93*01      1336        97,85% (273/279 nt)
S65298 Musmus IGKV19-93*02        1318        97,13% (271/279 nt)
AF441453 Musmus IGKV10-94*04      859         78,49% (219/279 nt)
M54904 Musmus IGKV10-94*03        850         78,14% (218/279 nt)
AF441457 Musmus IGKV10-94*08      850         78,14% (218/279 nt)


1. Alignment for V-GENE
                                 <---------------------------------- FR1-IMGT ---------------
RAC18_VK                         gacatccagatgacacagtctccatcctcactgtctgcatctctgggaggcaaagtcacc
AJ235935 Musmus IGKV19-93*01     ------------------------------------------------------------
S65298 Musmus IGKV19-93*02       ------------------------------------------------------------
AF441453 Musmus IGKV10-94*04     --t---------------a--a-------c--------c----------a--g-------
M54904 Musmus IGKV10-94*03       --t---------------a--a-------c--------c----------a--g-------
AF441457 Musmus IGKV10-94*08     --t---------------a--a-------c--------c----------a--g-------

                                 -----------------> CDR1-IMGT <-----
RAC18_VK                         atcacttgcaaggcaagccaagacatt.................aacaaatatatagct
AJ235935 Musmus IGKV19-93*01     ---------------------------.................-----g---------
S65298 Musmus IGKV19-93*02       ---------------------------.................-----g---------
AF441453 Musmus IGKV10-94*04     ----g-----g------t--g-----..................-g---t---t--aac
M54904 Musmus IGKV10-94*03       ----g-----g------t--g--t---..................-g---t---t--aac
AF441457 Musmus IGKV10-94*08     ----g-----g------t--g--t---..................-g---t---t--aac
```

```
                                 ---------- FR2-IMGT ------------------>__________ CDR
RAC18_VK                         tggtaccaacacaaggctggaaaaggtcctaggctgatcatgcattacaca.........
AJ235935 Musmus IGKV19-93*01     ---------------c-------------------c----a---------.........
S65298 Musmus IGKV19-93*02       ---------------c---------------a---c----a---------.........
AF441453 Musmus IGKV10-94*04     -----t--g--g--ac-a-atgg-ac-gt--aa--ac-g--ct-c------.........
M54904 Musmus IGKV10-94*03       -----t--g--g--ac-a-atgg-ac-gt--aa--cc-g--ct-c------.........
AF441457 Musmus IGKV10-94*08     -----t--g--g--ac-a-atgg-ac-gt--aa--cc-g--ct-c------.........

                                 2-IMGT ________<-------------------------------------------
RAC18_VK                         ............tctacattacagccaggcatccca...tcaaggttcagtggaagtggg
AJ235935 Musmus IGKV19-93*01     ............----------------------------..--------------------
S65298 Musmus IGKV19-93*02       ............----------------------------..----------------c---
AF441453 Musmus IGKV10-94*04     ..............--a-g------ct----ag-----...--------------c------
M54904 Musmus IGKV10-94*03       ..............--a-g------ct----ag-----...--------------c------
AF441457 Musmus IGKV10-94*08     ..............--a-g------ct----ag-----...--------------c------

                                 --------- FR3-IMGT ---------------------------------------
RAC18_VK                         ......tctgggagagattattccttcagcatcatcaacctggagcctgaagatattgga
AJ235935 Musmus IGKV19-93*01     ......----------------------------g----------------------c-
S65298 Musmus IGKV19-93*02       ......----------------------------g----------------------c-
AF441453 Musmus IGKV10-94*04     ......-------c---------tc---c-----g---------a-------------cc
M54904 Musmus IGKV10-94*03       ......-------c---------tc---c-----g---------a-------------cc
AF441457 Musmus IGKV10-94*08     ......-------c---------tc---c-----g---------a-------------cc

                                 ----------->_________ CDR3-IMGT _____
RAC18_VK                         acttattattgtctacagtatgataatctgtggacgttcggtggaggcaccaagctggaa
AJ235935 Musmus IGKV19-93*01     ----------------------------tctac-
S65298 Musmus IGKV19-93*02       ----------------------------tctac-
AF441453 Musmus IGKV10-94*04     -----c-------ag------ag---g--tcctc-
M54904 Musmus IGKV10-94*03       -----c-------ag------ag---g--tcctc-
AF441457 Musmus IGKV10-94*08     -----c-------ag------ag---g--tcctc-

RAC18_VK                         atcaaa
AJ235935 Musmus IGKV19-93*01
S65298 Musmus IGKV19-93*02
AF441453 Musmus IGKV10-94*04
M54904 Musmus IGKV10-94*03
AF441457 Musmus IGKV10-94*08
```

3. Alignment for J-GENE

	Score	Identity
V00777 Musmus IGKJ1*01	185	100,00% (37/37 nt)
M15559 Musmus IGKJ1*02	153	91,67% (33/36 nt)
V00777 Musmus IGKJ2*01	131	83,78% (31/37 nt)
M15559 Musmus IGKJ2*02	113	78,38% (29/37 nt)
M27036 Musmus IGKJ2*03	113	78,38% (29/37 nt)

```
RAC18 VK                         gtggacgttcggtggaggcaccaagctggaaatcaaa
V00777 Musmus IGKJ1*01           ------------------------------------c
M15559 Musmus IGKJ1*02           .cc---------------------------------tc
V00777 Musmus IGKJ2*01           --ac--------a--g--g-------------a---c
M15559 Musmus IGKJ2*02           --at--------atcg--g-------------g---c
M27036 Musmus IGKJ2*03           --at--------atcg--g-------------a---c
```

7. V-REGION translation

```
                              <------------------------------------------  FR1 - IMGT
                              1               5                  10                  15
                               D   I   Q   M   T   Q   S   P   S   S   L   S   A   S   L
RAC18_VK                      gac atc cag atg aca cag tct cca tcc tca ctg tct gca tct ctg

AJ235935 Musmus IGKV19-93*01  --- --- --- --- --- --- --- --- --- --- --- --- --- --- ---

                              ----------------------------------------> ________________
                                              20                  25                  30
                               G   G   K   V   T   I   T   C   K   A   S   Q   D   I
RAC18_VK                      gga ggc aaa gtc acc atc act tgc aag gca agc caa gac att ...

AJ235935 Musmus IGKV19-93*01  --- --- --- --- --- --- --- --- --- --- --- --- --- --- ...

                              __  CDR1 - IMGT  _______________ <--------------------------
                                              35                  40                  45
                                                  N   K   Y   I   A   W   Y   Q   H   K
RAC18_VK                      ... ... ... ... ... aac aaa tat ata gct tgg tac caa cac aag

AJ235935 Musmus IGKV19-93*01  ... ... ... ... ... --- --g --- --- --- --- --- --- --- ---

                               FR2 - IMGT  -------------------------> _________________  CDR2
                                              50                  55                  60
                               A   G   K   G   P   R   L   I   M   H   Y   T
RAC18_VK                      gct gga aaa ggt cct agg ctg atc atg cat tac aca ... ... ...
                               P                       L   I
AJ235935 Musmus IGKV19-93*01  c-- --- --- --- --- --- --- c-- --a --- --- --- ... ... ...

                               - IMGT  __________ <-------------------------------------
                                              65                  70                  75
                                               S   T   L   Q   P   G   I   P       S   R
RAC18_VK                      ... ... ... ... tct aca tta cag cca ggc atc cca ... tca agg

AJ235935 Musmus IGKV19-93*01  ... ... ... ... --- --- --- --- --- --- --- --- ... --- ---

                              ------------------------------  FR3 - IMGT  ---------------
                                              80                  85                  90
                               F   S   G   S   G               S   G   R   D   Y   S   F   S
RAC18_VK                      ttc agt gga agt ggg ... ... tct ggg aga gat tat tcc ttc agc

AJ235935 Musmus IGKV19-93*01  --- --- --- --- --- ... ... --- --- --- --- --- --- --- ---

                              ----------------------------------------------------------> ____
                                              95                  100             104
                               I   I   N   L   E   P   E   D   I   G   T   Y   Y   C   L
RAC18_VK                      atc atc aac ctg gag cct gaa gat att gga act tat tat tgt cta
                                   S                               A
AJ235935 Musmus IGKV19-93*01  --- -g- --- --- --- --- --- --- --- -c- --- --- --- --- ---

                              ______  CDR3 - IMGT  ______

                               Q   Y   D   N   L   W   T   F   G   G   G   T   K   L   E
RAC18_VK                      cag tat gat aat ctg tgg acg ttc ggt gga ggc acc aag ctg gaa
                                                   L
AJ235935 Musmus IGKV19-93*01  --- --- --- --- --t cta c-
```

```
                              I   K
RAC18_VK                      atc aaa

AJ235935 Musmus IGKV19-93*01
```

References:

Amukele, T. K., & Schramm, V. L. (2004). Ricin A-chain substrate specificity in RNA, DNA, and hybrid stem-loop structures. *Biochemistry*, 43(17), 4913-4922. doi:10.1021/bi0498508

Audi, J., Belson, M., Patel, M., Schier, J., & Osterloh, J. (2005). Ricin poisoning: A comprehensive review. *The Journal of the American Medical Association*, 294(18), 2342-2351.

Bai, Y., Watt, B., Wahome, P. G., Mantis, N. J., & Robertus, J. D. (2010). Identification of new classes of ricin toxin inhibitors by virtual screening. *Toxicon*, 56(4), 526-534.

Balint, G. A. (1974). Ricin: The toxic protein of castor oil seeds. *Toxicology*, 2(1), 77-102.

Barbieri, L., Ciani, M., Girbes, T., Liu, W. Y., Van Damme, E. J., Peumans, W. J., et al. (2004). Enzymatic activity of toxic and non-toxic type 2 ribosome-inactivating proteins. *FEBS Letters*, 563(1-3), 219-222.

Berry, J. D. (1999). Antibody gene markers and their relationship to the chlamydial major outer outer membrane protein (MOMP) immune response. (Ph.D., University of Manitoba).

Binder, P., Attre, O., Boutin, J. P., Cavallo, J. D., Debord, T., Jouan, A., et al. (2003). Medical management of biological warfare and bioterrorism: Place of the immunoprevention and the immunotherapy. *Comparative Immunology, Microbiology and Infectious Diseases*, 26(5-6), 401-421.

Blancou, J., & Pearson, J. E. (2003). Bioterrorism and infectious animal diseases. *Comparative Immunology, Microbiology and Infectious Diseases*, 26(5-6), 431-443.

Boese, D. J. (2009). Development and characterization of a neutralizing chimeric murine-human IgG1/K monoclonal antibody to the protective antigen toxin of *Bacillus anthracis*. (M.Sc. University of Manitoba).

Bomlitz, L. J., & Brezis, M. (2008). Misrepresentation of health risks by mass media. *Journal of Public Health*, 30(2), 202-204.

Bradberry, S. M., Dickers, K. J., Rice, P., Griffiths, G. D., & Vale, J. A. (2003). Ricin poisoning. *Toxicological Reviews*, 22(1), 65-70.

Challoner, K. R., & McCarron, M. M. (1990). Castor bean intoxication. *Annals of Emergency Medicine*, 19(10), 1177-1183.

Cook, D. L., David, J., & Griffiths, G. D. (2006). Retrospective identification of ricin in animal tissues following administration by pulmonary and oral routes. *Toxicology*, 223(1-2), 61-70.

Coopman, V., De Leeuw, M., Cordonnier, J., & Jacobs, W. (2009). Suicidal death after injection of a castor bean extract (ricinus communis L.). *Forensic Science International*, 189(1-3), e13-20.

Correll, C. C., Munishkin, A., Chan, Y. L., Ren, Z., Wool, I. G., & Steitz, T. A. (1998). Crystal structure of the ribosomal RNA domain essential for binding elongation factors. *Proceedings of the National Academy of Sciences of the United States of America*, 95(23), 13436-13441.

Crompton, R., & Gall, D. (1980). Georgi markov--death in a pellet. *The Medico-Legal Journal*, 48(2), 51-62.

Dall'Acqua, W. F., Damschroder, M. M., Zhang, J., Woods, R. M., Widjaja, L., Yu, J., et al. (2005). Antibody humanization by framework shuffling. *Methods*, 36(1), 43-60.

David, J., Wilkinson, L. J., & Griffiths, G. D. (2009). Inflammatory gene expression in response to sub-lethal ricin exposure in Balb/c mice. *Toxicology*, 264(1-2), 119-130.

Day, P. J., Owens, S. R., Wesche, J., Olsnes, S., Roberts, L. M., & Lord, J. M. (2001). An interaction between ricin and calreticulin that may have implications for toxin trafficking. *The Journal of Biological Chemistry*, 276(10), 7202-7208.

Dessain, S. K., Adekar, S. P., & Berry, J. D. (2008). Exploring the native human antibody repertoire to create antiviral therapeutics. *Current Topics in Microbiology and Immunology*, 317, 155-183.

Doan, L. G. (2004). Ricin: Mechanism of toxicity, clinical manifestations, and vaccine development. A review. *Journal of Toxicology*, 42(2), 201-208.

Eccles, S. A. (2001). Monoclonal antibodies targeting cancer: 'magic bullets' or just the trigger? *Breast Cancer Research* : BCR, 3(2), 86-90.

Endo, Y., Mitsui, K., Motizuki, M., & Tsurugi, K. (1987). The mechanism of action of ricin and related toxic lectins on eukaryotic ribosomes. the site and the characteristics of the modification in 28 S ribosomal RNA caused by the toxins. *The Journal of Biological Chemistry*, 262(12), 5908-5912.

Endo, Y., & Tsurugi, K. (1987). RNA N-glycosidase activity of ricin A-chain. mechanism of action of the toxic lectin ricin on eukaryotic ribosomes. *The Journal of Biological Chemistry*, 262(17), 8128-8130.

Fulton, R. J., Blakey, D. C., Knowles, P. P., Uhr, J. W., Thorpe, P. E., & Vitetta, E. S. (1986). Purification of ricin A1, A2, and B chains and characterization of their toxicity. *The Journal of Biological Chemistry*, 261(12), 5314-5319.

Funatsu, G., Islam, M. R., Minami, Y., Sung-Sil, K., & Kimura, M. (1991). Conserved amino acid residues in ribosome-inactivating proteins from plants. *Biochimie*, 73(7-8), 1157-1161.

Garland, T., & Bailey, E. M. (2006). Toxins of concern to animals and people. *Revue Scientifique Et Technique*, 25(1), 341-351.

Gerber, D. E. (2008). Targeted therapies: A new generation of cancer treatments. *American Family Physician*, 77(3), 311-319.

Girbes, T., Ferreras, J. M., Arias, F. J., & Stirpe, F. (2004). Description, distribution, activity and phylogenetic relationship of ribosome-inactivating proteins in plants, fungi and bacteria. *Mini Reviews in Medicinal Chemistry*, 4(5), 461-476.

Gorman, C., Leandro, M., & Isenberg, D. (2003). B cell depletion in autoimmune disease. *Arthritis Research & Therapy*, 5 Suppl 4, S17-21.

Guarner, J., & Zaki, S. R. (2006). Histopathology and immunohistochemistry in the diagnosis of bioterrorism agents. *The Journal of Histochemistry and Cytochemistry*, 54(1), 3-11.

Hamburg, M. A. (2002). Bioterrorism: Responding to an emerging threat. *Trends in Biotechnology*, 20(7), 296-298.

Hartley, M. R., & Lord, J. M. (2004). Cytotoxic ribosome-inactivating lectins from plants. *Biochimica Et Biophysica* Acta, 1701(1-2), 1-14.

Hassani, M., Patel, M. C., & Pirofski, L. A. (2004). Vaccines for the prevention of diseases caused by potential bioweapons. *Clinical Immunology*, 111(1), 1-15.

He, X., Brandon, D. L., Chen, G. Q., McKeon, T. A., & Carter, J. M. (2007). Detection of castor contamination by real-time polymerase chain reaction. *Journal of Agricultural and Food Chemistry*, 55(2), 545-550.

Hilleman, M. R. (2002). Overview: Cause and prevention in biowarfare and bioterrorism. *Vaccine*, 20(25-26), 3055-3067.

Ho, M. C., Sturm, M. B., Almo, S. C., & Schramm, V. L. (2009). Transition state analogues in structures of ricin and saporin ribosome-inactivating proteins. *Proceedings of the National Academy of Sciences of the United States of America*, 106(48), 20276-20281.

Hoiseth, G., & Olsnes, S. (2005). Ricin--a therapeutic agent and a biological weapon. [Ricin--terapeutisk agens og biologisk vapen] Tidsskrift for Den Norske Laegeforening : *Tidsskrift for Praktisk Medicin, Ny Raekke*, 125(18), 2477-2479.

Hudson, P. J., & Souriau, C. (2003). Engineered antibodies. *Nature Medicine*, 9(1), 129-134.

Huxsoll, D. L., Patrick, W. C.,3rd, & Parrott, C. D. (1987). Veterinary services in biological disasters. *Journal of the American Veterinary Medical Association*, 190(6), 714-722.

Hwang, W. Y., & Foote, J. (2005). Immunogenicity of engineered antibodies. *Methods*, 36(1), 3-10.

Jetzt, A. E., Cheng, J. S., Tumer, N. E., & Cohick, W. S. (2009). Ricin A-chain requires c-jun N-terminal kinase to induce apoptosis in nontransformed epithelial cells. The International *Journal of Biochemistry & Cell Biology*, 41(12), 2503-2510.

Jetzt, A. E., Cheng, J. S., Tumer, N. E., & Cohick, W. S. (2009). Ricin A-chain requires c-jun N-terminal kinase to induce apoptosis in nontransformed epithelial cells. *The International Journal of Biochemistry & Cell Biology*, 41(12), 2503-2510.

Kalwy, S., Rance, J., & Young, R. (2006). Toward more efficient protein expression: Keep the message simple. *Molecular Biotechnology*, 34(2), 151-156.

Khardori, N. (2006). Bioterrorism and bioterrorism preparedness: Historical perspective and overview. *Infectious Disease Clinics of North America*, 20(2), 179-211.

Kim, S. J., Park, Y., & Hong, H. J. (2005). Antibody engineering for the development of therapeutic antibodies. *Molecules and Cells*, 20(1), 17-29.

Kohler, G., & Milstein, C. (1975). Continuous cultures of fused cells secreting antibody of predefined specificity. *Nature*, 256(5517), 495-497.

Kopferschmitt, J., Flesch, F., Lugnier, A., Sauder, P., Jaeger, A., & Mantz, J. M. (1983). Acute voluntary intoxication by ricin. Human *Toxicology*, 2(2), 239-242.

Kortepeter, M. G., & Parker, G. W. (1999). Potential biological weapons threats. *Emerging Infectious Diseases*, 5(4), 523-527.

Kreitman, R. J. (2001). Toxin-labeled monoclonal antibodies. *Current Pharmaceutical Biotechnology*, 2(4), 313-325.

Laffly, E., & Sodoyer, R. (2005). Monoclonal and recombinant antibodies, 30 years after .. *Human Antibodies*, 14(1-2), 33-55.

Lane, H. C., Montagne, J. L., & Fauci, A. S. (2001). Bioterrorism: A clear and present danger. *Nature Medicine*, 7(12), 1271-1273.

Ler, S. G., Lee, F. K., & Gopalakrishnakone, P. (2006). Trends in detection of warfare agents. detection methods for ricin, staphylococcal enterotoxin B and T-2 toxin. *Journal of Chromatography*, 1133(1-2), 1-12.

Lipman, N. S., Jackson, L. R., Trudel, L. J., & Weis-Garcia, F. (2005). Monoclonal versus polyclonal antibodies: Distinguishing characteristics, applications, and information resources. *ILAR Journal*, 46(3), 258-268.

Lonberg, N. (2008). Human monoclonal antibodies from transgenic mice. *Handbook of Experimental Pharmacology*, (181), 69-97.

Mackinnon, P. J., & Alderton, M. R. (2000). An investigation of the degradation of the plant toxin, ricin, by sodium hypochlorite. *Toxicon*, 38(2), 287-291.

Maddaloni, M., Cooke, C., Wilkinson, R., Stout, A. V., Eng, L., & Pincus, S. H. (2004). Immunological characteristics associated with the protective efficacy of antibodies to ricin. *Journal of Immunology* 172(10), 6221-6228.

Mantis, N. J., McGuinness, C. R., Sonuyi, O., Edwards, G., & Farrant, S. A. (2006). Immunoglobulin A antibodies against ricin A and B subunits protect epithelial cells from ricin intoxication. *Infection and Immunity*, 74(6), 3455-3462.

Marconescu, P. S., Smallshaw, J. E., Pop, L. M., Ruback, S. L., & Vitetta, E. S. (2010). Intradermal administration of RiVax protects mice from mucosal and systemic ricin intoxication. *Vaccine*, 28(32), 5315-5322.

Marsden, C. J., Smith, D. C., Roberts, L. M., & Lord, J. M. (2005). Ricin: Current understanding and prospects for an antiricin vaccine. *Expert Review of Vaccines*, 4(2), 229-237.

Matsuura, T., & Yomo, T. (2006). In vitro evolution of proteins. *Journal of Bioscience and Bioengineering*, 101(6), 449-456.

Mushtaq, A., El-Azizi, M., & Khardori, N. (2006). Category C potential bioterrorism agents and emerging pathogens. *Infectious Disease Clinics of North America*, 20(2), 423-441.

Narayanan, S., Surendranath, K., Bora, N., Surolia, A., & Karande, A. A. (2005). Ribosome inactivating proteins and apoptosis. *FEBS Letters*, 579(6), 1324-1331.

Neal, L. M., O'Hara, J., Brey, R. N., & Mantis, N. J. (2010). A monoclonal immunoglobulin G antibody directed against an immunodominant linear epitope on the ricin A chain confers systemic and mucosal immunity to ricin. *Infection and Immunity*, 78(1):552-61.

Nissim, A., & Chernajovsky, Y. (2008). Historical development of monoclonal antibody therapeutics. *Handbook of Experimental Pharmacology*, (181), 3-18.

Olsnes, S. (2004). The history of ricin, abrin and related toxins. *Toxicon*, 44(4), 361-370.

Olsnes, S., & Kozlov, J. V. (2001). Ricin. *Toxicon*, 39(11), 1723-1728.

Olsnes, S., & Pihl, A. (1972). Ricin - a potent inhibitor of protein synthesis. *FEBS Letters*, 20(3), 327-329.

Olsnes, S., Refsnes, K., Christensen, T. B., & Pihl, A. (1975). Studies on the structure and properties of the lectins from abrus precatorius and ricinus communis. *Biochimica Et Biophysica Acta*, 405(1), 1-10.

Pappas, G., Panagopoulou, P., Christou, L., & Akritidis, N. (2006). Category B potential bioterrorism agents: Bacteria, viruses, toxins, and foodborne and waterborne pathogens. *Infectious Disease Clinics of North America*, 20(2), 395-421.

Park, S. W., Vepachedu, R., Sharma, N., & Vivanco, J. M. (2004). Ribosome-inactivating proteins in plant biology. *Planta*, 219(6), 1093-1096.

Patocka, J., & Streda, L. (2006). Protein biotoxins of military significance. *Acta Medica*, 49(1), 3-11.

Peumans, W. J., Hao, Q., & Van Damme, E. J. (2001). Ribosome-inactivating proteins from plants: More than RNA N-glycosidases? *The FASEB Journal*, 15(9), 1493-1506.

Poupard, J. A., & Miller, L. A. (1992). History of biological warfare: Catapults to capsomeres. *Annals of the New York Academy of Sciences*, 666, 9-20.

Ramsden, C. S., Drayson, M. T., & Bell, E. B. (1989). The toxicity, distribution and excretion of ricin holotoxin in rats. *Toxicology*, 55(1-2), 161-171.

Rapak, A., Falnes, P. O., & Olsnes, S. (1997). Retrograde transport of mutant ricin to the endoplasmic reticulum with subsequent translocation to cytosol. *Proceedings of the National Academy of Sciences of the United States of America*, 94(8), 3783-3788.

Robertus, J. D., & Monzingo, A. F. (2004). The structure of ribosome inactivating proteins. *Mini Reviews in Medicinal Chemistry*, 4(5), 477-486.

Roy, C. J., Hale, M., Hartings, J. M., Pitt, L., & Duniho, S. (2003). Impact of inhalation exposure modality and particle size on the respiratory deposition of ricin in BALB/c mice. *Inhalation Toxicology*, 15(6), 619-638.

Rutenber, E., Katzin, B. J., Ernst, S., Collins, E. J., Mlsna, D., Ready, M. P., et al. (1991). Crystallographic refinement of ricin to 2.5 Å. *Proteins*, 10(3), 240-250.

Rutenber, E., & Robertus, J. D. (1991). Structure of ricin B-chain at 2.5 Å resolution. *Proteins*, 10(3), 260-269.

Salfeld, J. G. (2007). Isotype selection in antibody engineering. *Nature Biotechnology*, 25(12), 1369-1372.

Sandvig, K., & van Deurs, B. (2002). Transport of protein toxins into cells: Pathways used by ricin, cholera toxin and shiga toxin. *FEBS Letters*, 529(1), 49-53.

Sanz, L., Cuesta, A. M., Compte, M., & Alvarez-Vallina, L. (2005). Antibody engineering: Facing new challenges in cancer therapy. *Acta Pharmacologica Sinica*, 26(6), 641-648.

Schep, L. J., Temple, W. A., Butt, G. A., & Beasley, M. D. (2009). Ricin as a weapon of mass terror - separating fact from fiction. *Environment International*, 35(8), 1267-1271.

Shawler, D. L., Bartholomew, R. M., Smith, L. M., & Dillman, R. O. (1985). Human immune response to multiple injections of murine monoclonal IgG. *Journal of Immunology*, 135(2), 1530-1535.

Smallshaw, J. E., Richardson, J. A., & Vitetta, E. S. (2007). RiVax, a recombinant ricin subunit vaccine, protects mice against ricin delivered by gavage or aerosol. *Vaccine*. 25(42), 7459-7469.

Spirin, A. S. (2002). Ribosome as a molecular machine. *FEBS Letters*, 514(1), 2-10.

Spirin, A. S. (2004). The ribosome as an RNA-based molecular machine. *RNA Biology*, 1(1), 3-9.

Spooner, R. A., Smith, D. C., Easton, A. J., Roberts, L. M., & Lord, J. M. (2006). Retrograde transport pathways utilised by viruses and protein toxins. *Virology Journal*, 3, 26.

St John, R., Finlay, B., & Blair, C. (2001). Bioterrorism in canada: An economic assessment of prevention and postattack response. *The Canadian Journal of Infectious Diseases*, 12(5), 275-284.

Stechmann, B., Bai, S. K., Gobbo, E., Lopez, R., Merer, G., Pinchard, S., et al. (2010). Inhibition of retrograde transport protects mice from lethal ricin challenge. *Cell*, 141(2), 231-242.

Stirpe, F. (2004). Ribosome-inactivating proteins. *Toxicon*, 44(4), 371-383.

Stirpe, F., & Battelli, M. G. (2006). Ribosome-inactivating proteins: Progress and problems. *Cellular and Molecular Life Sciences*, 63(16), 1850-1866.

Thorpe, S. C., Kemeny, D. M., Panzani, R., & Lessof, M. H. (1988). Allergy to castor bean. I. its relationship to sensitization to common inhalant allergens (atopy). *The Journal of Allergy and Clinical Immunology*, 82(1), 62-66.

van Deurs, B., Tonnessen, T. I., Petersen, O. W., Sandvig, K., & Olsnes, S. (1986). Routing of internalized ricin and ricin conjugates to the golgi complex. *The Journal of Cell Biology*, 102(1), 37-47.

van Egmond, M. (2008). Neutrophils in antibody-based immunotherapy of cancer. *Expert Opinion on Biological Therapy*, 8(1), 83-94.

Vitetta, E. S., Smallshaw, J. E., Coleman, E., Jafri, H., Foster, C., Munford, R. & Schindler, J (2006) . A pilot clinical trial of a recombinant ricin vaccine in normal humans.

Proceedings of the National Academy of Sciences of the United States of America, 103:2268–2273.

Watson, W. A., Litovitz, T. L., Klein-Schwartz, W., Rodgers, G. C.,Jr, Youniss, J., Reid, N., et al. (2004). 2003 annual report of the american association of poison control centers toxic exposure surveillance system. *The American Journal of Emergency Medicine*, 22(5), 335-404.

Wesche, J., Rapak, A., & Olsnes, S. (1999). Dependence of ricin toxicity on translocation of the toxin A-chain from the endoplasmic reticulum to the cytosol. *The Journal of Biological Chemistry*, 274(48), 34443-34449.

Weston, S. A., Tucker, A. D., Thatcher, D. R., Derbyshire, D. J., & Pauptit, R. A. (1994). X-ray structure of recombinant ricin A-chain at 1.8 Å resolution. *Journal of Molecular Biology*, 244(4), 410-422.

Wilhelmsen, C. L., & Pitt, M. L. (1996). Lesions of acute inhaled lethal ricin intoxication in rhesus monkeys. *Veterinary Pathology*, 33(3), 296-302.

Xiao, X., & Dimitrov, D. S. (2007). Monoclonal antibodies against viruses and bacteria: A survey of patents. *Recent Patents on Anti-Infective Drug Discovery*, 2(3), 171-177.

Yoo, E. M., Wims, L. A., Chan, L. A., & Morrison, S. L. (2003). Human IgG2 can form covalent dimers. *Journal of Immunology*, 170(6), 3134-3138.

Youle, R. J., Murray, G. J., & Neville, D. M.,Jr. (1981). Studies on the galactose-binding site of ricin and the hybrid toxin Man6P-ricin. *Cell*, 23(2), 551-559.

Yuan, X., Gubbins, M. J., & Berry, J. D. (2004). A simple and rapid protocol for the sequence determination of functional kappa light chain cDNAs from aberrant-chain-positive murine hybridomas. *Journal of Immunological Methods*, 294(1-2), 199-207.

Zhu, Z., Dimitrov, A. S., Chakraborti, S., Dimitrova, D., Xiao, X., Broder, C. C., et al. (2006). Development of human monoclonal antibodies against diseases caused by emerging and biodefense-related viruses. *Expert Review of Anti-Infective Therapy*, 4(1), 57-66.